



Federal Republic of Iraq
Kurdistan Region Government
Ministry of Higher Education
and Scientific Research
Koya University

Antifungal activity of Iron and Zinc oxide nanoparticles against air-borne fungi isolated from hospital environments in Koya city

A thesis submitted to the Faculty of Science and Health at Koya University as a partial fulfilment for the degree of Masters of Science (MSc.) in Medical Microbiology

By

Iman Mohammed Mirza

BSc. In Medical Microbiology Department in (2016)
From the College of Health Sciences /Hawler Medical
University

Supervised by

Assist. Prof. Dr. Taha Jalal Omar

December 2023

بِسْمِ اللَّهِ الرَّحْمَنِ الرَّحِيمِ

﴿فَتَعَالَى اللَّهُ الْمَلِكُ الْحَقُّ وَلَا تَعْجَلْ بِالْقُرْآنِ مِنْ قَبْلِ أَنْ

يُنزَلَ إِلَيْكَ وَخِيئَةٌ وَقَدْ رَجَعِ خَيْرِي عَلَمًا﴾.

سورة طه، آية: ١١٤

Dedication

I dedicate this thesis to my lovely parents, my husband, and to the smile of my life sisters and brothers. Their love, faith and encouragement have kept me on track and helped me in this amazing journey.

To my child, who is my heart living outside of my body.

To my dear colleagues and friends.

Acknowledgments

Praise be to Allah the lord of the worlds. Mercy, kindness, and prayers and Peace upon Mohammed the prophet of God and upon his purified family.

I feel pleasure to acknowledge my supervisor, **Assist. Prof. Dr. Taha Jalal Omar** for providing all the necessary guidance and moral support throughout research work.

I would also like to give special thanks to my family (father and mother) and my husband as a whole for their continuous support and understanding when undertaking my research and writing my project. Your prayer for me was what sustained me this far.

I would also like to thank **Koya University, Faculty of Science and Health, Medical Microbiology Department** and, all of the members of the **science and health research center** of Koya University for helping me.

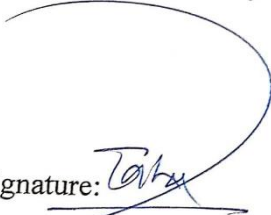
Special thanks to the Dean of the Faculty of Science and Health **Prof. Dr. Zrar Saleem Kareem** and head of the Medical Microbiology Department **Assist. Prof. Dr. Aqeel Ismael Gheni** for his enhancements and supports.

In the end, thanks to everyone who helped me even one word.

Supervisor's Approval

Hereby I'm Assist. Professor. Dr. Taha Jalal Omar state that this thesis entitled (**Antifungal activity of Iron and Zinc oxide nanoparticles against air-borne fungi isolated from hospital environments in KOYA city**) was prepared under my supervision, at the Department of Medical Microbiology, Faculty of Science and Health, Koya University, by (Iman Mohammed Mirza) , as partial fulfilment for the degree of Master of Science (MSc.) in Medical Microbiology.

I have read and reviewed this work and I confirm that it is an original work to the best of my knowledge.

Signature: 

Name: Dr.Taha Jalal Omar

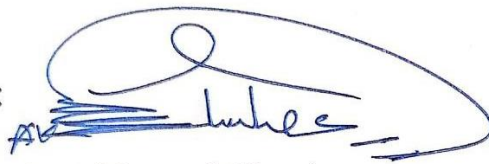
Academic title: Assistant Professor

Date: / / 2023

Head of Department Approval

Upon recommendation of the supervising faculty whose name and signature appear above, I have forwarded this thesis for review by the examining committee.

Signature:

A handwritten signature in blue ink, enclosed in a large, loopy oval. The signature appears to be 'Aqeel Ismael Gheni' with some stylized flourishes.

Name: Dr. Aqeel Ismael Gheni

Academic title: Assistant Professor

Academic position: Head of Medical Microbiology Department/ Koya

University

Date 28/12 2023

Viva Examining Committee Approval

We, the viva examining committee confirm that we have read this thesis as entitled (**Antifungal activity of Iron and Zinc oxide nanoparticles against air-borne fungi isolated from hospital environments in KOYA city**). We have examined the student (**Iman Mohammed Mirza**) in relation to all aspects of this thesis. In our opinion, it meets the standards of a thesis for the degree of Master of Science (MSc.) in Medical Microbiology.

Signature: 

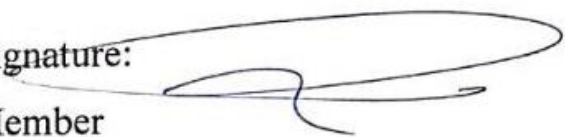
Chairman

Name: Dr. Khattab A. M. Shekhany

Academic title: Assist Professor

Academic position: University of Sulaimani

Date: / / 2023

Signature: 

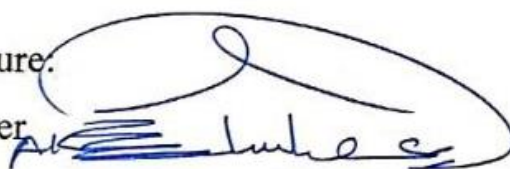
Member

Name: Dr. Qasim Abdulla Marzani

Academic title: Assist Professor

Academic position: Salahaddin University- Erbil

Date: / / 2023

Signature: 

Member

Name: Dr. Aqeel Ismael Ghani

Academic title: Assist Professor

Academic position: Koya University

Date: 14 / 12 / 2023

Signature: 

Member and supervisor

Name: Dr. Taha Jalal Omer

Academic title: Assist Professor

Academic position: Koya University

Date: / / 2023

Approved by the Council of the Faculty of Science and Health

Signature: 

Name: Dr. Zrar Saleem Marzany

Academic title: Professor

Academic position: Dean of the Faculty of Science and Health

Date: / / 2023

List of Abbreviation

Abbreviations	Expansion
SDA	Sabouraud dextrose agar
XRD	X-ray Diffraction
SEM	Scan Electron microscope
ITS	Internal Transcribe Spacer
MIC	Minimum inhibitory concentration
NPs	Nanoparticles
ZnO-NPs	Zinc oxide Nanoparticles
IONPs	Iron-oxide Nanoparticles
ROS	Reactive oxygen species
HSCT	Hematopoietic stem cell transplantation
HIV	Human immunodeficiency virus
PCR	Polymerase Chain Reaction
DNA	Deoxyribonucleic acid
RNA	Ribonucleic acid
FLU	Fluconazole
ICUs	Intensive Care Units
NICUs	Neonatal intensive care units
HAIs	Hospital-acquired infections
HEPA	High Efficiency Particulate Air
CNS	Central nervous system
TLR2	Toll-like receptor1
TLR6	Toll-like receptor6
IA	Invasive aspergillosis
ABPA	Allergic bronchopulmonary aspergillosis
IPA	Invasive pulmonary aspergillosis
CGD	Chronic granulomatous disease
TB	Tuberculosis
COVID-19	Coronavirus disease
rDNA	Ribosomal deoxyribonucleic acid
rRNA	Ribosomal ribonucleic acid

ITR	Itraconazole
VRC	Voriconazole
POS	Posaconazole
Rpm	Round per minute
GRAS	Generally recognised as safe
MRI	Magnetic Resonance Imaging
ddH ₂ O	Double distilled water
SDB	Sabouraud Dextrose Broth
PDA	Potato Dextrose Agar
PDB	Potato Dextrose Broth

Abstract

Despite the fact that spores are present in various environments, hospital indoor surroundings might cause the spread of pathogenic fungi among patients in hospitals. Nosocomial infections, also called hospital-acquired infections, frequently occur by pathogenic airborne organisms that are found in hospitals and the areas around them.

The aim of this study was to isolate and identify airborne fungi presented in the hospital environments in Koya city and Molecular identification for *candida* species isolates; with a band size of 375-871 bp and evolution of Zinc oxide and Iron-oxide nanoparticles activity against candida species. The investigation was done in five government hospitals and healthcare facilities, which included; Shahid Doctor Khalid Hospital, Shahid Doctor Handren Health Center, Haji Qadr Health Center, Bawaji Health Center and Shahid Doctor Kawa &Dental Center. A total of 225 air samples from various wards in each of these hospitals were cultured. They were isolated on sterile petri dishes filled with Sabouraud Dextrose Agar (SDA) amended with chloramphenicol. These plates were left open in the investigation site for 20 minutes. Each sample is properly identified then taken to a lab for routine microbiological processing and analysis. 16 genera of pathogenic and opportunistic fungi have been observed in the selected hospitals.

These isolates were distributed in Shahid Doctor Khalid Hospital (32%), Shahid Doctor Handren Health Center (17%), Haji Qadr Health Center (15%), Bawaji Health Center (12%) and Shahid Doctor Kawa &Dental Center (23%). The results of the laboratory analysis revealed that out of the 198 positive samples analyzed, a total of 60.5% were identified as filamentous fungi, while the remaining 39.5% were identified as yeast isolates. The most common airborne fungi included: The filamentous fungi which was distributed as *Aspergillus* spp. (25.26%), *Penicillium* sp. (8.25%) and *Curvularia* sp. (6.19%). The yeast isolates were distributed as *Candida* spp. (28.35%), *Cryptococcus* sp. (6.87%) and *Rhodotorula* sp. (3.61%).

To identify the most isolated species of candida, molecular diagnosis using PCR was used. Polymerase chain reaction using ITS1(18S) and ITS4 (28S) oligonucleotide universal primers amplified rRNA genes and the 5.8S gene of the fungi. *C. albicans*, *C. glabrata*, *C. parapsilosis*, *C. krusei* and *C. lusitaniae* were identified using these primers. They were registered in the National Centre for Biotechnology Information database (NCBI).

An additional part of this study was aimed to evaluate the antifungal activity of metal oxide nanoparticles, particularly zinc oxide and Iron-oxide against different *Candida* spp. and compared with fluconazole (FLU). Zinc oxide and Iron-oxide nanoparticles were characterized by X-ray Diffraction Analysis (XRD) and Scanning Electron microscope (SEM).

The efficacy of ZnONPs and IONPs were studied at concentrations (1000,500,250,125 and 62.5) µg/ml against 5 isolates of *Candida* spp. by agar plate well diffusion assay. The results showed high inhibition effect of ZnONPs on *C. lusitaniae* and *C. glabrata* followed by, *C. krusei*. While high inhibition effect of IONPs presented in *C. parapsilosis* and *C. glabrata*. The results showed that *Candida* spp. were susceptible to NPs and the inhibition rate increases with the increase of concentration.

For the minimum inhibitory concentration (MIC) by broth microdilution methods, it is found that MIC of ZnO-NPs and IONPs against *Candida* spp. were reported to be 64–512 µg/ml ,16-128 and 64–512 µg/ml for the FLU. The results revealed that MICs for antifungals against *Candida* spp. were had very good invitro activity, the lowest MIC of IONPs in *C. glabrata* and *C. lusitaniae* were 16 µg/ml. While the lowest MIC of ZnO-NPs was observed for *C. lusitaniae* and *C. albicans* were 64 µg/ml.

List of Contents

Titles		Page
Dedication		I
Acknowledgment		II
List of Abbreviations		VI
Abstract		VIII
List of contents		X
List of tables		XV
List of figures		XVI
Chapter One: Introduction		
1.1	Introduction	۱
1.2	Objective of the study	۳
Chapter Two: Literature Review		
2.	Literature Review	۴
2.1	Airborne Fungi in hospital	۴
2.2	Nosocomial fungal infections	7
2.3	Major fungi present in hospital environments	8
2.3.1	<i>Aspergillus spp.</i>	8
2.3.1.1	<i>Aspergillus fumigatus</i>	۸
2.3.1.2	<i>Aspergillus flavus</i>	9
2.3.1.3	<i>Aspergillus Niger</i>	9
2.3.1.4	<i>Aspergillus versicolor</i>	۹
2.3.1.5	<i>Aspergillus terreus</i>	10
2.3.1.6	<i>Aspergillus nidulans</i>	10
2.3.2	<i>Penicillium sp.</i>	۱۰
2.3.3	<i>Alternaria spp.</i>	۱1
2.3.4	<i>Chrysosporium sp.</i>	۱1
2.3.5	<i>Cladosporium spp.</i>	۱۱
2.3.6	<i>Blastomyces dermatitidis</i>	۱2
2.3.7	<i>Mucorales</i>	۱2
2.3.8	<i>Candida spp.</i>	۱3
2.3.9	<i>Naganishia albida (Cryptococcus albidus)</i>	۱4

2.3.10	<i>Rhodotorula Spp.</i>	15
2.3.11	<i>Exophiala dermatitidis</i>	15
2.4	Molecular assay	16
2.5	Antifungal agents	18
2.5.1	Polyenes	18
2.5.2	Echinocandins	18
2.5.3	Allylamines	19
2.5.4	Azole	19
2.5.5	Fluorinated pyrimidine analogues	19
2.6	Nanotechnology	20
2.6.1	Zinc Oxide Nanoparticles	20
2.6.2	Iron-oxide Nanoparticle	22
Chapter Three: Material and Methods		
3.	Material and Methods	23
3.1	Materials	23
3.1.1	Equipment and Laboratory Instruments	23
3.1.2	Chemical substances	24
3.1.3	Media	25
3.1.4	Diagnostic Kit	25
3.2	Methods	25
3.2.1	Sterilization	25
3.2.1.1	Moist heat sterilization	25
3.2.1.2	Dry heat sterilization	25
3.2.1.3	Sterilization by filtration	26
3.2.2	Preparation of culture media	26
3.2.2.1	Sabouraud Dextrose Agar (SDA)	26
3.2.2.2	Sabouraud Dextrose Broth (SDB)	26
3.2.2.3	Potato Dextrose Agar (PDA)	27
3.2.2.4	Potato Dextrose Broth (PDB)	27
3.2.3	Isolation and Identification of fungi	27
3.2.3.1	Air Sampling	27
3.2.3.2	Morphological examination of fungal colonies	28

3.2.3.3	Microscopical examination	۲۸
3.2.4	Biochemical test for Yeast	۲۸
3.2.4.1	Germ tube test	۲۸
3.2.4.2	Diagnostic testing with the Vitek2 Compact System	۲۹
3.2.5	Maintenance of Isolate	۲۹
3.2.5.1	Short term preservation	۲۹
3.2.5.2	Long term preservation	۲۹
3.2.6	Molecular identification	30
3.2.6.1	Fungal DNA Extraction	30
3.2.6.2	Estimation of extracted DNA	30
3.2.6.3	PCR Reaction mixture	31
3.2.6.4	PCR Thermocycler Conditions	۳۱
3.2.6.5	DNA primers	۳۲
3.2.6.6	PCR product analysis	۳۲
3.2.6.7	Fragment sizes of ITS1-ITS4 PCR products for <i>Candida</i> spp.	33
3.2.6.8	Sequencing of PCR amplicons	۳۳
3.2.7	Preparation and determination of Characterization of ZnO-NPs and IONPs.	۳۴
3.2.7.1	X-ray diffraction	۳۴
3.2.7.2	Field emission scanning electron microscopy (FESEM)	۳۴
3.2.7.3	Susceptibility Test	۳۵
3.2.7.4	Agar well diffusion method	۳۵
3.2.7.5	Microdilution Method for MIC determination	۳۶
3.2.8	Data analysis	۳۶
Chapter Four: Results and Discussion		
4.	Results and Discussion	۳۷
4.1	Isolation of airborne fungi	۳۷
4.1.1	Isolated Yeasts from the air of hospitals	40
4.1.2	Isolated <i>Aspergillus</i> spp. from the air of hospitals	41
4.1.3	Isolated <i>Candida</i> spp. from the air of hospitals	۴۳
4.1.4	Distribution of airborne fungi in each Hospital	۴۴
4.3	Germ tube formation	۴۵

4.2	Identification of airborne fungi	ε6
4.2.1	<i>Aspergillus</i> spp.	ε6
4.2.1.1	Cultural and Microscopic Characteristics	ε6
4.2.1.2	<i>Aspergillus Niger</i>	ε7
4.2.1.3	<i>Aspergillus flavus</i>	ε8
4.2.1.4	<i>Aspergillus fumigatus</i>	ε9
4.2.1.5	<i>Aspergillus terreus</i>	50
4.2.1.6	<i>Aspergillus nidulans</i>	51
4.2.1.7	<i>Aspergillus versicolor</i>	52
4.2.2	<i>Alternaria</i> sp.	53
4.2.3	<i>Mucor</i> sp.	5ε
4.2.4	<i>Trichophyton verrucosum</i>	55
4.2.5	<i>Pencillium</i> sp.	56
4.2.6	<i>Curvularia</i> sp.	57
4.2.7	<i>Blastomyces dermatitidis</i>	ε8
4.2.8	<i>Chaetomium</i>	ε9
4.2.9	<i>Trichoderma</i>	60
4.2.10	<i>Chrysosporium</i>	61
4.2.11	<i>Aureobasidium</i> sp.	62
4.2.12	<i>Cladosporium</i>	6ϣ
4.2.13	<i>Candida</i> spp.	64
4.2.14	<i>Rhodotorula mucilaginosa</i>	67
4.2.15	<i>Cryptococcus albidus</i> (<i>Naganishia albida</i>)	68
4.2.16	<i>Exophiala dermatitidis</i>	69
4.3	Molecular identification	70
4.3.1	Polymerase Chain Reaction	70
4.3.2	Sequencing Analysis	71
4.4	Properties of Nanoparticles	73
4.4.1	XRD crystallography analysis and thermal stability	73
4.4.2	SEM analysis of nanoparticles	76
4.4.3	MICs Determination of ZnO-NPs, IONPs compared to FLU against different <i>Candida</i> species	78

4.4.4	Inhibitory effect of IONPs Against <i>Candida</i> species by Agar plate Well Diffusion assay	81
4.4.5	Inhibitory effect of ZnO-NPs Against <i>Candida</i> species by Agar plate well Diffusion assay	84
4.4.6	Inhibitory effect of FLU Against <i>Candida</i> species by Agar plate well Diffusion assay	87
Chapter Five: Conclusions and Recommendations		
5.1	Conclusions	89
5.2	Recommendations	90
References		
References		91

List of Tables

No.	Title	Page
3-1	Lists of all of the tools and devices that have been used in the study.	23
3-2	The chemical substances used in the study and their origin.	24
3-3	The culture media used in the study and their origin.	25
3-4	Diagnostic Kit used in the study and their origin.	25
3-5	PCR reaction mixture of 40 ul.	31
3-6	Conditions PCR Thermocycler.	31
3-7	Primer sequences used for molecular identification.	32
3-8	Expected fragment length of amplification the ITS region.	33
4-1	Fungal genera isolated from the air of hospitals.	39
4-2	Yeast species isolated from the air of hospitals.	41
4-3	Colony number and percentage of <i>Aspergillus</i> spp. isolated from air of hospitals in koya.	39
4-4	Colony number and percentage of <i>Candida</i> spp. of airborne fungi in the hospitals.	43
4-5	<i>Candida</i> spp. isolates obtained from airborne of hospitals in koya city and accession numbers of DNA sequenced of isolates registered in NCBI and Examples of GenBank accession numbers matching to our result.	71
4-6	Zone of inhibition of IONPs at various concentrations against different <i>Candida</i> species (mm).	82
4-7	Zone of inhibition of ZnO-NPs at various concentrations against different <i>Candida</i> species (mm).	85
4-8	Zone of inhibition of FLU at various concentrations against different <i>Candida</i> species (mm).	87

List of Figures

N o.	Title	Pa ge
4- 1	Distribution of air-borne fungi in five koya hospitals.	44
4- 2	Germ tube of <i>C. albicans</i> grown on human serum at 37°C for 2hrs and half (40 X).	45
4- 3	(A) <i>A. niger</i> Culture on SDA at 37°C for 5 days, and (B) microscopic morphology of conidiophores and conidia of <i>A. niger</i> colony mounted with LPCB stain magnify at 40x.	47
4- 4	(A) <i>A. flavus</i> culture on SDA at 37°C for 5 days, and (B) microscopic morphology of conidiophores and conidia of <i>A. flavus</i> colony mounted with LPCB stain magnify at 40x.	48
4- 5	(A) <i>A. fumigatus</i> culture on SDA at 37°C for 5 days, and (B) microscopic morphology of conidiophores and conidia of <i>A. fumigatus</i> colony mounted with LPCB stain magnify at 40x.	49
4- 6	(A) <i>A. terreus</i> culture on SDA at 37°C for 5 days, and (B) microscopic morphology of conidiophores and conidia of <i>A. terreus</i> colony mounted with LPCB stain magnify at 40x.	50
4- 7	(A) <i>A. nidulans</i> culture on SDA at 37°C for 5 days, and (B) microscopic morphology of Hülle cells of <i>A. nidulans</i> colony mounted with LPCB stain magnify at 40x.	51
4- 8	(A) <i>A. versicolor</i> culture on SDA at 37°C for 5 days, and (B) microscopic morphology of conidiophores and conidia of <i>A. versicolor</i> colony mounted with LPCB stain magnify at 40x	52
4- 9	(A) <i>Alternaria</i> sp. culture on PDA at 37°C for 7 days, and (B) microscopic morphology of conidiophores and conidia of <i>Alternaria</i> sp. colony mounted with LPCB stain magnify at 40x.	53
4- 10	(A) <i>Mucor</i> spp. culture on PDA at 37°C for 5 days, and (B) microscopic morphology of <i>Mucor</i> spp. sporangiophores of <i>Mucor</i> spp. colony mounted with lactophenol cotton blue stain magnify at 40x.	54
4- 11	(A) <i>Trichophyton verrucosum</i> culture on SDA at 37°C for 10 days, and (B) microscopic morphology of macroconidia and microconidia of <i>Trichophyton verrucosum</i> colony mounted with LPCB stain magnify at 40x.	55
4- 12	(A) <i>Penicillium</i> sp. culture on PDA at 37°C for 7days, and (B) microscopic morphology of conidiophores and conidia of <i>Penicillium</i> sp. colony mounted with LPCB stain magnify at 40x.	56

4-13	(A) <i>Curvularia</i> sp. culture on PDA at 37°C for 8days, and (B) microscopic morphology of conidiophores of <i>Curvularia</i> sp. colony mounted with LPCB stain magnify at 40x.	57
4-14	(A) <i>B. dermatitidis</i> culture on SDA at 37°C for 10 days, and (B) microscopic morphology of conidia of <i>B. dermatitidis</i> colony mounted with LPCB stain magnify at 40x.	58
4-15	(A) <i>Chaetomium</i> culture on PDA at 37°C for 6 days, and (B) microscopic morphology of perithecia of <i>Chaetomium</i> colony mounted with LPCB stain magnify at 40x.	59
4-16	(A) <i>Trichoderma</i> culture on PDA at 37°C for 5 days, and (B) microscopic morphology of conidiophores and conidia of <i>Trichoderma</i> colony mounted with LPCB stain magnify at 40x.	60
4-17	(A) <i>Chrysosporium</i> culture on PDA at 37°C for 8 days, and (B) microscopic morphology of hyphae and conidia of <i>Chrysosporium</i> colony mounted with LPCB stain magnify at 40x.	61
4-18	(A) <i>Aureobasidium</i> sp. culture on PDA at 37°C for 7 days, and (B) microscopic morphology of arthroconidia of <i>Aureobasidium</i> sp. colony mounted with LPCB stain magnify at 40x.	62
4-19	(A) <i>Cladosporium</i> culture on PDA at 37°C for 10 days, and (B) microscopic morphology of conidiophores and conidia of <i>Cladosporium</i> colony mounted with LPCB stain magnify at 40x.	63
4-20	(A) <i>C.albicans</i> growth on SDA at 37°C for 24-48 hours h and(B) microscopic characteristic of colony mounted with Gram stain observed in a 40x magnification.	64
4-21	(A) <i>C.glabrata</i> growth on SDA at 37°C for 24-48 hours h and(B) microscopic characteristic of colony mounted with Gram stain observed in a 40x magnification.	65
4-22	(A) <i>C.parapsilosis</i> growth on SDA at 37°C for 24-48 hours h and(B) microscopic characteristic of colony mounted with Gram stain observed in a 40x magnification.	65
4-23	(A) <i>C.krusei</i> growth on SDA at 37°C for 24-48 hours h and(B) microscopic characteristic of colony mounted with Gram stain observed in a 40x magnification.	66
4-24	(A) <i>C. lusitania</i> growth on SDA at 37°C for 24-48 hours and(B) microscopic characteristic of colony mounted with Gram stain observed in a 40x magnification.	66

4-25	(A) <i>Rhodotorula mucilaginosa</i> growth on SDA medium at 37°C for 3 days and (B) microscopic characteristic of blastoconidia mounted with Gram stain observed in a 40x magnification.	67
4-26	(A) <i>Cryptococcus albidus</i> growth on SDA medium at 37°C for 3 days and (B) microscopic characteristic of blastoconidia mounted with Gram stain observed in a 40x magnification.	68
4-27	(A) <i>Exophiala dermatitidis</i> growth on SDA medium at 37°C for 10 days and (B) microscopic characteristic of conidia of <i>Exophiala dermatitidis</i> colony mounted with LPCB stain observed in a 40x magnification.	69
4-28	The agarose gel electrophoresis technique was used to visualize the ITS-PCR products of <i>Candida</i> isolates, which showed distinct bands. Lane 1: Ladder 100 bp (Genedirex), Lane 2: negative control (NC), Lane 3: <i>C. albicans</i> (535bp), Lane 4: <i>C. glabrata</i> (871bp), Lane 5: <i>C. lusitaniae</i> (375bp), Lane 6: <i>C. albicans</i> (535bp), Lane 7: <i>C. krusei</i> (510bp), Lane 8: <i>C. parapsilosis</i> (520bp) respectively by using 1X TBE buffer/ Agarose gel 1.14%.	70
4-29	Examples of Chromatograms of the Sequenced Data. A) <i>C. albicans</i> , B) <i>C. parapsilosis</i> , C) <i>C. lusitaniae</i> , D) <i>C. krusei</i> , E) <i>C. glabrata</i> .	72
4-30	X-ray diffraction pattern of the zinc oxide nanoparticles.	74
4-31	X-ray diffraction pattern of the iron oxide nanoparticles.	74
4-32	SEM photomicrograph of zinc oxide nanoparticles at magnifications of 10 µm (A), 5 µm (B), 4 µm (C), and 3 µm (D).	76
4-33	SEM photomicrograph of iron oxide nanoparticles at magnifications of 10 µm (A), 5 µm (B), 3 µm (C), and 3 µm	77
4-34	Minimum inhibitory concentration (MIC) of ZnO-NPs, IONPs and FLU against different <i>Candida</i> species (µg/ml).	80
4-35	Zone of inhibition of IONPs at various concentrations against different <i>Candida</i> species. A- <i>C. albicans</i> , B- <i>C. parapsilosis</i> , C- <i>C. krusei</i> , D- <i>C. lusitaniae</i> , E- <i>C. glabrata</i> .	83
4-36	Zone of inhibition of ZnO-NPs at various concentrations against different <i>Candida</i> species. A- <i>C. albicans</i> , B- <i>C. parapsilosis</i> , C- <i>C. krusei</i> , D- <i>C. lusitaniae</i> , E- <i>C. glabrata</i> .	86

4- 37	Zone of inhibition of FLU at various concentrations against different <i>Candida</i> species. A- <i>C. albicans</i> , B- <i>C. parapsilosis</i> , C- <i>C. krusei</i> , D- <i>C. lusitaniae</i> , E- <i>C. glabrata</i> .	88
----------	---	----

Chapter One

Introduction

1.1 Introduction

The public health can be influenced by several agents present in both indoor and outdoor environments, including physical, chemical, and biological factors. Problems of indoor air quality in hospitals is a matter of concern due to the presence of an extensive variety of infectious airborne microorganisms, which have the potential to contribute to the occurrence of hospital-acquired infectious diseases (Sudharsanam *et al.*, 2012). The hospital environment has been identified as a potential habitat for various airborne diseases such as bacteria and fungi. Fungi are the most common types of microbes found in hospitals. Because fungi grow slowly, mycoses are often cause chronic disorders. Mycoses are divided into five categories based on the degree of tissue involvement and mechanism of entry: superficial, cutaneous, subcutaneous, systemic, and opportunistic Mycoses. The spread of fungal spores by free-living fungi, which enter the host via inhalation or injury, results in the development of numerous serious illnesses. Some fungi secrete mycotoxins, which are fungal toxins that cause disease (Tortora *et al.*, 2010).

Fungi are quite similar to humans and animals since they are all eukaryotic organisms, and their structures and metabolism are similar to those of their hosts. As a result, anti-fungal that damage fungal cells may also affect human and animal cells. Because of this, fungal infections in both humans and animals are frequently difficult to treat. The damage caused by these fungi is caused by their poisons and enzymes, which cause penetration of the tissues and hypersensitivity (Tormo-Molina *et al.*, 2012)

Immunocompromised patients are more sensitive to nosocomial infections since their defensive ability has been reduced, either related to cancer, hemolymphoproliferative disorders, elderly patients or HIV infection, medical therapy, or organ transplantation. The most common potential causes of infection in the hospital air are bioaerosols. Fungi are the most common forms of bioaerosols seen in hospital environments (Park *et al.*, 2013)

Filamentous fungi from the *Aspergillus* spp., *Penicillium* sp., *Mucorales* (*Rhizopus* sp.), *Fusarium* spp., *Trichophyton* spp., *Chrysosporium* sp., *Cladosporium* sp., and *Acremonium* sp. dominate airborne micro-fungi in indoor hospital environments. *Candida* spp., *Trichosporon*, *Rhodotorula*, *Saccharomyces*, and *Cryptococcus* yeast isolates have also been discovered. The concentration and

variability of bioaerosols in the hospital can be used to assess the sanitation of these environments (Martínez-Herrera *et al.*, 2016) .

PCR techniques may identify extremely small amounts of DNA, resulting in rapid identification of pathogenic fungi and, as a result, earlier initiation of antifungal therapy, which may enhance survival prospects. These approaches have a high degree of specificity and sensitivity in detecting the presence of fungus (Allothman, 2012). The ITS region has been suggested as the universal fungal barcode sequence since it is the most frequently sequenced DNA region in fungi molecular identification (Peay *et al.*, 2008).

Candida yeasts are among the most commonly observed pathogens in healthcare-associated infections (HAIs). Due to the fact that the clinical isolates of *Candida* are becoming more resistant to antifungals (Costa *et al.*, 2016), it was essential to explore alternative treatments that exhibit strong efficiency against pathogenic fungus. Notably, nanoparticles have emerged as an excellent choice due to their great effectiveness in preventing pathogenic fungi (Torabi & Doudi, 2016).

Nanotechnology is an emerging field of study that specifically focuses on particles within the size range of around 1 to 100 nm. Nanoparticles (NPs) are extensively employed in the field of nanomedicine for preventing bacterial and fungal infections, with a low possibility of pathogens acquiring resistance to their effects. NPs are widely accepted as viable options for facilitating the delivery of therapeutic medicines to specific target sites (Brandelli, 2012). Many different types of metal and metal oxide nanoparticles (NPs), including silver (Ag), silver oxide (Ag₂O), titanium dioxide (TiO₂), zinc oxide (ZnO), gold (Au), iron oxide, calcium oxide (CaO), silica (Si), copper oxide (CuO), and magnesium oxide (MgO), are currently demonstrated to be capable of antimicrobial effects.(Dizaj *et al.*, 2015).

The toxicity of zinc oxide nanoparticles (ZnO-NP) was found to be the highest among other types of metal oxide nanoparticles when evaluated against *Candida* species. The disruption of membrane integrity by ZnO is attributed to the generation of reactive oxygen species, which subsequently induce fungal destruction (Hosseini SS *et al.*, 2011). Furthermore, the synthesis of hydrogen peroxide by zinc oxide nanoparticles has been found to play a crucial role in their antifungal action. ZnO nanoparticles

demonstrate selective toxicity towards fungal organisms, while demonstrating minimal effect on both human and animal cells (Eskandari *et al.*, 2009).

Iron-oxide nanoparticles (IONPs) are widely recognised as highly adaptable and safe nanomaterials, additionally considered as non-toxic substances. Iron oxide nanoparticles become widespread use in several applications related to their biodegradability, minimal cytotoxicity, and the presence of a reactive surface that may be altered with biocompatible coatings (Abdeen *et al.*, 2013). With the development of nanotechnology, IONPs have been shown to be effective against many different kinds of viruses (Kumar *et al.*, 2019) antiparasitic (Shukla *et al.*, 2015), bactericidal (Tran *et al.*, 2010), antibiofilm (Prodan *et al.*, 2013), antifungal (Prucek *et al.*, 2011) and wound healing (Tocco *et al.*, 2012). The antimicrobial efficacy of the IONPs exhibits a strong association with the oxidative stress induced by reactive oxygen species (ROS). Reactive oxygen species (ROS), which encompass hydrogen peroxide, superoxide radicals (O_2^-), hydroxyl radicals ($-OH$), and singlet oxygen (1O_2), have the potential to induce damages to DNA and proteins within pathogenic microorganisms, which includes bacteria and fungi (Rudramurthy *et al.*, 2016).

1.2 Objectives of the study:

- 1- Isolation and identification of airborne fungi from hospitals environment in Koya city, which will be helpful in future to reduce fungal hospital-acquired infection (HAI) rates.
- 2- Molecular diagnosis to characterize isolates of *Candida* species from hospital environment.
- 3- Characterization of ZnONPs, IONPs nanoparticles by scanning electron microscope (SEM), and X-ray diffraction (XRD).
- 4- Evaluate the antifungal activity of ZnONPs and IONPs against different *Candida* spp. compared with fluconazole (FLU).
- 5- Determination of the minimum inhibitory concentration of ZnONPs, IONPs and FLU.

Chapter Two

Literatures Review

2.Literature Review

2.1 Airborne Fungi in hospital

Fungi are a type of microorganism that belong to the eukaryotic domain. Fungi have the ability to manifest as either yeasts, moulds, or a combination of both morphological forms. Certain types of fungi have the ability to induce various forms of diseases, including superficial, cutaneous, subcutaneous, systemic, or allergic reactions. Yeasts are unicellular fungi that undergo a kind of asexual reproduction known as budding. In contrast, moulds are characterised by the presence of elongated filaments called hyphae, which exhibit growth through apical extension (McGinnis & Tyring, 1996).

Fungal spores are microscopic particles responsible for the reproduction of fungi. They typically range in size from 2 to 50 µm in diameter, with most allergenic spores in the respirable size range of 3 to 10 µm (Filippo *et al.*, 2013). Meteorological and climate conditions, such as temperature and relative humidity, influence the concentrations of spores in the air (Ponce-Caballero *et al.*, 2013). For example, dry air spore fungi can disperse long distances under low relative humidity and high wind speed. Wet weather spores tend to disperse during and after rainfall (Khattab & Levetin, 2008).

Fungi that disperse via the atmosphere are referred to as airborne fungi, and due to their opportunistic nature, they have the potential to induce diseases in people. Airborne fungi have a significant impact on human health, mostly due to their ability to induce allergic reactions, irritate mucous membranes and skin, and cause fungal infections in those who are sensitive to their spores and toxic products (Setlhare *et al.*, 2014).

Within healthcare facilities, the composition of the airborne microbiota primarily consists of filamentous fungi, with a particular emphasis on species such as *Aspergillus*, *Cladosporium*, *Paecilomyces*, *Penicillium*, and *Scopulariopsis*. Yeasts, specifically *Candida*, *Rhodotorula*, *Cryptococcus*, and *Trichosporon* species, have also been discovered in the airborne environment. However, there is limited knowledge regarding the mechanisms by which these yeasts maintain their suspension in the air.

All of the genera mentioned before have been identified and documented as possible infections in humans, especially the *Candida* genus. *Candida* is recognised as the most common causal agent of fungemia in hospitals (Cordeiro *et al.*, 2010). Invasive candidiasis is a potentially fatal infection attributed to these fungal organisms, primarily manifesting within Intensive Care Units (ICU) environments (Presente *et al.*, 2023). Invasive candidiasis is the main factor in mortality and morbidity in low birth weight and premature neonates in neonatal intensive care units (NICUs) (Caggiano *et al.*, 2017). Furthermore, the incidence of opportunistic infections caused by *Candida* species may be correlated with newborns who require invasive therapies, such as the insertion of catheters (Ezenwa *et al.*, 2017).

Exposure to airborne microorganisms provides a significant risk factor for human health. Research has demonstrated that microbes originating from environmental reservoirs have the ability to disseminate across considerable distances through the movement of air currents, which leads to their inhalation, ingestion, or contact with persons who have not been in direct contact with the infectious source (Fernstrom & Goldblatt, 2013).

The quality of the air inside hospitals is an important part of preventing nosocomial respiratory diseases. Microorganisms can be found in places like soil, water, dust, and decaying organic matter, among other places. Once these substances are brought into a hospital by people, air currents, or building materials, the microorganisms that live in them can grow and spread in different indoor ecological areas (Shelton *et al.*, 2002). The inhalation of fungal spores has the potential to give rise to a range of fungal diseases in individuals who are susceptible to such infections. The recognition of the significance of environmental data on fungus is growing with the increase of the populations of elderly patients, cancer patients, solid organ transplantation patients, premature babies, and hematopoietic stem cell transplantation (HSCT) recipients (Gangneux *et al.*, 2016). Despite the fact that mortality and morbidity rates related to invasive fungal diseases are still extremely prevalent, the number of antifungal treatment medicines that are now available is rather low when compared to antibacterial agents (Roemer & Krysan, 2014).

Numerous investigations indicate that the quantitative and qualitative distribution of fungi in the atmosphere exhibits geographical variations and is further affected by seasonal climate and environmental variables. These factors include temperature, air humidity, time of day, the direction and speed of the wind, the presence of human activity, and the type of ventilation used in enclosed spaces (Kim *et al.*, 2010).

While it is uncommon for fungi to induce symptoms in humans, this can be attributed to the presence of immunity and other effective defence mechanisms, such as cell-mediated (T-dependent) immunity. However, in cases where the host's immune system is impaired, it might result in the uncontrolled proliferation of fungus and then lead to the development of an infection. Approximately 11% of infections observed in organ transplant patients, specifically in cases such as kidney transplants, can be attributed to fungal pathogens (Verma *et al.*, 2015).

Aspergillus and *Candida* species were found to be the cause of infections in 80% of solid organ transplant patients. In the last two decades, the number of weakened people who get invasive aspergillosis has steadily increased. This is a major problem that can be fatal. Exposure to fungi is a risk factor not just for people with weakened immune systems but also for healthy people who may develop a hypersensitivity to the fungal allergen. This hypersensitivity can lead to lung problems like asthma and allergic alveolitis. *Aspergillus fumigatus*, a saprophytic fungus, is commonly seen in diverse environmental settings and is known to regularly induce allergic reactions, including bronchopulmonary allergic aspergillosis. Numerous investigations have documented the potential emergence of respiratory diseases subsequent to hypersensitivity reactions to diverse fungal species, including *Penicillium*, *Cladosporium*, and *Rhizopus*. Multiple strains of *Aspergillus* and *Penicillium* appear to be significantly implicated in the development of asthma and allergic alveolitis (Shoham & Marr, 2012).

2.2: Nosocomial fungal infections

Nosocomial infections, which are also called "hospital-acquired infections", refer to infections that are acquired during a patient's hospital stay and were not present or in the incubation stage at the time of admission. Nosocomial infections are typically defined as infections that manifest more than 48 hours following a patient's admission to a healthcare facility (Sardi *et al.*, 2013).

Nosocomial fungal infections are important causes of mortality in patients who are admitted to healthcare facilities, particularly in populations with weakened immune systems. The main types of microorganisms involved are *Candida* spp., *Aspergillus* spp., *Mucor* sp., and *Fusarium* sp. Nosocomial fungal diseases will become more common in the coming decades because of the reasons behind them. The risk factors are due to the widespread use of invasive treatments like stem cell transplants, organ transplantation, chemotherapy, and immunosuppressive drugs, which weaken the immune system, which one of the risk factors. With the suggested infection control methods, immunocompromised hospital patients can avoid getting candidiasis from a catheter and also have less exposure to airborne *Aspergillus* spores. By teaching medical staff how to use medical equipment, many of these infections can be avoided without the need for high costs or modern equipment's. During times of severe immunosuppression, people who are likely to get invasive fungal illnesses should think about antifungal prophylaxis (Moazeni *et al.*, 2018).

In both intensive care units and neonatal intensive care units (ICUs) the predominant cause of fungal infections is attributed to yeasts belonging to the *Candida* genus, with *Candida albicans* being the most commonly seen species, accounting for approximately 80% of cases (Akeme Yamamoto *et al.*, 2012).

For instance, the rates of HAIs have exhibited considerable variation, with percentages ranging from 1% in selected regions of Europe and North America to over 40% in specific areas of Asia, Latin America, and Sub-Saharan Africa (Saxena & Mani, 2014).

According to a study done by Napoli *et al.*, (2012), the climate and other factors of hospitals play a significant role in the biological quality of their indoor air, and the quality of filtered air conditioning in hospitals is an effective means of reducing nosocomial infections. It has been reported that the High Efficiency Particulate Air

(HEPA) filtration system prevents invasive pulmonary aspergillosis in immunocompromised patients in isolation wards.

2.3: Major fungi present in hospital environments

2.3.1: *Aspergillus* spp.

The genus *Aspergillus* is classified as a phylum Ascomycota. This varied phylum was originally recognised by its sexual reproductive spore, the ascospore, which is found in cup fungi, morels, yeasts, and moulds (Lutzoni *et al.*, 2004). *Aspergillus* spp. are highly adaptable organisms that can grow on a wide variety of carbon and nitrogen sources, are quite thermotolerant (37–50 °C) because they have ribosomal biogenesis proteins, and are able to tolerate high osmotic pressure (Jacob Kizhakedathil *et al.*, 2017). *Aspergillus* species derive nutrition from decaying organic matter within the environment, and their reproductive process primarily occurs through asexual means, specifically by means of conidia (Latgé & Chamilos, 2019).

There are more than 24 *Aspergillus* species that can cause disease in humans, but *A. fumigatus*, followed by *A. terreus* and *A. flavus*, are the species that have been linked to the most infectious diseases (Gibbons & Rokas, 2013). Depending on the immunological condition of the host, aspergillosis can manifest as a variety of different symptoms. As a result, the consequences can range from being life-threatening, as shown in invasive pulmonary aspergillosis and invasive rhinosinusitis observed in highly immunocompromised individuals, to not being urgent, as seen in the case of small aspergillomas in immunocompetent individuals (Montone, 2016).

2.3.1.1: *Aspergillus fumigatus*

Aspergillus fumigatus is the predominant causative agent responsible for a substantial majority (60 to 90%) of reported infections. Infections induced by *Aspergillus* are frequently found in the lower respiratory tract, lungs, sinuses, and skin. Direct or hematogenous spread might have an impact on both the central nervous system (CNS) and cardiovascular system. *A. fumigatus* is the predominant causative agent of pulmonary aspergillosis (S. M. Rudramurthy *et al.*, 2019). When Toll-like receptors (TLR), especially TLR2 and TLR6, interact, airway epithelial cells consume and eliminate conidia with antimicrobial peptides. Alveolar macrophages complete the microbicidal effect by phagocytosing escaped conidia. Low neutrophil counts increase

the likelihood of invasive aspergillosis (IA), therefore neutrophils are also necessary for pathogen clearance (Humphrey *et al.*, 2016; Kaur *et al.*, 2017).

2.3.1.2: *Aspergillus flavus*

Aspergillus flavus is an opportunistic pathogen causing invasive and non-invasive aspergillosis in humans, *A. flavus* is responsible for around 10% of bronchopulmonary infections, with rhino-cerebral aspergillosis being the predominant manifestation. In the environment of healthcare facilities, outbreaks of *A. flavus* have been linked to infections affecting the skin, mucous membranes, and subcutaneous tissues (Vonberg & Gastmeier, 2006). *A. flavus* produces aflatoxin, which can cause acute hepatitis, hepatocellular carcinoma, and neutropenia in humans. *A. flavus* grow well at 37°C and 42°C, thermotolerance is considered key for *Aspergillus* pathogenicity in general.

2.3.1.3: *Aspergillus Niger*

Aspergillus niger is a widespread opportunistic pathogen found in numerous both indoor and outdoor environments. *A. niger* spores can be quickly aerosolized (Li *et al.*, 2019) and possess the capacity to be deposited within the bronchioles of the respiratory system of humans (White *et al.*, 2020). Infections attributed to *A. niger* have the potential to give rise to allergic bronchopulmonary aspergillosis (ABPA) or invasive aspergillosis, both of which can result in fatality among susceptible individual patients (Barac *et al.*, 2018).

2.3.1.4: *Aspergillus versicolor*

Aspergillus versicolor is a common fungus that has been linked to osteomyelitis, ocular disease, cutaneous infection, otomycosis, and onychomycosis. It is a common respiratory tract coloniser with uncommon occurrences of invasive pulmonary aspergillosis (IPA) (Charles *et al.*, 2011). Several species of *Aspergillus* have been seen to create metabolites, including mycotoxins such as (3-nitro propionic acid, aflatoxins, and ochratoxin). These metabolites have been reported to negatively affect the process of phagocytosis (Singh *et al.*, 2021).

2.3.1.5: *Aspergillus terreus*

Aspergillus terreus is a widespread soil saprophyte and the only species of the genus *Aspergillus* that forms globose, thick-walled hyaline cells termed accessory conidia or aleurioconidia (Balajee, 2009). The presence of accessory conidia in infected individuals' tissues strongly suggests *A. terreus* infection, According to (Deak *et al.*, 2009) it has been proposed that accessory conidia might have a function in the transmission of disease. Furthermore, new evidence has demonstrated that accessory conidia can lead to increased inflammatory responses in a model of pulmonary aspergillosis. The pathogen *A. terreus* is responsible for a spectrum of diseases, including aspergilloma, allergic bronchopulmonary aspergillosis, superficial infections , and invasive disease (Steinbach *et al.*, 2004).

2.3.1.6: *Aspergillus nidulans*

Aspergillus nidulans is an opportunistic fungal pathogen in patients with immunocompromised, and it is the most common infectious organism among patients with chronic granulomatous disease (CGD). Although infection with *A. nidulans* occurs in non-CGD patients. (Bastos *et al.*, 2020).

The primary route of infection of *A. nidulans* is via the inhalation of conidia (asexual spores). In immunocompetent individuals, inhaled conidia are rapidly cleared by pulmonary resident and recruited neutrophils and macrophages, together preventing the onset of infection. However, disturbances to the immune system may render an individual susceptible to infection by *A. nidulans* (Henriet *et al.*, 2012).

2.3.2: *Penicillium* sp.

The majority of *Penicillium* species are opportunistic infections. They are typically seen in people with weakened immune systems, and HIV patients are most frequently affected by them (Le *et al.*, 2010). The exclusive causative agent responsible for this disease is a thermally regulated dimorphic fungus known as *talaromyces marneffeii*. The inhalation of spores from the environment leads to the infection of human beings (Narayanasamy *et al.*, 2021). The disease has the potential to affect various anatomical systems, including the respiratory tract, skin, intestinal tract, bones, and joints, and can also exhibit systemic dissemination throughout the body. *Penicilliosis* has the potential to affect the respiratory system. There is a frequent occurrence of confusion between this condition and tuberculosis (TB) (Qiu *et al.*, 2019).

2.3.4: *Alternaria* sp.

The *Alternaria* genus encompasses a variety of melanized hyphomycetes species that are known to induce opportunistic infections in humans. The fungus known as *Alternaria* is commonly linked to the development of chronic allergic lung or sinus disease. However, *Alternaria* is being recognised more frequently as a causative agent of cutaneous and subcutaneous diseases, rhinosinusitis, and oculomycosis in individuals with impaired immune systems. This is particularly notable in individuals who have undergone solid-organ transplantation or who have haematological malignancies (NaPier & Redd, 2022).

2.3.5: *Chrysosporium* sp.

Chrysosporium are common saprobes in soil. A lot of them are keratinophilic fungi that dissolve shed keratin substrates. People can get infections of the skin and onychomycosis from *Chrysosporium* sp. *Chrysosporium* species have also been found in systemic infections in people who have had a bone marrow donation or who have a disease called chronic granulomatous disease (CGD). The high fatality rate associated with systemic *Chrysosporium* infections is notable. These fungi are occasionally seen in the diagnostic laboratory, primarily as contamination in cutaneous or respiratory specimens (Gopal *et al.*, 2020).

2.3.6: *Cladosporium* sp.

Cladosporium species are widely distributed, saprophytic, dematiaceous fungi, which are rarely implicated in opportunistic infections in humans and animals. *Cladosporium* is commonly encountered as one of the dominant airborne fungi (Ellis *et al.*, 2007). In most cases, allergic rhinitis may be linked back to *Cladosporium* (Sellart-Altisent *et al.*, 2007) or localized superficial or deep lesions (Sang *et al.*, 2012) but, rarely, can cause disseminated infections (Lalueza *et al.*, 2011).

2.3.7: *Blastomyces dermatitidis*

Blastomyces dermatitidis causes blastomycosis. Spores of the fungus cause a lung infection that might be asymptomatic or life-threatening, like acute respiratory distress syndrome (Miceli & Krishnamurthy, 2023). After inhalation, conidia enter the lower respiratory tract. Some people have asymptomatic infections because bronchopulmonary mononuclear cells phagocytize and neutrophils and macrophages destroy conidia. When *Blastomyces dermatitidis* becomes yeast, its thick wall resists phagocytosis and destruction, causing symptomatic lung infection. The skin is the most prevalent site of extrapulmonary diseases in 25% to 30% of individuals after hematogenous spread from the lungs (Lohrenz *et al.*, 2018).

2.3.8: *Mucor* sp.

Mucormycosis, which used to be called zygomycosis, is an uncommon, invasive, and deadly fungal disease that has become more common in the last few years (Baldin & Ibrahim, 2017). After candidiasis and aspergillosis, this disease is the third most prevalent invasive fungal infection in patients of haematological and allogeneic stem cell transplants. An elderly population, the increased number of patients with immune deficiencies, and the most recent COVID-19 pandemic all contribute to an increase in the number of people who are at increased risk for Mucorales infections (García-Carnero & Mora-Montes, 2022).

Lungs, rhinocerebral spaces, sinuses, soft tissue, skin, gastrointestinal tract, and circulation are all possible infection sites. While spore inhalation is the most prevalent mode of transmission. The disease can also be contracted cutaneously or gastrointestinally. This potentially fatal condition primarily affects immunodeficient, diabetic, and all other forms of immunocompromised people who have a primary bacterial or fungal infection (Choi *et al.*, 2019).

2.3.9: *Candida* spp.

Candida is derived from the Latin word "candid" which means white. Fungal diseases, especially candidemia, are becoming more common in hospitals, which raises the risk of morbidity and mortality (Delavy *et al.*, 2019). The term candidiasis or candidosis is used to refer to infections caused by *Candida* spp. Candidiasis includes a wide range of diseases affecting the skin, mucous membranes, and internal organs, which are caused by fungi belonging to the *Candida* genus. The term "invasive candidiasis" relates to infections in the bloodstream caused by *Candida* spp., commonly known as candidemia, as well as deep-seated diseases such as intra-abdominal abscesses and peritonitis (Pappas *et al.*, 2018).

The occurrence of invasive candidiasis has been seen to be on the rise, primarily due to the advancements in medical equipment within healthcare facilities (McCarty & Pappas, 2016). *Candida albicans*, *Candida glabrata*, *Candida tropicalis*, *Candida parapsilosis*, *Candida lusitanae*, and *Candida krusei* are the most common *Candida* spp. that cause human diseases (Kullberg & Arendrup, 2015). In certain parts of the world, a previously rare organism, *Candida auris*, has emerged as a major pathogen (Diekema *et al.*, 2012; Lockhart *et al.*, 2017).

Candida infections can be attributed to a variety of risk factors. These factors refer to the use of wide spectrum antibiotics, decreased immunity, malignancy, operation, diabetes, and prolonged periods of hospitalisation. The transmission of *Candida* spp. can occur by direct contact between hands, and subsequent survival on hands may remain for a duration of up to 45 minutes (Seneviratne *et al.*, 2008). Numerous habitats can support the growth of *Candida* spp. They are able to persist in a hospital environment for up to four months (Ha *et al.*, 2011).

Various virulence features, such as the ability to adhere to both living and non-living surfaces and the production of hydrolytic enzymes, contribute to the pathogenesis of *Candida* spp. Extracellular hydrolytic enzymes make it easier for the pathogen to adhere to the host tissue, invade it, and destroy it (Deorukhkar & Saini, 2015). The principal occurrence in *Candida* colonization and infection involves the process of adhesion to host cells (Silva *et al.*, 2012).

Approximately 50% of nosocomial infections can be attributed to the use of medical devices (Kojic & Darouiche, 2004). *Candida* spp. have the ability to develop biofilm on a wide range of medical equipment, including shunts, implants, stents,

catheters, endotracheal tubes, and pacemakers. The capacity to produce biofilms is a significant virulence determinant in the context of candidiasis (Deorukhkar & Saini, 2013). The creation of biofilms serves as a means of protection against host defence systems and is also associated with the development of resistance to drugs (Sardi *et al.*, 2013).

The yeast microorganism *C. albicans* is the predominant *Candida* spp. that commonly causes pathogenic infections in humans. *C. albicans* is the predominant species associated with onychomycosis, vulvovaginitis, and oral lesions. *C. krusei* is a prominent fungal pathogen known for its ability to induce invasive candidiasis, predominantly because to its inherent resistance to fluconazole (Gong *et al.*, 2018).

Candida lusitanae is a major opportunistic pathogen commonly found in individuals with impaired immune systems in healthcare settings. It is mainly obtained through the respiratory tract, urine, and blood (Deorukhkar & Saini, 2016).

C. parapsilosis is considered one of the most widespread species responsible for candidemia worldwide. Infections predominantly manifest in individuals who have been hospitalised in intensive care units (Lockhart *et al.*, 2008), and particularly in certain populations such as infants, transplant recipients, those with COVID-19, and cancer patients (Thomaz *et al.*, 2021).

2.3.10: *Naganishia albida* (*Cryptococcus albidus*)

Cryptococcus species, belonging to the basidiomycetous yeasts, are recognised as causative agents for many different types of diseases. Notably, *C. neoformans* and *C. gattii* are known as the predominant pathogenic species within this group (Hagen *et al.*, 2017). Infections caused by non-neoformans cryptococcal species such as *Papiliotrema laurentii* (also known as *C. laurentii*) and *Naganishia albida* have lately increased (Burnik *et al.*, 2007). *Naganishia albida* is a type of yeast that is sometimes found on the human skin, in soil, and in the air (Kano *et al.*, 2008). Several cases of *Naganishia albida* caused infections, including encephalitis, pneumonia, keratitis, and cutaneous and disseminated cryptococcosis, have been documented (Huang *et al.*, 2015).

Cryptococcus sp. pathogenicity factors include capsule formation against phagocytosis, laccase enzyme expression, and melanin synthesis. *Cryptococci* change

their cell wall integrity, avoid the immune system, and are less likely to respond to antifungal treatment when melanin produces up on their surfaces (Khawcharoenporn *et al.*, 2007).

2.3.11: *Rhodotorula* sp.

Rhodotorula is a prevalent yeast species that is widely distributed in several environmental habitats, including the atmosphere, soil, freshwater bodies, ocean, dairy products, and fruit juices. *Rhodotorula* species, belonging to the phylum Basidiomycota, have the ability to establish colonies in various organisms, including plants, humans, and other mammals. *Rhodotorula* is a genus that contains eight different species, three of which have been identified to be responsible for disease in humans: *R. mucilaginosa*, *R. glutinis*, and *R. minuta* (Wirth & Goldani, 2012).

In the past, *Rhodotorula* species were regarded as non-pathogenic; however, they have now been recognised as opportunistic pathogens capable of colonising and causing infections in individuals who are susceptible (Lunardi *et al.*, 2006). The majority of incidents of *Rhodotorula* fungemia infection are linked to the presence of central catheters in individuals diagnosed with hematologic malignancies (García-Suárez *et al.*, 2011). Localised infections in both immunocompetent and immunodeficient individuals have been documented, including prosthetic joint infections, meningitis, onychomycosis, endophthalmitis and peritonitis (Wirth & Goldani, 2012).

2.3.12: *Exophiala dermatitidis*

Exophiala is a taxonomic classification encompassing a variety of opportunistic black yeasts. This genus belongs to the category of Ascomycota and is characterised by its melanized, thermophilic, dimorphic, dematiaceous, and hyphal growth fungus (Babič *et al.*, 2018).

Infections caused by *Exophiala* are often long-lasting and difficult to get eliminate, and the number of cases keeps going up in both people with weak immune systems and people with strong immune systems. The most common symptoms of an *Exophiala* infection are skin infections, and the most common type of deep infection is

pulmonary infection caused by inhalation. The invasive disease can start with a skin or subcutaneous infection and spread to internal organs (Usuda *et al.*, 2021).

2.4 Molecular assay

In the past few years, there has been an increase of DNA-based methodologies aimed at enhancing the diagnostic capabilities for mycotic infections and the detection of pathogenic fungi. Molecular diagnostic methods for fungi encompass various techniques that detect and identify fungal species based on their genetic material. Some prominent methods include: Polymerase Chain Reaction (PCR), DNA Sequencing, DNA microarray and microarray, fluorescence *in situ* hybridization, loop-mediated isothermal amplification (LAMP) and Matrix-Assisted Laser Desorption/Ionization Time-of-Flight Mass Spectrometry (MALDI-TOF MS). These methods offer rapid, sensitive, and accurate means of identifying fungal pathogens, aiding in clinical diagnosis, epidemiological studies, and environmental monitoring in healthcare settings (Aslam *et al.*, 2017).

The polymerase chain reaction (PCR) amplifies single copies of fungal DNA millions of times over and allows for the detection of small amounts of target DNA in clinical specimens. The methods of polymerase chain reaction (PCR) exhibit considerable promise due to their basic simplicity, specificity, and sensitivity. PCR-based methodologies have made significant contributions to the identification of fungal species derived from clinical specimens. PCR technology includes multiplex PCR, nested PCR, real-time PCR and reverse transcriptase (RT)-PCR and Digital PCR each of these PCR techniques has its strengths and specific applications in fungal diagnostics (Allothman, 2012).

PCR has the ability to make a quick diagnosis, which could lead to an earlier diagnosis and a quicker start of antifungal therapy, if needed. Internal Transcribe Spacer (ITS) is the most frequently sequenced DNA region in fungal molecular ecology (Peay *et al.*, 2008) and has been recommended as the universal fungal barcode sequence. It has typically been most useful for molecular systematics at the species level, and even

within species (e.g., to identify geographic races). Because of its higher degree of variation than other genetic regions of rDNA (for small- and large-subunit rRNA), variation among individual rDNA repeats can sometimes be observed within both the internal transcribed spacer (ITS) and intergenic spacer (IGS) regions (Schoch *et al.*, 2012).

PCR primers are short pieces of single-stranded DNA, usually around 20 nucleotides in length. Two primers are used in each PCR reaction, and they are designed so that they flank the target region (region that should be copied). The PCR primers "ITS1" and "ITS4" were the first to be widely used for studying fungal Internal Transcribe Spacer (ITS). These primers target the ITS1 and ITS2 sequences, which are highly variable and located between the Small Subunit-coding sequence (SSU) and the Large Subunit-coding sequence (LSU) of the ribosomal operon. The primers employed in this study exhibit a broad amplification capacity for several fungal targets, proving to be effective in the analysis of DNA extracted from individual organisms (Martin & Rygiewicz, 2005).

In general, for *Candida* spp. identification, a single-step polymerase chain reaction (PCR) methodology is employed, utilising a set of universal primers that specifically target the conserved areas of 18S, 5.8S, and 28S rRNA. The resulting PCR fragments are further analysed using agarose gel electrophoresis to estimate their lengths, and the accuracy of these fragment lengths is further verified through DNA sequencing. The ITS1-ITS4 primer pair was used to amplify the intervening 5.8S rDNA and also the adjacent ITS1 and ITS2 regions, while the ITS3-ITS4 primer pair was used to amplify a large portion of the 5.8S rDNA and the adjacent ITS2 region (Barbedo *et al.*, 2016). The exact identification of *Candida* spp. has important due to the varying antifungal susceptibility patterns observed towards these species. Additionally, an accurate identification aids in the appropriate selection of antifungal medications for both preventive and therapeutic purposes (Nejad *et al.*, 2020).

2.5: Antifungal agents

In comparison to antibacterial medications, there are fewer antifungal agents available for clinical use. They result from the high number of drug targets in fungi and the similarity of their eukaryotic cells to those of humans. In the genomic era, however, the search for novel cell targets has increased significantly. Patients undergoing long-

term antifungal prophylaxis or treatment exhibit favourable circumstances for antifungal resistance (Brion *et al.*, 2007). The most common antifungals used to treat candidiasis, and how they work, are outlined here.

2.5.1: Polyenes

Polyenes are a category of naturally occurring chemicals characterised by the presence of a heterocyclic amphipathic molecule, which exhibits both hydrophilic charged properties on one side and hydrophobic uncharged properties on the other side. The mechanism of action involves the specific targeting of ergosterol within the fungal membrane. This is achieved through the insertion of the substance into the lipid bilayers, thereby generating pores which affect the integrity of the plasma membrane. Consequently, this disruption facilitates the diffusion of small molecules across the membrane, ultimately leading to the death of the fungal cell (Pemán *et al.*, 2009). This class includes nystatin and amphotericin B. Nystatin is most commonly used topically and serves a significant role in the prevention of oral and systemic candidiasis in full-term and preterm neonates, infants, and immunocompromised patients (Howell *et al.*, 2009). Amphotericin B is still thought to be the most effective medication to treat most fungal diseases, mainly severe invasive infections (Lacerda & Oliveira, 2013).

2.5.2: Echinocandins

Echinocandins are currently the first choice treatment for invasive *Candida* diseases (Pappas *et al.*, 2016). These chemicals have been shown to be fungicidal against the yeasts. Caspofungin, micafungin, and anidulafungin are the three medications that are now accessible for usage in clinical. Echinocandins inhibit 1,3--glucan synthase, which causes disruption in the process of cell wall production (Cannon *et al.*, 2009). The enzyme under consideration is accountable for the synthesis of 1,3- β -glucan, an important component that enhances the structural integrity of the cell wall in both *C. albicans* and *S. cerevisiae*. The absence of the glucan components within the cellular wall leads to osmotic instability, eventually resulting in the lysis of the cell (Ripeau *et al.*, 2002).

2.5.3: Allylamines

Two of the most common allylamines used to treat fungal infections are terbinafine and naftifine. This group of antifungal chemicals is fungicidal (effective

against dermatophytes) and fungistatic (effective against *Candida albicans*) (Cannon *et al.*, 2009). Allylamines exert their inhibitory effects on the formation of ergosterol through a mechanism that is independent on cytochrome P-450 enzymes. This inhibition occurs by through the process of binding to squalene epoxidase (Erg1p), leading to the intracellular accumulation of squalene in large quantities. Because of this process results in heightened membrane permeability, disruption of cellular structure, and finally leads cellular death (Minnebruggen *et al.*, 2010).

2.5.4: Azole

Azole antifungal drugs exhibit fungistatic properties against *Candida* species (Robbins *et al.*, 2011). Various drugs belonging to this particular class, such as fluconazole (FLU), itraconazole (ITR), voriconazole (VRC), and posaconazole (POS), are frequently used for the treatment of mycoses. Heterocyclic synthetic chemicals have been identified as inhibitors of the fungal cytochrome P450 14 α -lanosterol demethylase, which is encoded by the ERG11 gene (CYP51). This enzyme plays a crucial role in the final stage of ergosterol production. The inhibition of this particular enzyme leads to a reduction in the ergosterol content inside the cell membrane, as well as an accumulation of toxic methylation compounds. As a result, the normal functioning of the fungal cell membrane is disrupted, resulting in the suppression of growth and, in certain cases, cell death (Xiao *et al.*, 2004).

2.5.5: Fluorinated pyrimidine analogues

Flucytosine, also known as (5-fluorocytosine or 5-FC), is a pyrimidine cytosine derivative that is fluorinated. It is frequently used in the treatment of candidiasis (Barker & Rogers, 2006). The mechanism of action involves the enzymatic conversion of cytosine to 5-fluorouracil by cytosine deaminase. This converted compound is then integrated into both DNA and RNA, leading to the inhibition of cellular activity and division (Pemán *et al.*, 2009).

2.6: Nanotechnology

Nanotechnology has revolutionised practically in every part of human life, and its potential uses in agriculture, health, cosmetics, electronics, and textiles have recently gained momentum. Because of their high surface-to-volume ratio, their surface reactivity is substantially enhanced, which causes outstanding antibacterial, antifungal,

catalytic, and wound healing characteristics not found in their bulk equivalent (Marimuthu *et al.*, 2020).

Nanotechnology has been effectively employed to design new methods for delivering drugs using nanoparticles (NPs), which have contributed to precision medicine currently. Advancements in nanoparticle design have assured that NPs can overcome heterogeneous delivery barriers and intelligently enhance efficacy (Mitchell *et al.*, 2021). Nanoparticles (NPs) are categorised according to their morphology, dimensions, and characteristics. The primary classifications include metallic, ceramic, polymeric, and fullerene NPs, with sizes including from 1 to 100 nm (Khan *et al.*, 2019).

NPs have similarities in size to macromolecules found inside the human body and use existing cellular machinery to carry out their intended function. Due to high effectiveness delivery that provides therapeutic potential in minimal dosage, supports prolonged drug release, and modifies drug distribution and clearance, NPs have also successfully aided in minimising drug toxicity and side effects. Although the precise method of action of nanoparticles is unknown, it may be reliant on the following factors: composition, surface modifications, inherent nanoparticle characteristics, nanoparticle concentration, and the fungal genus (Bamrungsap *et al.*, 2012).

2.6.1: Zinc Oxide Nanoparticles

Zinc, recognised as a crucial trace element, is widely distributed across many bodily tissues, which includes the brain, muscles, bones, skin, and other organs. Zinc, being a fundamental constituent of numerous enzyme systems, actively participates in the metabolic processes of the human body. It assumes vital functions in the formation of proteins and nucleic acids, as well as in hematopoiesis and neurogenesis (Kołodziejczak-Radzimska & Jesionowski, 2014).

The small size of nano-ZnO particles makes it easier for the body to take in zinc. nano-ZnO is often added to food to make it taste better. Also, the US Food and Drug Administration (FDA) says that ZnO is "GRAS" (generally recognised as safe) (Rasmussen *et al.*, 2010).

Due to their unique characteristics, zinc oxide nanoparticles (ZnO NPs) have garnered increased interest in the field of biological applications. In contrast to other

metal oxide nanoparticles, zinc oxide nanoparticles (ZnO NPs) possess advantageous biomedical properties due to their relatively low cost and reduced toxicity. Consequently, they have demonstrated remarkable potential in several biomedical applications, including anticancer therapies, drug delivery systems, antimicrobial agents, diabetic treatment, anti-inflammatory actions, wound healing, and bioimaging techniques (Zhang & Xiong, 2015).

The toxicity mechanisms exhibited by ZnO nanoparticles (NPs) against fungus are primarily influenced by factors such as the size, shape, and concentration of the ZnO NPs, as well as the specific type of media used. In general, it can be observed that a reduction in particle size is associated with an increase in the ratio of surface area to volume. This phenomenon, in turn, results in increasing antifungal efficacy (Reddy *et al.*, 2007).

The physical interaction between zinc oxide nanoparticles (ZnO NPs) and the fungal cell wall results in the disruption of the cell wall's structural integrity. This disruption triggers an excessive generation of reactive oxygen species (ROS) within the fungal cells, including hydroxyl groups, superoxide anion radicals, and hydrogen peroxide. The accumulation of these ROS can ultimately induce cell death. The formation of reactive oxygen species (ROS) exhibits a direct correlation with the extent of surface area of the organism that is exposed to zinc oxide nanoparticles (ZnO NPs). Furthermore, numerous studies have also demonstrated that the antimicrobial activity of ZnO nanoparticles (NPs) operates in a dose-dependent manner. This implies that as the concentration of ZnO NPs increases, the antimicrobial effectiveness also increases (Djearmane *et al.*, 2020; Karimiyan *et al.*, 2015).

2.6.2: Iron-oxide Nanoparticle

Iron is an essential microelement that is required for the proper functioning of a variety of different systems found in biological processes. The prevalence of iron and the physiological roles it plays raise questions about the capacity of iron compounds in the same quantities to suppress the growth of microorganisms while simultaneously having a beneficial effect on mammalian cells (Gudkov *et al.*, 2021). Nanoparticle (NP)-based drug delivery systems have been shown to enhance absorption of drugs in patients, facilitate drug accumulation at the target location, promote rapidly drug

distribution, and ultimately improve therapeutic efficacy while reducing the toxic effects of drugs (Gontero *et al.*, 2017).

Iron-oxide nanoparticles (IONPs) are well recognised as highly adaptable and safe nanomaterials, so determining as non-toxic agents (Dissanayake *et al.*, 2015). Iron oxide nanoparticles (IONPs) are composed of maghemite (γ -Fe₂O₃) and/or magnetite (Fe₃O₄) particles. The diameter of these nanoparticles varies between 1 and 100 nm. Iron oxide nanoparticles (IONPs) are extensively utilised in many medical applications according to their magnetic and biological characteristics, as well as their low cost. The significant uses of iron oxide nanoparticles (IONPs) includes diagnostic magnetic resonance imaging (MRI), medication delivery, gene therapy, biosensing, protein separation, thermal therapy (Wu *et al.*, 2015). The fungicidal effects of iron oxide nanoparticles are attributed to their ability to generate reactive oxygen species (ROS). The efficacy of these substances stems from their chemical composition and subsequent release of metal ions (Ezealigo *et al.*, 2021).

Chapter Three

Materials & Methods

3. MATERIALS AND METHODS

3.1: Materials

3.1.1: Equipment and Laboratory Instruments

(Table 3-1) Lists of all tools and devices that have been used in the study.

Instruments and Equipment's	Manufacturer	Country
Incubator	Memmert	Germany
Refrigerator	Vestel	USA
centrifuge	Hettieh zentrifugen	Germany
Sensitive electronic balance	AND	Japan
Light microscope	Leica	China
Vortex mixer	Vortex 2 Genic	USA
Autoclave	HICLAVG	Japan
Distiller	GFL	Germany
Thermocycler (PCR)	BIO-RAD	USA
Nanodrop spectrophotometer	Nanovue Plus	UK
Electrophoresis	Consort	Bel Glum
Disposable petri dishes	Biozek	China
Micro pipette (0.5-10)	Eppendroph	Germany
Plate 96 well	Sorfa	China
Eppendorf tubes	Kirgen	China
Loop	Himedia	India
Slide and covers	Superstar	India
Ultrasonic	G.heinemann	Germany
Water bath	GFL	Germany
Flask	ISOLAB	Germany

Sterile cotton swabs	Biozek	Netherlands
Gloves	Top Glove Sdn. Bhd.	Malaysia
UV - Transilluminator	CYNGENE	UK
Screw cap bottles	Sorfa	China
Parafilm	BEMIS	USA
X-Ray diffraction	Panalytical	UK
SEM	QUANTA 450	USA

3.1.2: Chemical substances

Table (3-2) Chemical substances used in the study and their origin

Material	Company	Country
Glycerol	Biosolve	France
Agarose	Gene Direx	USA
McFarland standard	BioMérieux	France
Ethanol 99%	Scharlab S.L.	Spain
Dimethyl sulphoxide DMSO	Sigma	USA
Chloramphenicol	Wave pharmaceuticals Ltd.	India
Ethidium bromide	Sinnagen	Iran
Lactophenol Cotton blue stain	Chem-Lab NV	Belgium
Alcohol	Cedrah beaty	Jordan
TBE buffer 5 X	ADDBIO	Korea
Ladder 100 bp	Gene Direx	USA
Nuclease free water	Inn-otrain-diagnostik	Germany
Fluconazole	Sigma	USA
Taq master mix	ADDBIO	Korea

3.1.3: Media

Table (3-3) The culture media used in the study and their origin

Media Name	Company	Country
Sabouraud Dextrose Agar	Himedia	India
Sabouraud Dextrose Broth	Himedia	India
Potato Dextrose Agar	Himedia	India
Potato Dextrose Broth	Himedia	India

3.1.4: Diagnostic Kit

Table (3-4) Diagnostic Kit used in the study and their origin

Kit	Company	Country
Vitek2 Compact System ID-yist Kit	Biommerieux	(U.S.A.)

3.2: Methods

3.2.1: Sterilization

3.2.1.1: moist heat sterilization

The sterilization process is the most commonly used procedure for sterilizing solutions, equipment, and media using a (autoclave) sterilizer at 121°C and 15 lb/in² pressure during 15 minutes (Rashed *et al.*, 2020).

3.2.1.2: Dry heat sterilization

In this way of sterilization, glassware and materials that couldn't get wet were sterilized using dry heat. Dry heat sterilization required higher temperatures in an electric oven, typically at a temperature of 160°C, and longer exposure times, usually for 1 hour or more (Rogers, 2012).

3.2.1.3: Sterilization by filtration

The liquid and heat-affected solutions were sterilized using microfilters with a diameter of 0.22 µm. This filtration method ensured the removal of microorganisms, guaranteeing the sterility of the liquids and solutions (Rajniak *et al.*, 2008).

3.2.2 Preparation of culture media

Several culture media were used for isolation, identification and preservation of fungi. They were prepared according to the manufacturer's instructions.

3.2.2.1: Sabouraud Dextrose Agar (SDA)

This medium was used for the cultivation of fungi. It was prepared by dissolving 65 g of the powder of medium in 1000 ml of distilled water, then shake to mix completely and to make sure that the powder mixes with the distilled water and put it on the water bath for one minute. Then sterilize in an autoclave at a temperature of 121 °C and under a pressure of 15 pounds / inch² for 15 minutes and left to it cool down a before pouring it into the dishes, the temperature was approximately 45°C, then the antibiotic Chloramphenicol was added at a rate of 0.5 g per liter to prevent the growth of bacteria. The mixture was shaking a slightly to mix with the solution. Then it is poured into dishes and let to solidify.

3.2.2.2: Sabouraud Dextrose Broth (SDB)

This medium was prepared by dissolving 30 g of the powdered medium in a quantity of distilled water by shaking well, then the volume become 1000 ml and then placed it in an autoclave for 15 minutes at 121 °C and under a pressure of 15 pounds / inch². The prepared medium was poured in to tubes.

3.2.2.3: Potato Dextrose Agar (PDA)

The medium was prepared according to the producing company's instructions by dissolving 39 g of the medium powder in 1000 ml of distilled water. It was stirred well to mix thoroughly and then sterilized in an autoclave at a temperature of 121°C, under a pressure of 15 pounds/inch² for 15 minutes. Afterward, it was allowed to cool down a bit, and before pouring it into the dishes, its temperature was ensured to be approximately 45°C. Additionally, Chloramphenicol, at an amount of 0.5 g per liter, was added to prevent the growth of contaminants. The medium was left for 28 hours to ensure that there were no contaminants before being used for growing mycelium.

3.2.2.4: Potato Dextrose Broth (PDB)

The medium was prepared by dissolving 24 g of the powdered medium in a quantity of distilled water and shaking it well. Then, the volume was adjusted to 1000 ml and placed in the autoclave for 15 minutes at a temperature of 121°C and under a pressure of 15 pounds/inch². Afterward, it was implanted into a tube.

3.2.3: Isolation and Identification of Fungi

3.2.3.1: Air Sampling

The current study was conducted in the Koya hospitals for a period of November 2021 to March 2022. Five different hospitals and healthcare facilities in Koya city were chosen for this study, these included: Shahid Doctor Khalid Hospital, Shahid Handren Health Center, Haji Qadr Health Center, Bawaji Health Center and Shahid Doctor Kawa and Dental Center. A total of 225 air samples were taken from different wards of these hospitals by open plate method (passive sampling method). Two different types of media were used to cultivate fungi which are: Sabouraud dextrose agar (SDA) media and Potato dextrose agar with 0.5g/L of Chloramphenicol to suppress growth of bacteria. These petri dishes containing media were placed at the height of about 1.5 m above the ground then left it open in the morning after cleaning and disinfecting for 20 minutes to collect fungal particles according to Souza *et al.*, (2019). All the plates were kept on nearly clean areas on top of tables to capture the air-borne microorganisms in breathing zone. After plate collection, they were sealed and labeled properly then sent to a laboratory for examination. The plates were incubated at a temperature of 37°C for 24 hours to check and record the growth of yeast, and the incubation continued for 7 days to monitor the growth of mold. Different colonies were sub-cultured on SDA medium until a pure colony was obtained (Sivagnanasundaram *et al.*, 2019). Fungal colonies were counted and distinguished from each other on the basis of morphology and microscopic features.

3.2.3.2: Morphological examination of fungal colonies

After the appearance of growth on SDA, morphology of each colony was noted in color, size, margin, shape, and elevation on the culture medium (Kidd *et al.*, 2022).

3.2.3.3: Microscopical examination

The examination was done by taking a portion of the growing colony on a clean glass slide with a drop of lactophenol stain and lactophenol blue was fixed by heat and covered with the cover slip of the slide, then it was placed under the light microscope and examined at 40x magnification to observe the shape of cells for yeasts and the

shape of threads and present of conidia with their size, shape and structure (Chopra *et al.*, 2020a). Additionally, the yeast isolates were tested with Gram staining in order to observe their response to staining, as well as their morphology and budding characteristics.

3.2.4: Biochemical test for Yeast:

3.2.4.1: Germ tube test

Germ tube is a screening test, which is used to differentiate *C. albicans* from other yeasts (Matara *et al.*, 2017). The test was done as follow: 0.5 mL of human serum was transferred in a small tube. After that, using a bacteriological loop, 2-3 colonies of each yeast isolate were gently picked up and emulsified in the serum, and incubated at 37°C for 2-3 hours. After that a drop of the serum transfer to a slide covered with coverslip, then it was examined microscopically under low (40x) and at high (100x) power objectives. Yeast cells produced tube like extensions were considered positive.

3.2.4.2: Diagnostic testing with the Vitek2 Compact System

Fungal isolates were subjected to identification by VITEK 2 compact system. According to the instruction that were provided by the company, a sufficient amount of suspected *C. albicans* colonies were transferred to a glass tube containing 3 milliliters of sterile saline (sodium chloride inhalation solution 0.45%) to measure and adjust turbidity that represent fungal cells number per-milliliter which must be equal to (1.8-2.2) in MacFarland tube. Then measurable samples were entered to VITEK 2 compact system machine and this is done by transferring fungal suspension with (1.8-2.2) McFarland (Densi CHEK plus) to cassette by negative pressure. Then cassette was incubated to complete biochemical reaction within 18 hours. Interpretation of results were performed according to VITEK 2 compact system special software to identify fungal species and strains.

3.2.5: Maintenance of Isolates

3.2.5.1: Short term preservation

The isolates were preserved by growing them on special screw cap tube contain 20 ml of SDA for 2-7 days at 37°C. The isolates were kept in the refrigerator for two months. The cultures were renewed every two months (Gudlaugsson *et al.*, 2003; Nakasone *et al.*, 2004).

3.2.5.2: Long term preservation

To preserve the isolates for a long time, the fungi were grown in a SDB and PDB at 37°C for 2-7 days, then 1 ml of the culture was transferred to a sterile tube mixed well with 1 ml of sterile glycerol at a concentration of 15%, then kept at -20 °C for 12 to 18 months (Gudlaugsson *et al.*, 2003).

3.2.6: Molecular identification

3.2.6.1: Fungal DNA Extraction

The extraction of fungal genomic DNA from fungal isolates was performed using the colony PCR method. Colony PCR for fungal genomic DNA extraction involves directly using fungal colonies as the DNA template for PCR amplification, bypassing the traditional genomic DNA extraction process. 2-3 fresh *candida* spp. colonies grown on SDA agar plates are chosen. The selected colonies are transferred into 40 µl of double-distilled water. This step aims to suspend the fungal material in the water, allowing for the release of cellular components, including DNA.

The suspension containing the fungal colonies and water is then placed in incubation at high temperature 95°C for 20 minutes. This step is crucial as it helps in breaking down the fungal cell walls and membranes, releasing the genomic DNA into the solution. After the incubation, the suspension is centrifuged at a speed of 12,000 rpm for 2 minutes. Centrifugation helps to separate the cellular debris and any insoluble

material from the DNA-containing supernatant, which should be used as the template. A small volume 3µl of the supernatant, which contains released DNA, is directly used as the template for the PCR reaction according (Shekhany, 2021).

Advantages of colony PCR for fungal genomic DNA extraction include: time-saving, requires minimal material for PCR, simplifies the process by eliminating DNA extraction steps.

3.2.6.2: Estimation of extracted DNA

In order to identify the DNA that was obtained from fungal samples, a device called a Nanodrop spectrophotometer (NanoVue plus, UK) was used. This device detects and quantifies the concentration of nuclear DNA and RNA (ng/L), and it evaluated the purity of the DNA at absorbance of 260/280 nm as following steps:

- 1- After operating the device, then opening up the Nanodrop software, the application (Nucleic acid, DNA) was chosen.
- 2- The measurement pedestals was cleaned by a dry wipe for several times. Then carefully pipetted 1µl of ddH₂O and placed onto the surface pedestals for blank the system and then the ddH₂O was cleaned from the surface for measuring samples.
- 3- The Nanodrop sampling arm was lowered pressed ok after placing 1µl DNA sample, and then the instrument pedestals cleaned again to measure the next samples.
- 4- The purity of the samples was determined; the extracted DNA is considered pure when the absorbance ratio is (1.8).

3.2.6.3: PCR Reaction mixture

The ITS region was amplified by performing a PCR amplification reaction in a final quantity of 40 ul. The reaction component listed in the table (3-5).

Table (3-5) PCR reaction mixture of 40 ul

Component	Volume/ ul
Taq Master (2x conc.)	20 ul
Forward primer(10pmol)	2 ul
Reverse primer (10pmol)	2 ul
nuclease-free water	12 ul
DNA template	4 ul
Total volume	40 ul

After that PCR reaction mix components mentioned in the above table were put into 0.2 ml PCR tube, then all the tubes were transferred in to Exispin centrifuge vortex at 3000 rpm for three minutes and then placed in PCR Thermocycler.

3.2.6.4: PCR Thermocycler Conditions

PCR thermocycler conditions can vary depending on the specific requirements of the amplification reaction, the target DNA, primers, and the DNA polymerase used. The PCR thermocycler conditions with typical temperature ranges and times for each step was shown in table (3-6).

Table (3-6) Conditions PCR Thermocycler.

PCR Step	Temperature	Time	Repeat cycle
Initial denaturation	95°C	5 min.	1
Denaturation	95°C	30 sec.	35
Annealing	57°C	30 sec.	
Extension	72°C	40 sec.	
Final extension	72°C	5 min.	1
Hold	4 °C	Forever	

3.2.6.5: DNA primers

The primer sets of 18S rRNA genes and Internal Transcribed Spacer (ITS) regions are universal primers for amplicon sequencing fungal diversity studies. In the present study, the ITS1 and ITS4 primers were used to amplify the 5.8S rDNA gene was shown in table (3-7).

Table (3-7) Primer sequences used for molecular identification

Name of the primer	Sequence	References
ITS1(F)	TCCGTAGGTGAACCTGCGG	(White <i>et al.</i> , 1990)
ITS4 (R)	TCCTCCGCTTATTGATATGC	(White <i>et al.</i> , 1990)

3.2.6.6: PCR product analysis

The PCR products were analyzed by agarose gel electrophoresis method as following:

1-To prepare agarose gel, 1 gm of agarose powder was added with 100 ml of 1xTBE buffer. The mixture was heated in a microwave until the solution became transparent and free of any visible particles. Following that, the solution was allowed to cool down to 50 to 60 °C.

2-Then 3 ul of ethidium bromide stain was added into agarose solution

3- The agarose solution was poured into the tray after fixing the comb to generate wells and allowed to solidify at room temperature; after that, the comb was removed gently from the gel.

4- The gel tray was properly positioned into the electrophoresis tank, and a sufficient amount of 1XTBE buffer was poured to completely fill the tank and cover the gel.

5- 3ul of DNA marker (ladder) was put in the first well, followed by 3ul of PCR products in each well, and then an electric current of 80 V was run for 1h.

6- The results were visualized by using UV -Trans illuminator.

3.2.6.7: Fragment sizes of ITS1-ITS4 PCR products for *Candida* spp.

The size of different bands of PCR product was shown in table (3-8).

Table (3-8) Expected fragment length of amplification the ITS region.

Species	Fragment size found by PCR with ITS1-ITS4 primers
<i>C. albicans</i>	535 bp
<i>C. parapsilosis</i>	520 bp
<i>C. krusei</i>	510 bp
<i>C. glabrata</i>	871 bp
<i>C.lusitaniae</i>	375 bp

3.2.6.8: Sequencing of PCR amplicons

Nucleic acids Sequencing of PCR amplicons and the resolved PCR amplicons were commercially sequenced from forward directions, following to instruction manuals of the sequencing company (Macrogen Inc. Geumchen, Seoul, South Korea).

The NCBI BLAST analysis is used to identify homologous sequences and look for mutations. Eventually, the fungal isolates were deposited in the NCBI-Genbank database to get Genbank accession numbers.

3.2.7: Preparation and determination of Characterization of ZnO-NPs and IONPs.

ZnO-NPs and IONPs powders were purchased from US Research Nanomaterials, Inc (Houston, TX USA). The development of fluconazole powder was carried out by Pfizer, which afterwards purchased it from Sigma-Aldrich. The characterization of ZnO-NPs and IONPs was conducted using scanning electron microscopy (SEM) and X-ray diffraction (XRD) techniques. The scanning electron microscopy (SEM) images provided visual evidence of the shapes and size of the zinc oxide nanoparticles (ZnO-NPs) and iron oxide nanoparticles (IONPs). X-ray diffraction (XRD) was employed to determine the crystalline structure of the nanoparticles. A stock solution of nanoparticles is prepared by mixing 100 mg of the nanoparticles with 10 ml of deionized water, resulting in a concentration of 10 mg/ml. This mixture is then

exposed to ultrasonic bath and further homogenized using a vortex mixer. Subsequently, the stock solution is diluted to various concentrations (1000, 500, 250, 125, and 62.5 µg/ml) using the dilution equation ($N_1V_1 = N_2V_2$).

3.2.7.1: X-ray diffraction

The crystalline size and purity of ecofriendly produced Iron and Zinc oxide nanoparticles were determined employing an X-ray diffractometer and Cu-K α radiation with a wavelength of $\lambda=1.541 \text{ \AA}$. Scherrer's calculation was used to determine the crystalline size of the produced nanoparticles as follows $D \cong 0.9\lambda \div \beta \cos \theta$ Where D denotes the crystal size, λ denotes the X-ray wavelength, θ is the Bragg angle in radians, and β is the peak's full width at half maximum in radians (Wasly, 2018).

3.2.7.2: Field emission scanning electron microscopy (FESEM)

Field emission scanning electron microscopy was used to study the morphology of produced Iron and Zinc oxide nanoparticles utilizing a TM-1000, Hitachi, Japan. A thin film of the sample was formed by merely dropping a very small amount onto a carbon-coated copper grid. The film on the SEM grid was then allowed to dry for 5 minutes by placing it under a mercury lamp. The prepared sample is mounted onto a sample holder and inserted into the SEM chamber. Signals are collected by detectors and translated into an image displayed on a monitor, showing surface morphology, topography, and compositional information.

3.2.7.3: Susceptibility Tests

The assessment of antifungal activity was conducted using two methods: the agar well diffusion method, which measured inhibition diameters, and the microbroth dilution method, which determined the minimum inhibitory concentrations (MICs).

3.2.7.4: Agar well diffusion method

The determination of the antifungal activity of zinc oxide and iron oxide nanoparticles was conducted using the agar well diffusion method described in the study of (Arsène *et al.*, 2023). The present study aimed to assess the inhibitory effects of different concentrations of Zinc Oxide Nanoparticles (ZnONPs), Iron Oxide

Nanoparticles (IONPs), and Fluconazole (FLU) on *Candida* species. The concentrations examined included 1000, 500, 250, 125 and 62.5 µg/ml. The SDA was used as a growth medium for fungi. 20 ml of medium was carefully transferred onto sterile Petri plates and thereafter left for 30 minutes to allow for solidification. A suspension with a concentration of 1.5×10^6 colony-forming units per-millilitre (CFU/ml) of each of the five *Candida* spp. was cultivated on a Sabouraud dextrose agar medium, with a turbidity equal to a 0.5 McFarland standard. A sample of the *Candida* species which was found in isolation, was collected using a cotton swab and afterwards spread onto the culture medium. Subsequently, a corkborer was used to produce 5mm wells within the Sabouraud dextrose agar medium. Different concentration of zinc oxide (ZnONPs), iron oxide (IONPs) nanoparticles, and fluconazole (FLU) were introduced into the wells. The addition of a well deionized water (DW) was added as a negative control. The plates were incubated at 37°C for 24 hours. Following the incubation period, the measurements of the zones of inhibition for ZnONPs, IONPs, and FLU against each *Candida* species were recorded. The experiments were performed in triplicates for accuracy, during which the average widths of the zones of inhibition for ZnONPs, IONPs, and FLU were measured and recorded. The antifungal activity was assessed by quantifying the zone of inhibition using a standardized scale.

3.2.7.5: Microdilution Method for MIC determination

The minimum inhibitory concentration (MIC) refers to the lowest concentration of an antifungal drug that effectively prevents the growth of fungi. The MICs of ZnONPs, IONPs, and FLC were found using the microbroth dilution method in sterile 96-well flat-bottom microplates. This method was described by Arsène *et al.*,(2023) without any alterations. In this study, a serial 2-fold dilution of ZnONPs, IONPs and FLU was conducted in sterile 96-well microplates using Sabouraud Dextrose Broth (SDB). A volume of 100 µL of broth was introduced into all the wells of the plates, followed by the addition of 100 µL of each ZnONP, IONP, and FLC (1,024 µg/mL) to the first well. Serial dilutions were conducted by transferring a volume of 100 µL of the solution. In each well of the test plate, a volume of 10 µL of fungal suspension was added, with the turbidity level of the suspension being similar to a 0.5 McFarland scale. Two wells were employed as the positive and negative controls. The positive control consisted of a medium containing 10 µL of fungal suspension, while the negative control consisted of

a medium containing an antifungal agent that showed no growth. Subsequently, the plates were properly sealed and incubated at 37°C for 24 hours. After incubation, the fungal growth was measured using a spectrophotometer at 630 nm. The minimum inhibitory concentration (MIC) was defined as the lowest concentration of the tested substance that effectively suppressed the observable growth of the fungus.

3.2.8: Data analysis

The statistical analysis software program (Special Package for Statistical Science SPSS version 26) was applied for processing of the data, percentage and frequency analysis of the data was performed.

Chapter Four

Results & Discussion

4. Results and Discussion

4.1: Isolation of airborne fungi

During the investigation time from November 2021 to March 2022, a total of 225 collected plates exposed in to five wards of each hospital environment, where 198 plates (88%) showed growth of 582 filamentous and yeast fungi colonies, while 27 plates (12%) were giving negative results. The fungal isolates belonged to 16 genera (Table 4-1). Filamentous fungi were found to be 352 (60.5%) colonies, where 230(39.5%) was yeast colonies. Among the recovered fungi, *Candida* spp. was the most dominant species with a total of 165 isolates (28.35 %) in air samples collected from the wards of hospitals. *Aspergillus* spp. also exhibited a high number of isolates in the indoor air samples represented by 147 isolates (25.26 %) followed by *Penicillium* sp. (48 isolates with 8.25% These airborne fungal species had been reported in several studies that used different isolation and identification procedures.

The distribution of fungal species in our study exhibited similarities to previous research. For instance, Saleem *et al.*, (2017) demonstrated that the greatest fungal isolates in Azadi Teaching and Hevi Pediatric Hospitals were *Aspergillus* spp., indicating environmental contaminations. Additionally, *Candida* spp. was identified as the predominant yeast isolate.

According to our findings of the study, *Penicillium* sp. (which causes penicillioses) was the prevalent fungal genera with moderate percentage of 8.25% when compared to the remaining fungal genera. Our data align with those of Chopra *et al.*, (2020b) who reported the presence of *Penicillium* sp. (8.95%) in the air of a tertiary care hospital. Fungi of the genus *Penicillium* are common in most terrestrial habitats. Fungal infections developed by this fungi have become more common in recent years (Bassam Aboul-Nasr *et al.*, 2014). According to Abbasi & Samaei (2019), a wide range of clinical entities have been explained with allergic disorders and superficial mycoses becoming the most frequent. The role of *Penicillium* as a fungus that generates allergies and its prevalence in indoor air environments received considerable research attention nowadays. The study conducted by Sharpe *et al.*, (2015) highlights the correlation between the inhalation of fungal allergens produced by certain species in indoor air environments and the incidence of asthma.

According to the findings of our study, *Cladosporium* sp. with a percent of 2.23% found when compared to the remaining fungal isolates. Viegas *et al.*, (2011) and in line with what stated by Okten & Asan (2012) they found that *Cladosporium* sp. were the prevalent fungal genera with percentage 28,4% and 33.58% respectively. *Cladosporium* diseases include brain and skin lesions, brain abscesses associated with or without meningitis, as well as chromomycosis (Calumby *et al.*, 2019). While (Kiasat *et al.*, 2017) disagreed with our results who reported that was one of the most common type of mold. was *Cladosporium* sp. with a frequency of (35.3%).

The fungus known as *Alternaria* is widely distributed throughout the atmospheric air. The current study found that *Alternaria* sp. identified during the study, with a 3.44% frequency. In our study, *Alternaria* sp. had a lower concentrations of the spores than the study of (Chopra *et al.*, 2020b). Our result about the diagnosed *Alternaria* sp. is in similarity to what found by Demirel *et al.*, (2017) that detected *Alternaria* sp. with 6.22% in the air of hospital newborn units from Turkey.

In this study, we observed *Trichophyton Verrucosum* with the percentage of 1.03%. The results of this study, however, disagreed with those of Golah *et al.*, (2017) who found *Trichophyton* sp. (6%) isolated and identified the airborne pathogenic fungi from the hospitals environment at Dhamar governorate, Yemen. According to our findings, *Blastomyces dermatitidis* (which causes Blastomycosis) with percentage 3.61%. The fungus lives in the environment, Blastomycosis can be acquired through inhalation of airborne tiny fungus spores by individuals.

With regard to other genera of filamentous fungi *Curvularia* sp. presence with percentage of 6.19%. Similar to our results Kumar *et al.*, (2020)& Venceslau *et al.*, (2012) recorded that *Curvularia* sp. was isolated in low percentage of 12.5% and 5% in hospital environments. While the percentage of *Chrysosporium* sp. was 1.89%. The results are in agreement with that of (Golah *et al.*, 2017) who found *Chrysosporium* sp. with a percentage of 3%.

Table (4-1) Fungal genera isolated from the air of hospitals

Fungi genera	Number of colony	Percentage to isolates 582
<i>Aspergillus</i> spp.	147	25.26
<i>Penicillium</i> sp.	48	8.25
<i>Alternaria</i> sp.	20	3.44
<i>Cladosporium</i> sp.	13	2.23
<i>Blastomyces dermatitidis</i>	21	3.61
<i>Trichophyton verrucosum</i>	6	1.03
<i>Mucor</i> sp.	25	4.3
<i>Chrysosporium</i> sp.	11	1.89
<i>Curvularia</i> sp.	36	6.19
<i>Chaetomium</i> sp.	9	1.55
<i>Trichoderma</i> sp.	7	1.20
<i>Aureobasidium</i> sp.	9	1.55
<i>Candida</i> spp.	165	28.35
<i>Rhodotorula</i> sp.	21	3.61
<i>Cryptococcus</i> sp.	40	6.87
<i>Exophiala dermatitidis</i>	4	0.69
Total	582	100

4.1.1: Isolated Yeasts from the air of hospitals

In this study the results figure (4-2) has revealed that from 582 colonies of fungal isolate isolated 230 (39.52%) were colonies of yeast, 165 (71.74%) of them was *Candida* spp., *Rhodotorula* sp. 21(9.13%), *Cryptococcus* sp. 40 (17.39%) and *Exophiala dermatitidis* 4(1.74%). The confirmation of all isolates was conducted through using the methods of gram staining and germ tube test. Then, the identification process was carried out using the VITEK 2 Compact system (BiomeRieux, France) with the (ID-YST cards) which are specifically designed for the identification of yeast and yeast-like organisms.

According to our findings of *Rhodotorula* sp., the results of VITEK 2 Compact was *R. mucilaginosa* with a percentage of 9.13% when compared to the remaining yeasts isolated that were diagnosed from the air environment of hospitals.

This is in consistent with the results of Al-Bader *et al.*, (2018) who found frequency of isolated *Rhodotorula* sp. was 4.15% from five hospitals in Erbil city. According to the study by Lobato *et al.*, (2009) who found that isolating *Rhodotorula* sp. in about 32.69% of the ICU indoor air samples. While Viegas *et al.*, (2011) was found that regarding yeasts, *Rhodotorula* sp. was 45,2% identified in air of one Portuguese maternity hospitals.

According to our findings of *Cryptococcus* sp., the results of VITEK 2 Compact was *Cryptococcus albidus*, synonymous with *Naganishia albida* with a percentage of 17.39% when compared to the remaining yeasts. This pattern of results is consistent with the finding of Maldonado-Vega *et al.*, (2014) that *Cryptococcus albidus* account for 14% from air samples. However Viegas *et al.*, (2011) disagreed with our results and demonstrated *Cryptococcus neoformans* (3.2%) during the study.

According to our findings of black yeast *Exophiala* sp., showed the results of VITEK 2 Compact was *Exophiala dermatitidis* with low percentage of 1.74 % when compared to the remaining yeasts.

Table (4-2) Yeast species isolated from the air of hospitals

Yeast genera	N. of colony	Percentage to yeast Isolated	Percentage to fungal isolated
<i>Candida spp.</i>	165	71.74	28.35
<i>Rhodotorula sp.</i>	21	9.13	3.61
<i>Cryptococcus sp.</i>	40	17.39	6.87
<i>Exophiala sp.</i>	4	1.74	0.69
Total	230	100	39.52

4.1.2: Isolation of *Aspergillus* spp. from the air of hospitals

The current investigation revealed that *Aspergillus* spp. were the second most prevalent fungal isolates, accounting for a frequency of 25.26%. According to the data presented in Table (4-3), it is evident that among the several *Aspergillus* spp., *A. Fumigatus* exhibited the highest prevalence rate of 30.61% compared to the other isolated *Aspergillus* spp. (*A. flavus* 26.53%, *A. niger* 22.45 %, *A. terreus* 8.84%, *A. nidulantes* 6.80% and *A. versicolor* 4.76 %.).

Table (4-3) Colony number and percentage of *Aspergillus* spp. isolated from air of hospitals in koya.

<i>Aspergillus</i> spp.	N. of colony	Percentage to <i>Aspergillus</i> spp. isolated	Percentage to fungal isolated
<i>A. fumigatus</i>	45	30.61	7.73
<i>A. flavus</i>	39	26.53	6.70
<i>A. niger</i>	33	22.45	5.67
<i>A. terreus</i>	13	8.84	2.23
<i>A. nidulantes</i>	10	6.80	1.2
<i>A. versicolor</i>	7	4.76	1.20
Total	147	100	25.26

Based on the previous information about the distribution of *Aspergillus* isolates, it is demonstrated that *A. fumigatus* exhibited the highest prevalence among the identified species. *A. fumigatus* is a recognized pathogenic microorganism that has been associated with various health conditions, including allergic alveolitis, pulmonary aspergillosis, asthma and mycotoxicosis. In a study conducted by Tong *et al.*, (2017) an investigation was carried out to examine the distribution features of fungi within four different departments: the Respiratory Intensive Care Unit, Intensive Care Unit, Emergency Room, and Outpatient Department. At the species level, the frequency of *Aspergillus* fungi was found to be the highest, ranging from around 17% to 61%. Among the *Aspergillus* species, the prevalence of *A. fumigatus* was found to range from 34% to 50% throughout four departments.

The percentage of *Aspergillus* observed in our study was found to be higher in comparison with previous studies conducted by Kiasat *et al.*, (2017) in Iran, Gonçalves *et al.*, (2018) in Brazil, and Viegas *et al.*, (2011) in Portugal. These studies reported incidence rates of 15.1%, 13.92%, and 9.1%, respectively. In contrast, our findings demonstrated a lower prevalence compared to the studies conducted by Qudiesat *et al.*, (2009) in Jordan and Caggiano *et al.*, (2014) in Italy, which reported rates of 50.8% and 91.8%, respectively for *A. fumigatus*. Additionally, Jacob *et al.*, (2016) from Jordan recorded a prevalence of 20% for *A. niger*, indicating that it has a higher rate of isolation compared to other species of *Aspergillus*. The previously mentioned investigations demonstrate a diverse occurrence and provide further evidence of the variation in the predominance of *Aspergillus spp.* as the causative agent of Aspergillosis between various geographical areas.

4.1.3: Isolation of *Candida* spp. from the air of hospitals

The current study found that *Candida* is the most prevalent fungi identified in the hospital air, with a 28.35 % frequency. As seen in the table (4-4), among *Candida* spp. *Candida albicans* was the most common (37.58%) than the other isolated *Candida* species (*C.glabrata* 22.42%, *C.parapsilosis* 18.18%, *C.krusei* 12.73% and *C. lusitaniae* with 9.09%).

Table (4-4) Colony number and percentage of *Candida* spp. of airborne fungi in the hospitals

<i>Candida</i> spp.	N. of colony	Percentage to <i>Candida</i> spp. Isolated	Percentage to fungal isolated
<i>C. albicans</i>	62	37.58	10.65
<i>C. glabrata</i>	37	22.42	6.36
<i>C. parapsilosis</i>	30	18.18	5.15
<i>C. krusei</i>	21	12.73	3.61
<i>C. lusitaniae</i>	15	9.09	2.58
Total	165	100	28.35

Different distributions have been reported throughout the world. The study of Nnadi *et al.*, (2020a) found that *C. parapsilosis* as the most widespread *Candida* species in hospital environment, with an identification percentage of 31.25%. This was followed by *C. glabrata* and *C. krusei*, which had a prevalence of 28.13%. According to Nascimento *et al.*, (2023), *C. parapsilosis* exhibited the highest frequency of detection followed by other *Candida* species such as *C. glabrata*.

The results of current study agree with the results of Savastano *et al.*, (2016) in Brazil, in their study, they found a high occurrence of *C. albicans* followed by *C. glabrata* and *C. parapsilosis*. The high prevalence of *C. parapsilosis* is consistent with most studies that have shown a high occurrence of this species in hospital environment and in association with Catheter tips (Cordeiro *et al.*, 2010).

C. parapsilosis is a major cause of nosocomial infections that are becoming more common in hospital settings (Storti *et al.*, 2012). The formation of biofilms on prosthetic materials has been correlated to an increased virulence of *C. parapsilosis* (Branchini *et al.*, 1994). All *Candida* isolated and identified in this study were found to exhibit the ability to form biofilms.

4.1.4: Distribution of airborne fungi in each hospital

A total of 582 fungal colonies of opportunistic and pathogenic fungi were isolated from five hospitals and health care sector in Koya city. As depicted in Figure (4-1) these fungal isolates are distributed as: Shahid Doctor Khalid Hospital, Shahid Handren Health Center, Haji Qadr Health Center, Bawaji Health Center and Shahid Doctor Kawa & Dental Center represent with 186 (31.96%), 101 (17.35%), 90 (15.46%), 70 (12.03%) and 135(23.20%), respectively. The data generated from this study revealed that the highest fungal contamination 186 (31.96%) was founded from Shahid Doctor Khalid Hospital; whereas the lower fungal contamination 70 (12.03%) from Bawaji Health Center.

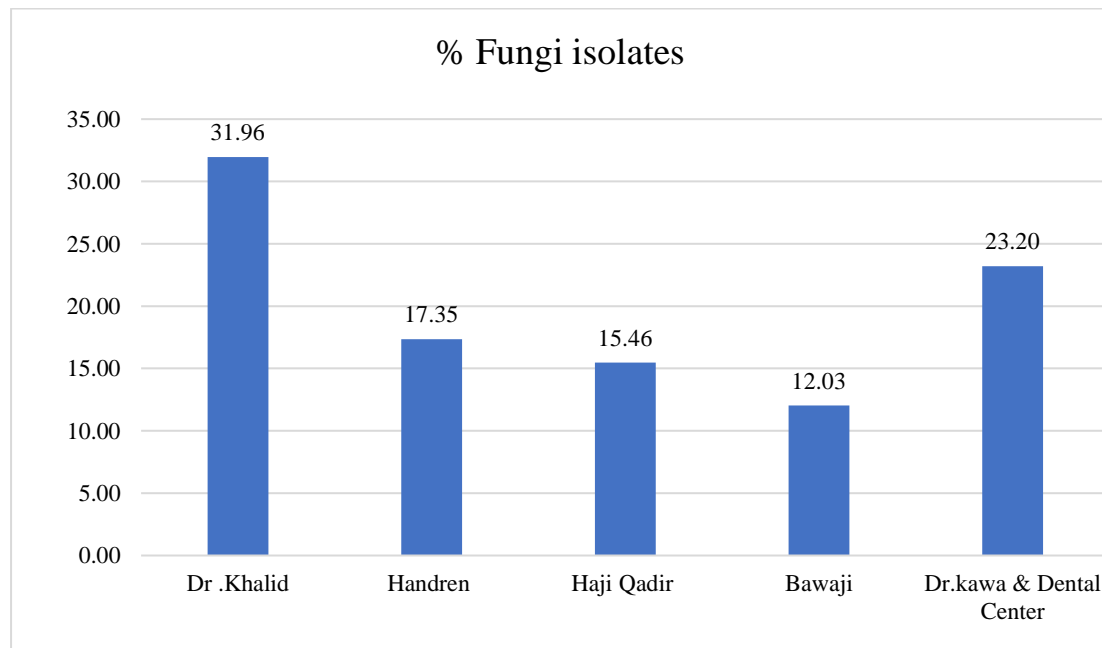


Figure (4-1) Distribution of air-borne fungi in five koya hospitals

4.3: Germ tube formation

A confirmation test for the presence of *Candida albicans* is the germ tube test. The germ tube test is a diagnostic test used in microbiology, specifically in the identification of *Candida albicans*, a yeast species. It's a simple and rapid test that helps differentiate *Candida albicans* from other non-*albicans* *Candida* species (Matare *et al.*, 2017).

Reynolds and Braude in 1956 were the first to describe germ tube formation; therefore, the germ tube test is referred to as the Reynolds-Braude Phenomenon. This is a quick way to distinguishing *C. albicans* from different *Candida* species. When *Candida* cells are incubated in serum at 37°C for 2-3 hours, *Candida albicans* generates germ tubes, which are short, slender, tube-like structures. The formation of germ tubes relates with greater production of proteins and ribonucleic acid production (Park & Lee, 2008).

Positive test: If germ tubes are observed, the test is positive, indicating the presence of *Candida albicans*. Negative test: The absence of germ tubes suggests the tested *Candida* isolate is likely a non-*albicans* species.

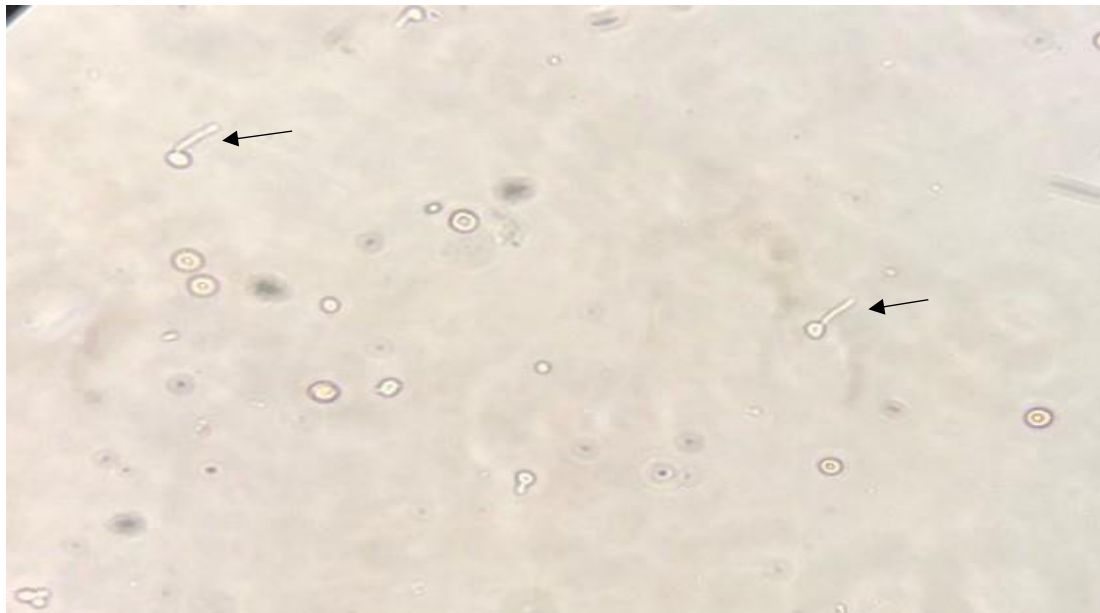


Figure (4-2) Germ tube of *C. albicans* grown on human serum at 37°C after 2hrs and half of incubation (40 X).

4.2: Identification of airborne fungi

4.2.1: *Aspergillus* spp.

4.2.1.1: Cultural and Microscopic Characteristics:

After a period of three to five days, the petri dishes containing Potato Dextrose Agar (PDA) and Sabouraud Dextrose Agar (SDA) exhibited visible colonies. These colonies displayed a cottony fluffy to velvety white mycelium growth, which was promptly covered with a substantial quantity of spores. These spores rapidly transitioned into various colors such as black, brown, orange, green, or yellow. Size and growth rate, generally fast-growing fungi, covering a significant area on agar plates. The colour on the reverse side of the colony can be different from the top surface and may provide additional diagnostic information.

A lactophenol cotton blue stain was used to look at the fungus isolate under a microscope and figure out what kind of fungus it was. *Aspergillus* species typically produce conidiophores (stalk-like structures) that bear conidia (asexual spores). Conidia are typically spherical, oval, or flask-shaped. The conidial heads, stipes, color, and length, the shape of the vesicles, and the size, shape, and roughness of the conidia were used to identify the fungus under a microscope. *Aspergillus* species exhibit septate hyphae (having cross-walls or septa) under microscopic examination.

The measurement of the colony after 7 days, the color of the spores, mycelia, exudates, and the reverse position, and the shape and texture of the colony were also used to identify the fungus (Diba *et al.*, 2007). A reference guide (Carmen , 2017; Kidd *et al.*, 2022) was to evaluate their morphological characteristics which include those (macroscopic and microscopic). For the purpose of being able to make the most accurate estimate as to their species, we identified each of the following:

4.2.1.2: *Aspergillus Niger*

The macroscopic examination of *Aspergillus niger* indicates that its growth initially appears white, but undergoes a transition to a black coloration after a few days, due to the production of dark pigments, turning green to black (olive-black or dark brown) in appearance, followed by the production of conidial spores. The colony surface is usually powdery or velvety in texture.

Aspergillus niger's mycelial, or thread-like, hyphae are clear and separated by a septum when seen under a microscope. Heads were biserial and the phialides are born on brown metulae that often have septate. Conidia are spherical or oval-shaped spores produced on the phialides in chains and consist of rough walls. Conidia are typically dark-colored, giving rise to the characteristic dark appearance of *A. niger* colonies (Figure 4-3).

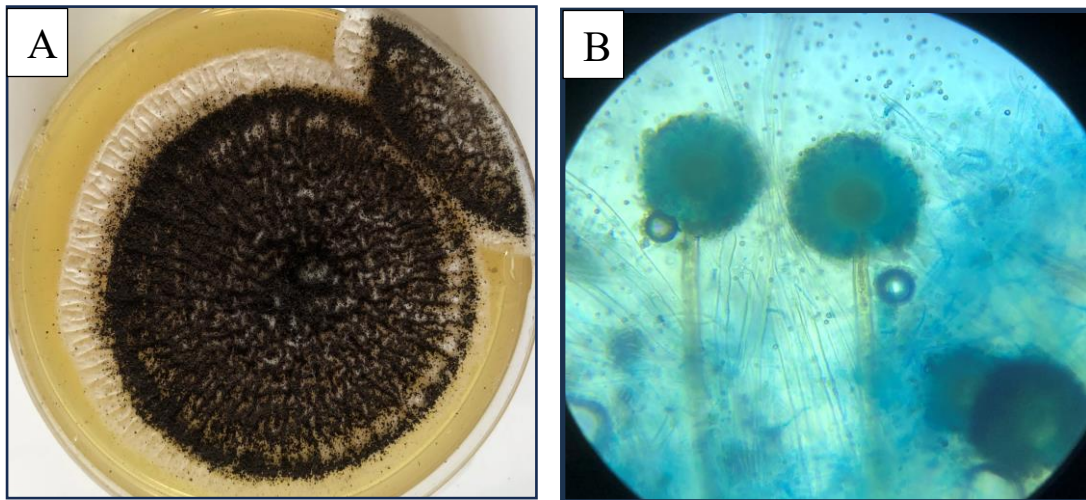


Figure (4-3) (A) *A. niger* Culture on SDA at 37°C for 5 days, and (B) microscopic morphology of conidiophores and conidia of *A. niger* colony mounted with LPCB stain magnify at 40x.

4.2.1.3: *Aspergillus flavus*

On culture media, Initially, colonies are usually white or yellow in color, becoming more yellow-green or olive-green with age. The colony surface is typically velvety or powdery in texture. The growth pattern may vary from initially circular to becoming more irregular with time.

The microscopic features of *A. flavus* showed the conidiophores are long, slender, and terminate in a vesicle. The conidiophores were rough and had thick walls that were not colored and didn't have any branches. Phialides produce conidia, forming chains or heads of spores.

The conidia were spherical to sub globose spores produced on the phialides in chains, they had thin walls and a rough surface. Conidia are typically greenish-yellow to yellow in color. Conidia and vesicles often display characteristic greenish-yellow to yellow pigmentation, contributing to colony coloration and aiding in species identification (Figure 4-4).

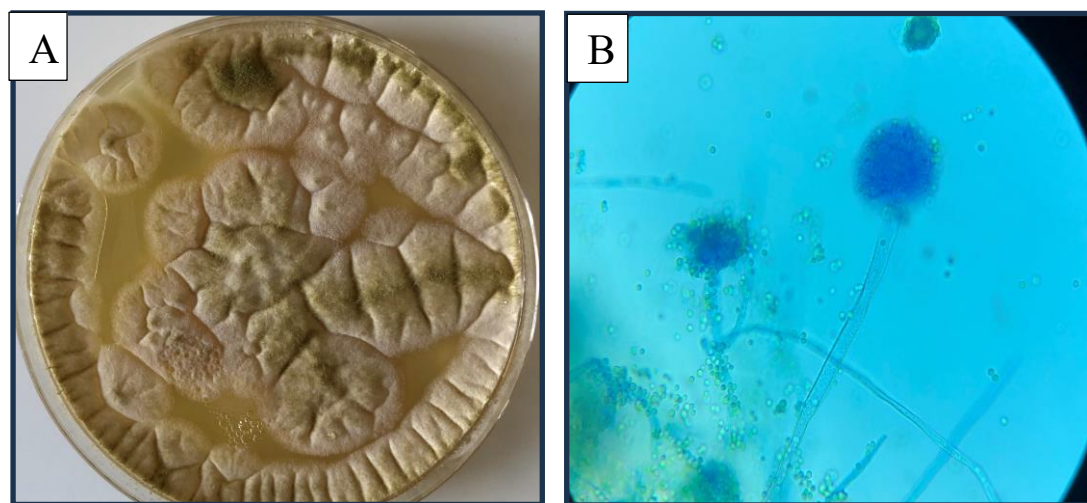


Figure (4-4) (A) *A. flavus* culture on SDA at 37°C for 5 days, and (B) microscopic morphology of conidiophores and conidia of *A. flavus* colony mounted with LPCB stain magnify at 40x.

4.2.1.4: *Aspergillus fumigatus*

The colonies feature of *A. fumigatus* on culture media are initially white, turning to shades of blue-green, gray-green, or olive-green with age. The colony surface is typically powdery or wooly in texture.

The microscopic characteristics observed in the sample consisted of conidiophores are typically long, slender, and terminate in a vesicle. Spherical to sub globose spores produced on the phialides in chains, flask-shaped vesicles with phialides covering approximately 50% to 75% of the vesicle.

Conidia and conidiophores are typically hyaline (colorless), visible in cluster and globose conidia exhibiting a finely rough texture and a simple green color (Figure 4-5).

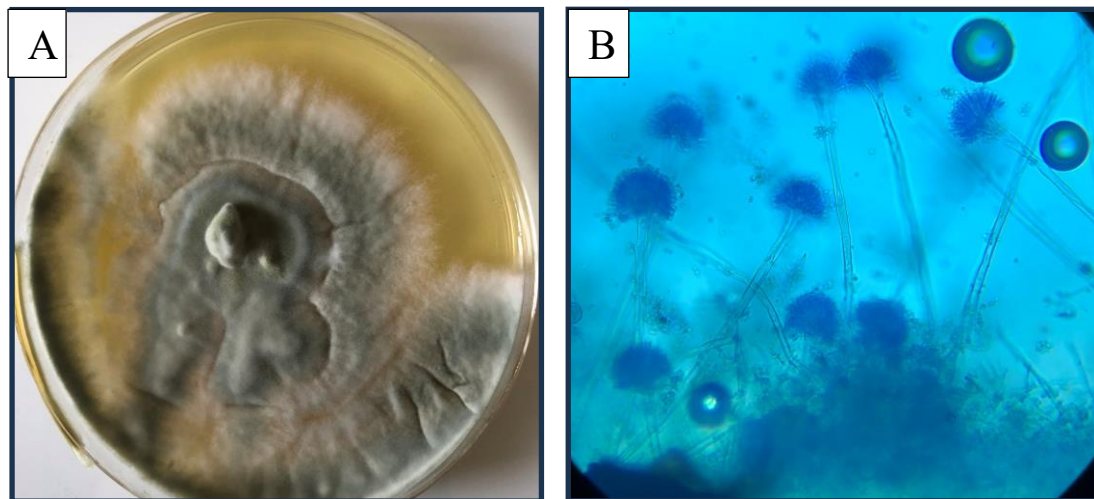


Figure (4-5) (A) *A. fumigatus* culture on SDA at 37°C for 5 days, and (B) microscopic morphology of conidiophores and conidia of *A. fumigatus* colony mounted with LPCB stain magnify at 40x.

4.2.1.5: *Aspergillus terreus*

The growth of *A. terreus* on culture media results in the formation of a colony that starts as white or yellowish, eventually turning to shades of yellow, brown, or tan, characterized by a surface coloration similar to cinnamon brown. The colony surface is often woolly, velvety, or granular in texture.

Conidiophores are typically long, slender, and terminate in a vesicle. Septate hyphae are characterized by cross-walls or septa dividing the hyphae into compartments. Conidia are spherical to elliptical spores produced on the phialides in chains. Biseriate phialides are shown to develop on the superior portion of vesicles, exhibiting chains of spherical conidia (Figure 4-6).

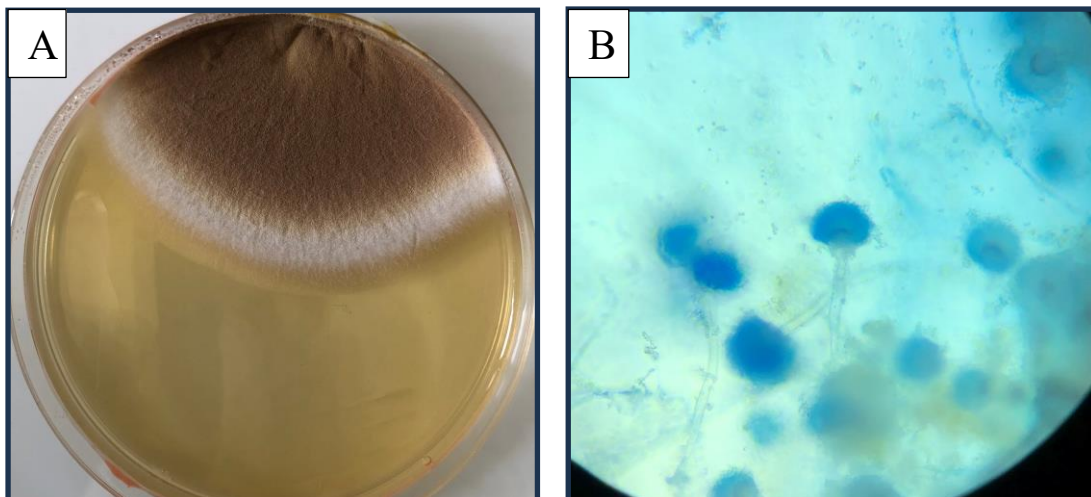


Figure (4-6) (A) *A. terreus* culture on SDA at 37°C for 5 days, and (B) microscopic morphology of conidiophores and conidia of *A. terreus* colony mounted with LPCB stain magnified at 40x.

4.2.1.6: *Aspergillus nidulans*

The initial appearance of *A. nidulans* on culture media typically start as white or cream-colored, eventually turning shades of blue-green, gray-green, or brown. ultimately turned entirely brown in matured cultures. Growth rate is slow to moderate in comparison with other clinically *Aspergillus* species.

Conidia are globose and rough. *A. nidulans* is a homothallic organism with the ability to generate the teleomorph, which represents its sexual stage. The ascomycetous teleomorph, *Emericella nidulans*, is known to generate globose cleistothecia with shades ranging from brown to black. These cleistothecia are surrounded by globose Hülle cells (Figure 4-7).

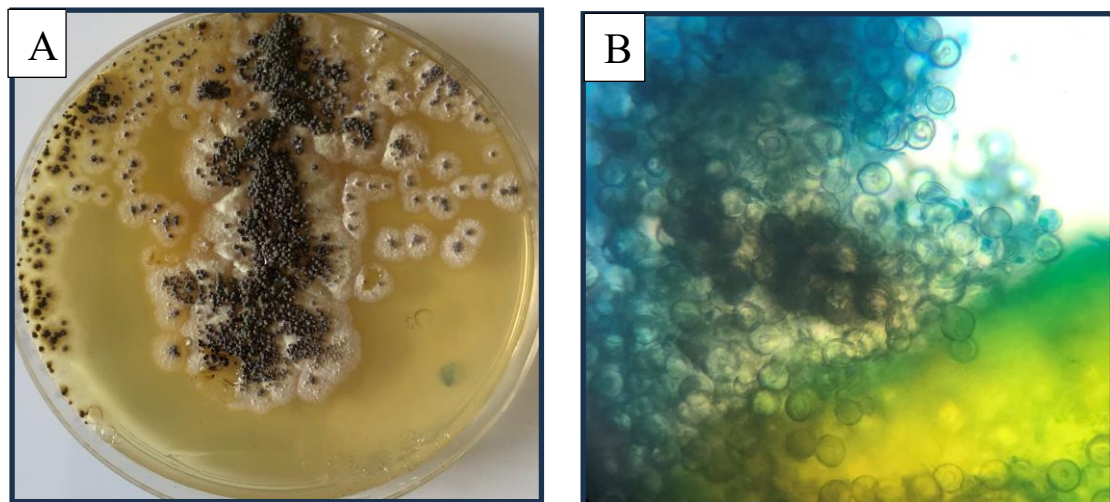


Figure (4-7) (A) *A. nidulans* culture on SDA at 37°C for 5 days, and (B) microscopic morphology of Hülle cells of *A. nidulans* colony mounted with LPCB stain magnify at 40x.

4.2.1.7: *Aspergillus versicolor*

A. versicolor on culture media the color of a colony typically starts as white or cream-colored, eventually turning shades of green, yellow, or olive-brown. Colonies are moderately fast-growing. The growth pattern may be initially circular but can become more irregular with time.

Hyphae have hyaline and septate parts that can be seen under a microscope. The conidiophores are long and hyaline to pale brown, smooth-walled and brittle. Biseriate phialides cover between half and all of vesicle and present round conidia in chains. Conidia are globose, and may be fine to distinctly roughened (Figure 4-8).

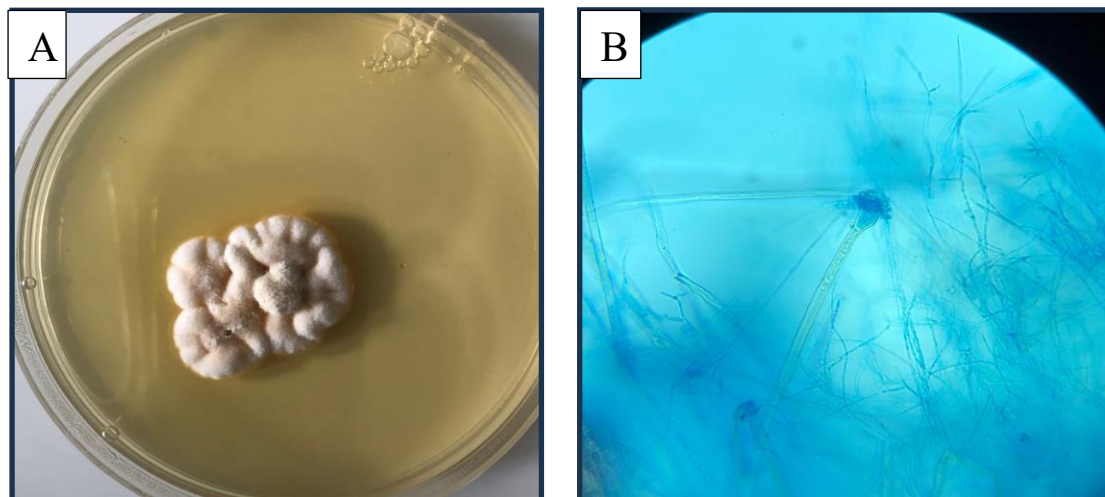


Figure (4-8) (A) *A. versicolor* culture on SDA at 37°C for 5 days, and (B) microscopic morphology of conidiophores and conidia of *A. versicolor* colony mounted with LPCB stain magnify at 40x.

4.2.2: *Alternaria* sp.

Alternaria species grow well on Potato Dextrose Agar (PDA). On culture media, colonies grow quickly and look like suede. Colonies typically exhibit various colors ranging from olive-green, brown, gray, to black. The colony surface is usually woolly, and suede-like in texture.

Under a microscope, conidiophores are tiny structures that can grow alone or in pairs and can be long or short. Conidia are darkly pigmented, multicellular, and multicelled spores produced on conidiophores.

Conidia are typically elongated, spindle-shaped, or oblong, with transverse and longitudinal septa, often with a short conical or cylindrical beak, pale brown, and have smooth walls. Conidia are usually dark-colored, ranging from brown, olive, to black, which contributes to the dark appearance of colonies (Figure 4-9).

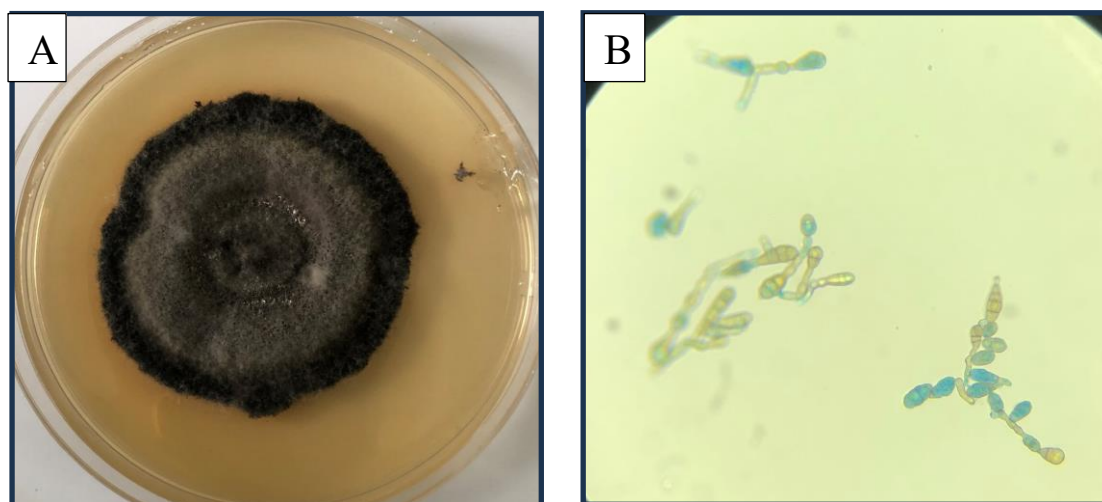


Figure (4-9) (A) *Alternaria* spp. culture on PDA at 37°C for 7 days, and (B) microscopic morphology of conidiophores and conidia of *Alternaria* spp. colony mounted with LPCB stain magnify at 40x.

4.2.3: *Mucor* sp.

The colonies on SDA and PDA were white or light-colored at first, but as sporangia developed, they turned brownish-grey to black. The colony surface is typically cottony, fluffy, or wooly in texture. Colonies are fast-growing and can cover a considerable area on agar plates.

Mucor species have broad, non-septate (aseptate), and ribbon-like hyphae, which are relatively wide compared to some other fungal species. *Mucor* species produce spores in structures called sporangia.

Sporangia are typically spherical or oval and dark brown to greyish black, have a raised base, can be seen protruding from hyphae. Sporangia release spores called sporangiospores when mature to facilitate reproduction and dispersal (Figure 4-10).

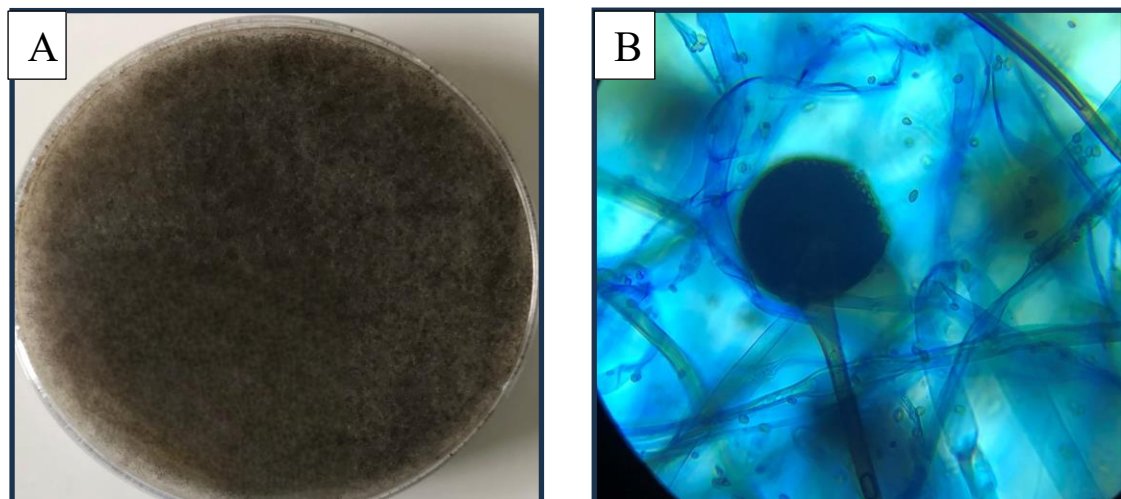


Figure (4-10) (A) *Mucor* spp. culture on PDA at 37°C for 5 days, and (B) microscopic morphology of *Mucor* spp. sporangiophores of *Mucor* spp. colony mounted with lactophenol cotton blue stain magnify at 40x.

4.2.4: *Trichophyton verrucosum*

Trichophyton verrucosum colonies was growing slowly. Colonies typically appear initially white, cream, or pale-colored, later becoming yellowish to tan. The colony surface can be cottony, fluffy colonies with a firm texture had formed. The growth pattern may be initially circular.

Trichophyton verrucosum produces both microconidia (smaller asexual spores) and macroconidia (larger asexual spores), both of them spherical to oval in shape. Microscopic examination allows the observation of the arrangement of conidia (microconidia and macroconidia) on hyphae, which grow together with the mycelium to produce hypha which appear like antlers (Guo et al., 2020) (Figure 4-11).

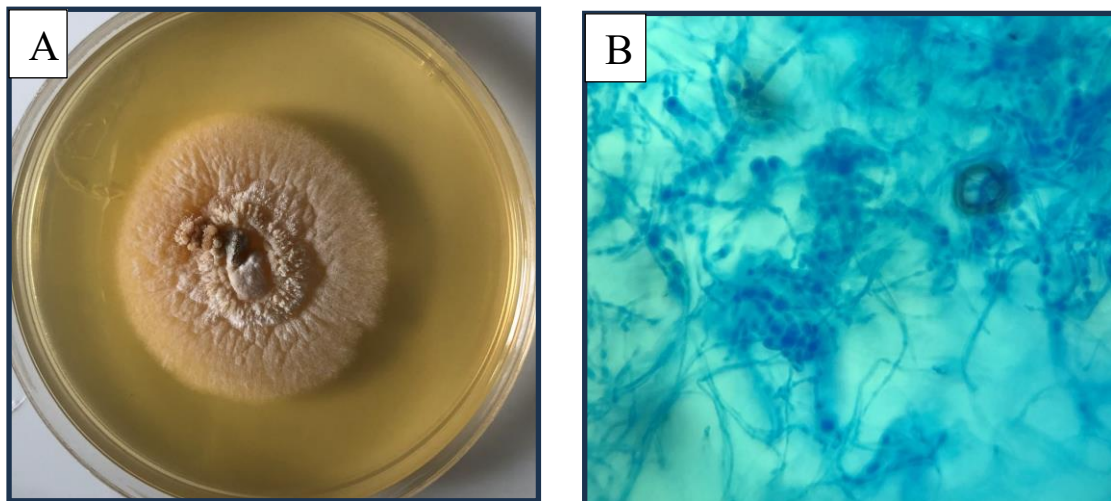


Figure (4-11) (A) *Trichophyton verrucosum* culture on SDA at 37°C for 10 days, and (B) microscopic morphology of macroconidia and microconidia of *Trichophyton verrucosum* colony mounted with LPCB stain magnify at 40x.

4.2.5: *Pencillium* sp.

Penicillium colonies are typically quickly developing, green or blue-green in color. The colony surface can range from velvety, powdery, or woolly in texture. The reverse side (underside) of the colony often shares the same color.

Penicillium species produce conidia (asexual spores) on structures called conidiophores. Conidia are typically spherical or oval and are produced in chains (forming a brush-like appearance). Phialides, which have a brush-like appearance, can be formed singularly, in clusters, or from branched metulae in *penicillium*. Both branches and metulae may be seen in the *penicillium*.

Conidia are usually hyaline (colorless) or can exhibit various colors, such as green, blue, or yellow-green, depending on the species and maturity (Figure 4-12).

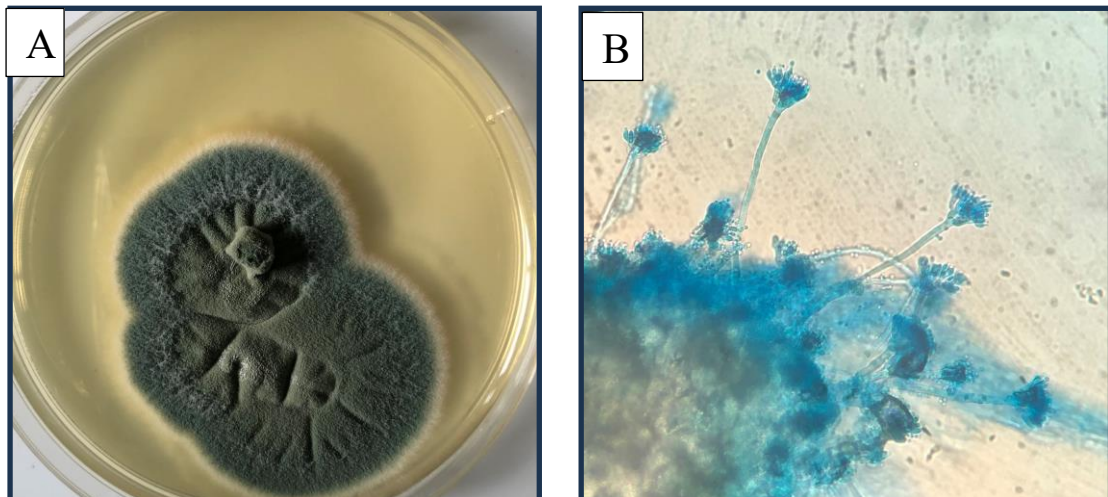


Figure (4-12) (A) *Penicillium* sp. culture on PDA at 37°C for 7 days, and (B) microscopic morphology of conidiophores and conidia of *Penicillium* sp. colony mounted with LPCB stain magnify at 40x.

4.2.6: *Curvularia* sp.

Colonies on PDA when they are young, they are white or light grey, when they become older, they are brown or have different shades of grey, mostly dark olivaceous grey, and have a cottony, raised or convex surface with papillate ridges.

You can see the septate, brown hyphae, brown conidiophores, and conidia. *Curvularia* species produce curved, cylindrical, or fusiform-shaped conidia, conidia are often septate (divided by septa) and are borne on conidiophores. Conidia are typically dark in color, ranging from brown, olive-green, to black.

Conidia and hyphae often show septations, with cross-walls or septa dividing them into compartments (Figure 4-13).

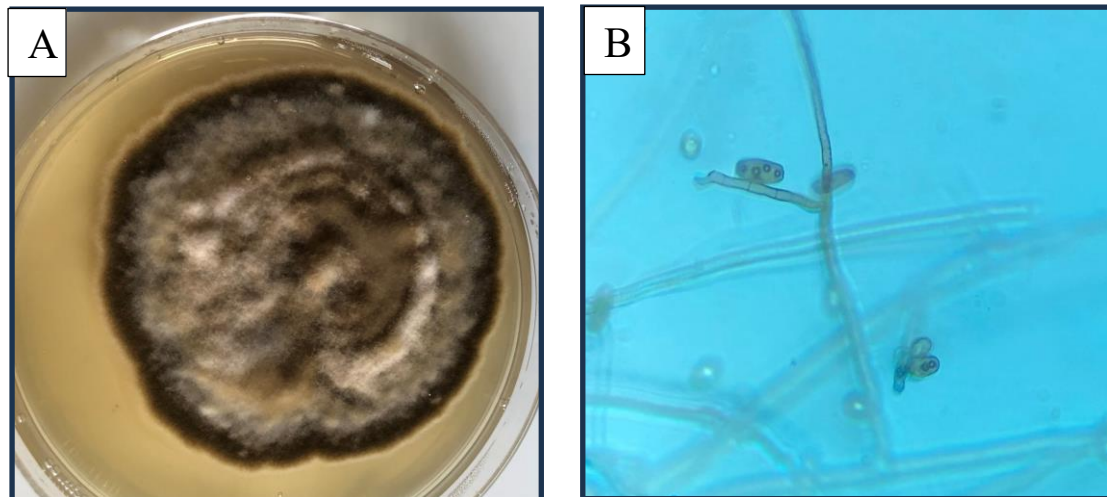


Figure (4-13) (A) *Curvularia* sp. culture on PDA at 37°C for 8 days, and (B) microscopic morphology of conidiophores of *Curvularia* sp. colony mounted with LPCB stain magnify at 40x.

4.2.7: *Blastomyces dermatitidis*

On SDA medium, *B. dermatitidis* typically begins to grow after 5 to 10 days. Colonies initially have a white to off-white appearance, but when aerial hyphae mature with time, they take on a grey or brown look. The colony surface was cottony, fluffy, or suede-like in texture.

The mold form of *B. dermatitidis* can be identified through microscopy by fragile, septate hyphae, more importantly for diagnosis, by oval or pyriform single-celled conidia and found individually at the tips of short or long conidiophores that resemble lollipops. Conidia might be observed as clusters or chains on conidiophores (Figure 4-14).

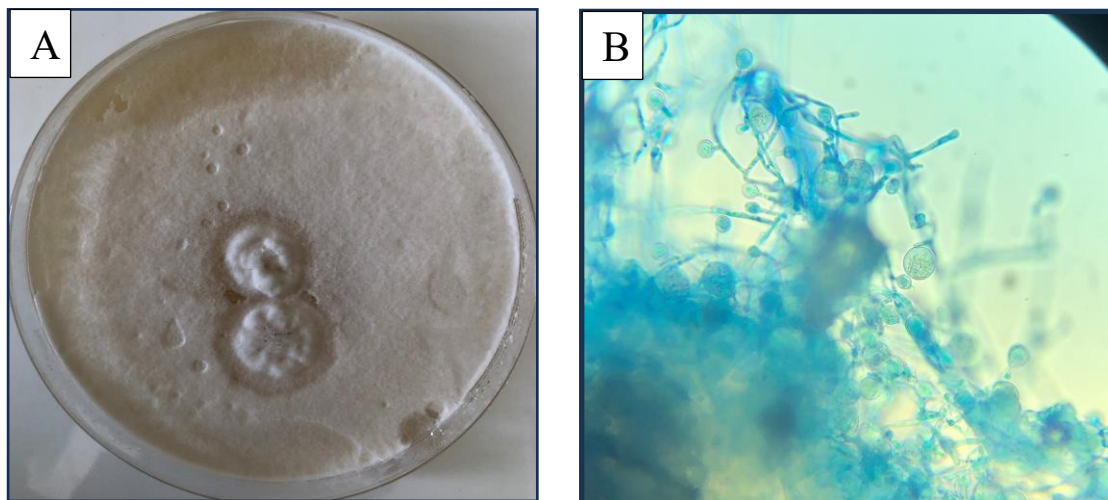


Figure (4-14) (A) *B. dermatitidis* culture on SDA at 37°C for 10 days, and (B) microscopic morphology of conidia of *B. dermatitidis* colony mounted with LPCB stain magnify at 40x.

4.2.8: *Chaetomium*

The colonies of *Chaetomium* have a quick growth rate and possess an initial appearance that is characterized by a cottony texture and a white coloration. As colonies reach maturity, they undergo a color transformation to a dark green, olive, or black coloration. The colony surface was cottony, wooly, or suede-like in texture

Under microscopic examination, the presence of septate hyphae, perithecia can be observed. *Chaetomium* species may produce distinctive perithecia (fruiting bodies) in culture, which are flask-shaped structures containing the asci (sac-like structures) that produce ascospores. The perithecia exhibit a large size, ranging from dark brown to black in color, their surface is covered with filamentous, hair-like appendages, which display a brown to black color. Ascospores are produced within the asci and are released for reproduction (Figure 4-15).

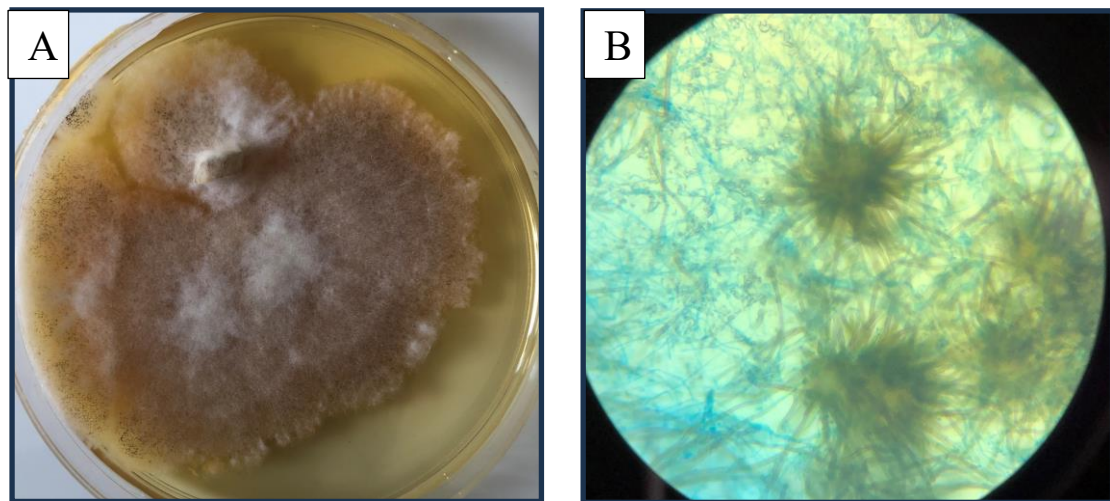


Figure (4-15) (A) *Chaetomium* culture on PDA at 37°C for 6 days, and (B) microscopic morphology of perithecia of *Chaetomium* colony mounted with LPCB stain magnify at 40x.

4.2.9: *Trichoderma*

Trichoderma colonies grow quickly and mature in 5 days. The colonies are fluffy and get compact over time. The color is white, and as the conidia form, it turns to blue-green or yellow-green.

Trichoderma isolates showed thick conidia, branched conidiophores, ampliform phialides, and slightly globose conidia under a microscope. Conidiophores can be observed as erect structures supporting conidia. Conidia are usually single-celled, smooth-walled. Phialides are structures that produce conidia and are often found at the tips of conidiophores (Figure 4-16).

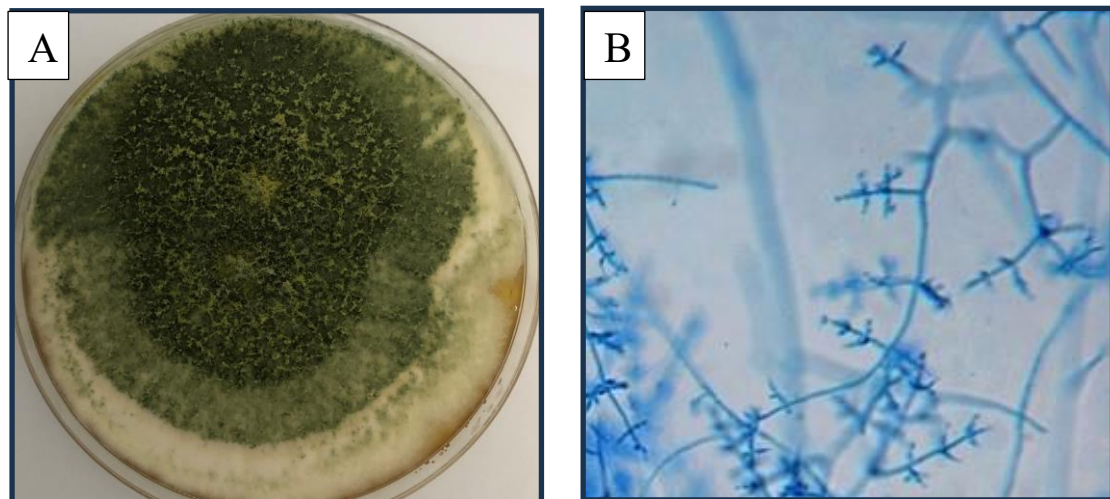


Figure (4-16) (A) *Trichoderma* culture on PDA at 37°C for 5 days, and (B) microscopic morphology of conidiophores and conidia of *Trichoderma* colony mounted with LPCB stain magnify at 40x.

4.2.10: *Chrysosporium*

Chrysosporium colonies grow at a modest rate. They can look grainy, woolly, cottony, or cottony and flat, or they can look raised and folded.

When you look at *Chrysosporium*. under a microscope, you can see that it makes hyphae, conidia (aleuriconidia), and arthroconidia. These conidia are wider than the vegetative hyphae and grow at the end of pedicels, along the sides of hyphae, or in spaces between hyphae. Conidia can be unicellular or multicellular, spherical, oval. *Chrysosporium* may have conidiophores, structures that bear conidia (Figure 4-17).

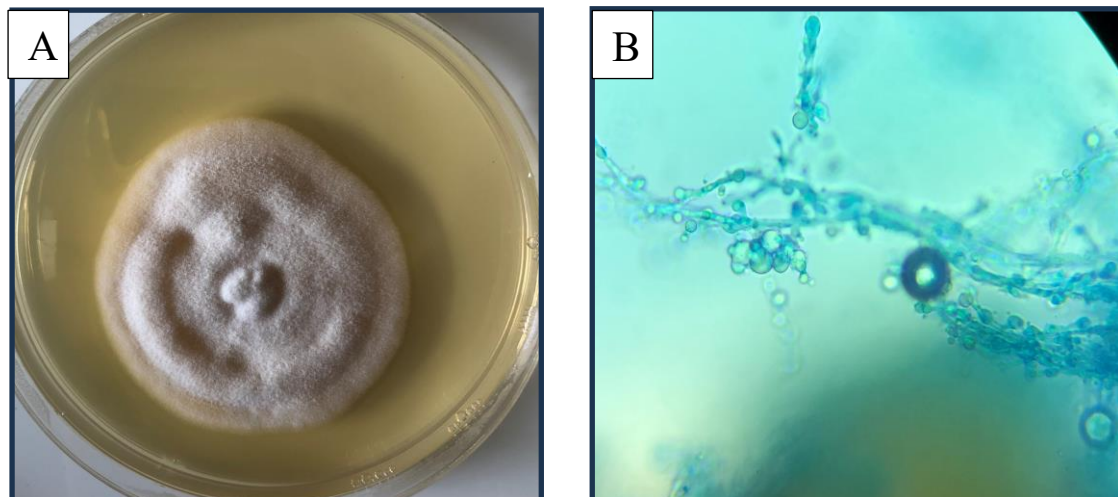


Figure (4-17) (A) *Chrysosporium* culture on PDA at 37°C for 8 days, and (B) microscopic morphology of hyphae and conidia of *Chrysosporium* colony mounted with LPCB stain magnify at 40x.

4.2.11: *Aureobasidium* sp.

Colonies grow quickly and soon become covered in slimy clumps of conidia. Colonies commonly appear dark-colored, ranging from shades of black, brown, olive-green, to dark gray. The colony surfaces are slightly rough.

Hyphae are hyaline and have holes in them. As they age, they often turn dark brown and form chains of one- to two-celled, thick-walled, darkly colored arthroconidia. These arthroconidia are actually the *Scytalidium* anamorph of *Aureobasidium*, but they are not the most important way to tell which species belong to this genus. Structures that bear conidia, observed as elongated structures supporting or carrying the conidia (Figure 4-18).

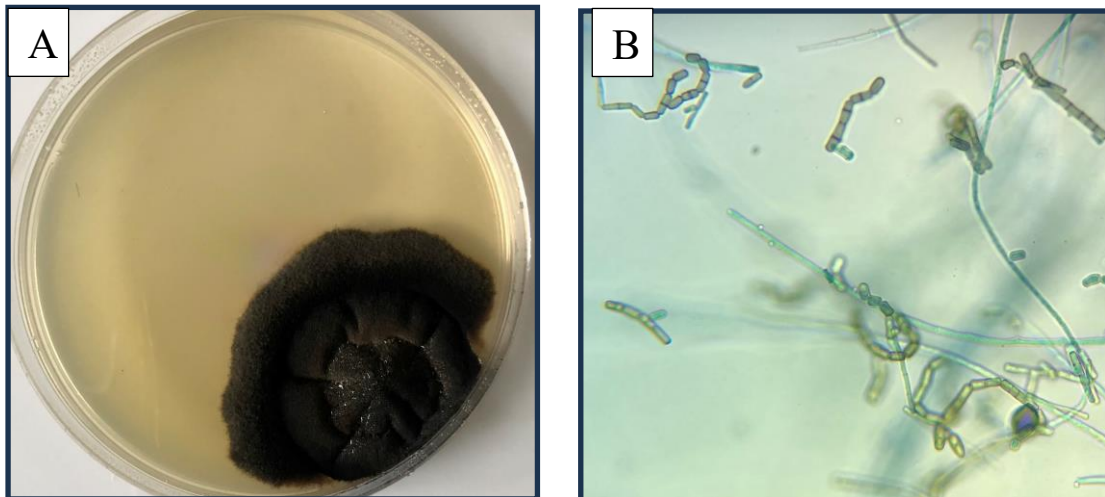


Figure (4-18) (A) *Aureobasidium* sp. culture on PDA at 37°C for 7 days, and (B) microscopic morphology of arthroconidia of *Aureobasidium* sp. colony mounted with LPCB stain magnify at 40x.

4.2.12: *Cladosporium*

The colonies grow slowly and colonies may vary in color, commonly appearing olive-green, dark green, brown, black, or grayish-green. the colony surface is velvety, powdery and wooly in texture.

Microscopy showed that Conidiophores are also darkly colored and may have branches like a tree. Conidia can be smooth, rough or spiky. They are often septate, with multiple cells, and may have distinctive shapes (e.g., cylindrical, ovoid, or curved). They have one to four cells and a dark spot in the middle called the hilum (Figure 4-19).

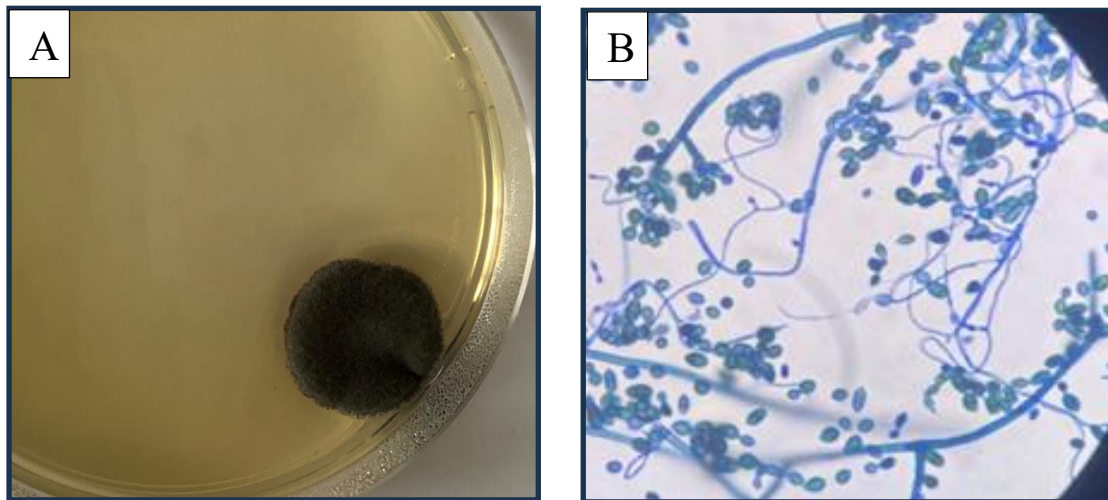


Figure (4-19) (A) *Cladosporium* culture on PDA at 37°C for 10 days, and (B) microscopic morphology of conidiophores and conidia of *Cladosporium* colony mounted with LPCB stain magnify at 40x.

4.2.13: *Candida* spp.

The colonies on Sabouraud Dextrose Agar (SDA) were white to creamy, smooth, and round. Different species shown in (Figure 4-20) (Figure 4-21) (Figure 4-22) (Figure 4-23) (Figure 4-24). SDA is incubated aerobically at 37°C for 24–48 hours. According to a study conducted by Hadi & Alsultany (2020) found that *Candida* colonies growing on SDA among different species have such morphological features, which aligns with the findings mentioned by Raju & Rajappa (2011) regarding the appearance of colonies are creamy, shiny, smooth, circular, and species differentiation is difficult.

When the yeast cells were stained with gram stain, they became darker and more oval-shaped. This is different from *C. albicans* cells, which are usually bright and round, as shown in (Figure 4-20). This result is in consistent with that of (Kemoi, 2012) findings.

After about 15 hours of growth, the VITEK 2 device automatically identified the species of yeast. The VITEK 2 method was able to identify the species of *C. albicans*, *C. parapsilosis*, *C. glabrata*, *C. krusei*, and *C. lusitaniae*.

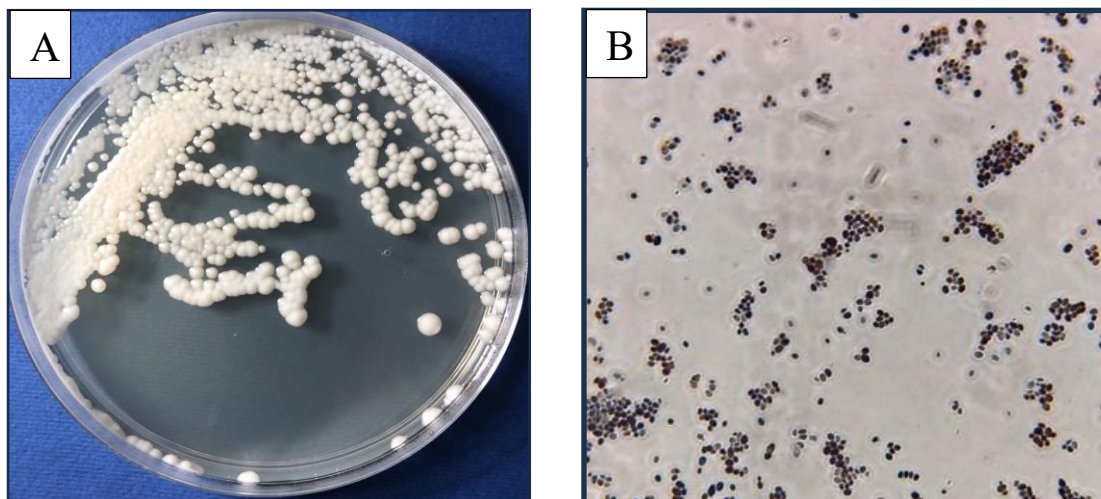


Figure (4-20) (A) *C.albicans* growth on SDA at 37°C for 24-48 hours h and(B) microscopic characteristic of colony mounted with Gram stain observed in a 40x magnification.

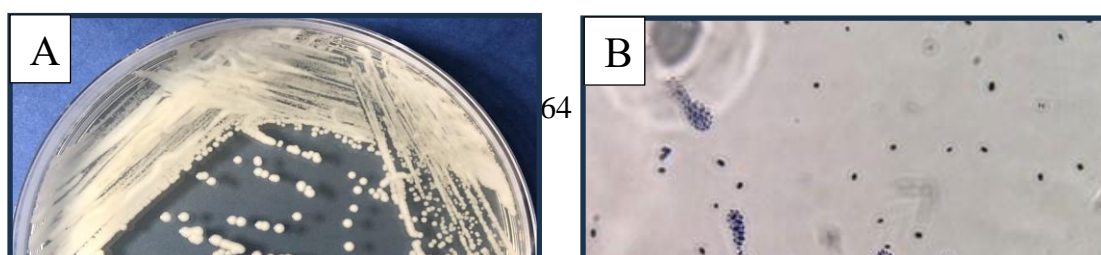


Figure (4-21) (A) *C.glabrata* growth on SDA at 37°C for 24-48 hours h and(B) microscopic characteristic of colony mounted with Gram stain observed in a 40x magnification.

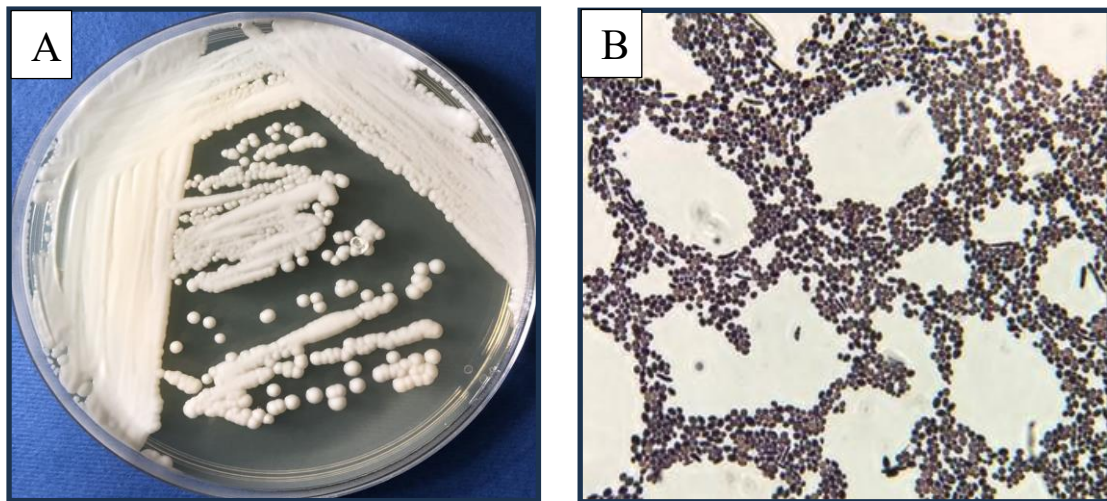


Figure (4-22) (A) *C.parapsilosis* growth on SDA at 37°C for 24-48 hours h and(B) microscopic characteristic of colony mounted with Gram stain observed in a 40x magnification.

A

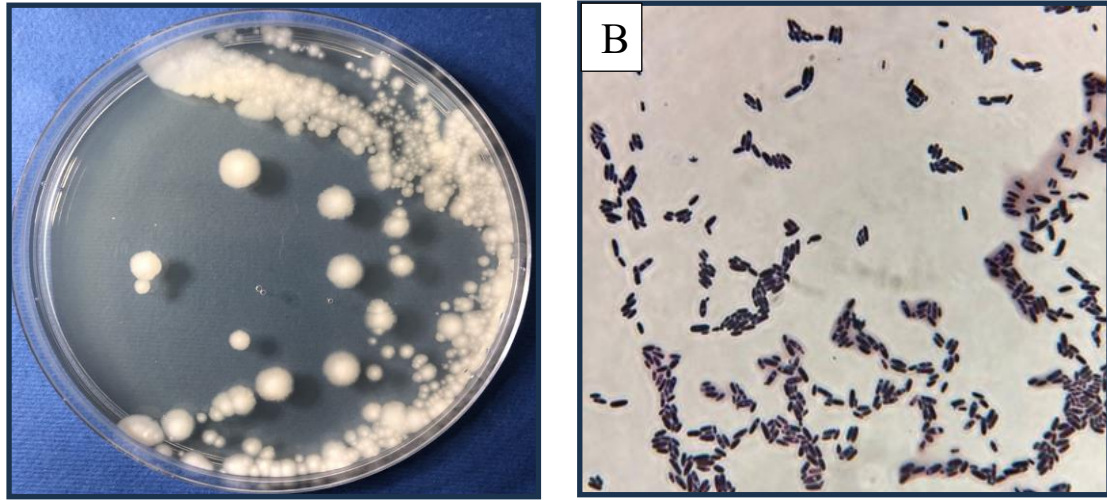


Figure (4-23) (A) *C.krusei* growth on SDA at 37°C for 24-48 hours h and(B) microscopic characteristic of colony mounted with Gram stain observed in a 40x magnification.

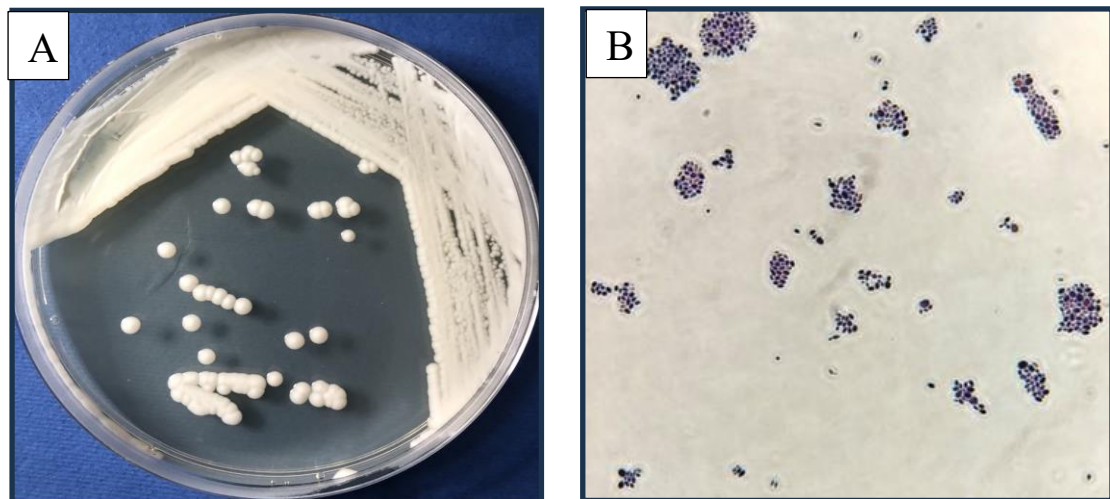


Figure (4-24) (A) *C. lusitania* growth on SDA at 37°C for 24-48 hours and(B) microscopic characteristic of colony mounted with Gram stain observed in a 40x magnification.

4.2.14: *Rhodotorula mucilaginosa*

Colonies are usually moderately fast-growing on SDA at 37°C. The colonies are often pink, crimson, or reddish-orange in color. Due to capsules are available, colonies produce a mucoid substance.

Rhodotorula mucilaginosa appears as spherical to ellipsoidal yeast cells under the microscope. The cells can be seen as single cells or in budding forms where daughter cells remain attached to the parent cell.

These fundamental findings are consistent with prior study by eifi *et al.*, (2013) and Garcia-Gutiérrez *et al.*, (2021) that shown that colonies of *R. mucilaginosa* are mucoid cells that appear orange on SDA (Figure 4-25). Under the microscope, they appear to be ovoid or spherical.

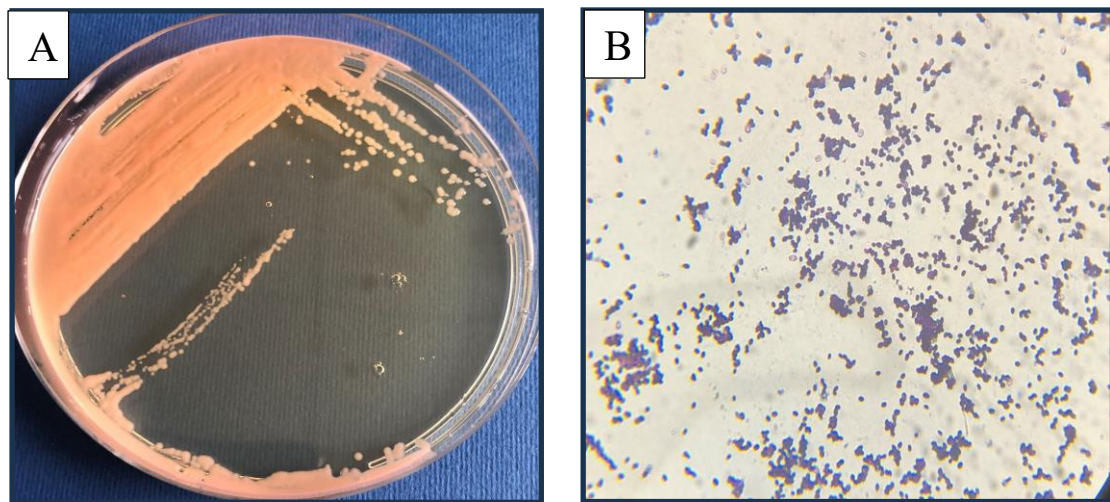


Figure (4-25) (A) *Rhodotorula mucilaginosa* growth on SDA medium at 37°C for 3days and (B) microscopic characteristic of blastoconidia mounted with Gram stain observed in a 40x magnification.

4.2.15: *Cryptococcus albidus* (*Naganishia albida*)

The colony morphology on SDA was determined by isolating yeast colonies exhibiting whitish, cream-colored, or slightly off-white, mucoid characteristics, which varied in relation to the thickness of the capsule.

This was achieved through the growth on fungal media for a period of 72 hours. The morphology of the yeast cells was observed using microscopy. The cells were found to be spherical-to-oval in shape and were enveloped by a mucopolysaccharide capsule. These cells may show budding forms or occur as individual yeast cells (Figure 4-26).

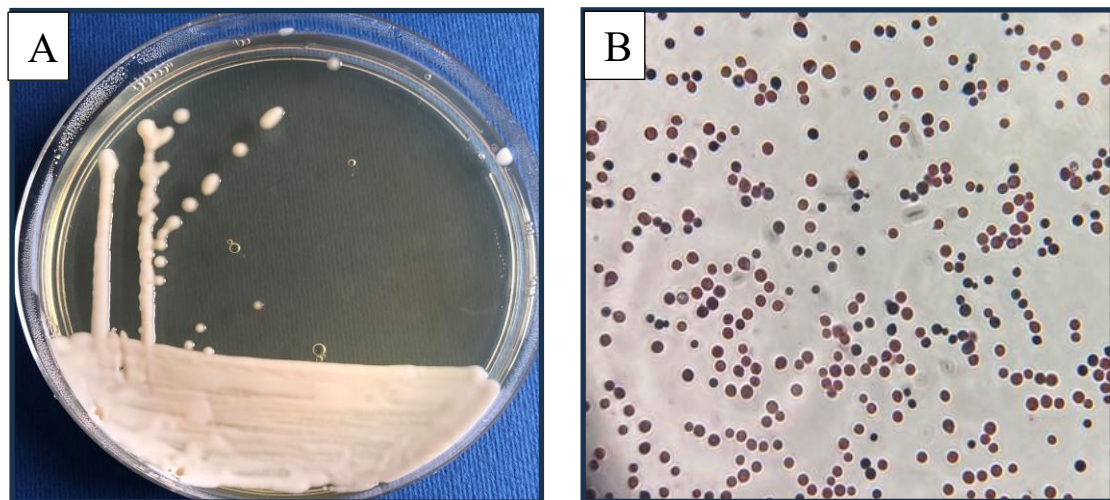


Figure (4-26) (A) *Cryptococcus albidus* growth on SDA medium at 37°C for 3 days and (B) microscopic characteristic of blastoconidia mounted with Gram stain observed in a 40x magnification.

4.2.16: *Exophiala dermatitidis*

Colonies grow slowly; and at first, they look like black yeast and feel like suede. Colonies are black to olive-black, and greyish or brownish colours often show through, particularly visible at the margins, where the formation is younger.

Exophiala dermatitidis typically appears as yeast-like cells under the microscope. The yeast cells are usually round to oval in shape. The conidia are one-celled, white to pale brown, and round to obovoid. Depending on the staining method and the presence of melanin, *Exophiala dermatitidis* structures may exhibit varying degrees of pigmentation (Figure 4-27).

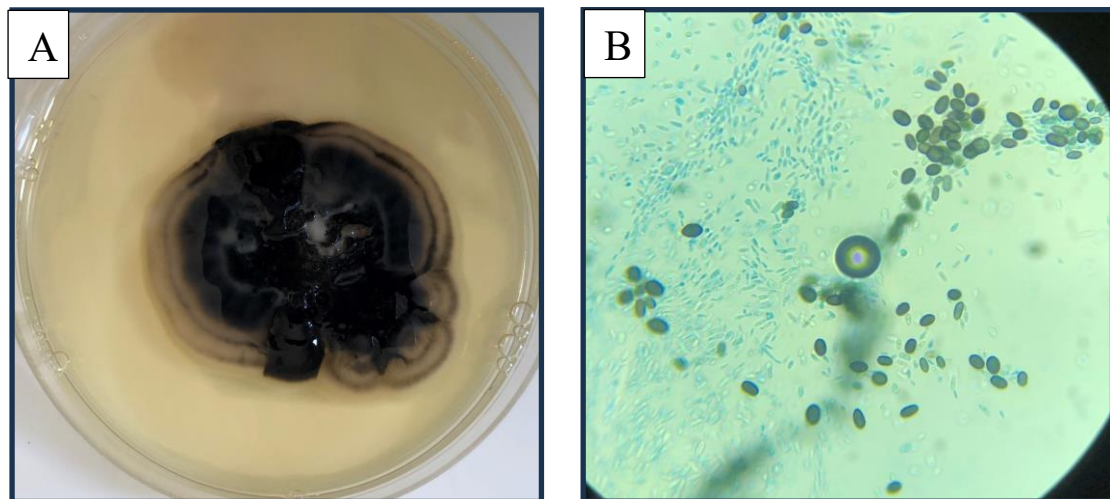


Figure (4-27) (A) *Exophiala dermatitidis* growth on SDA medium at 37°C for 10 days and (B) microscopic characteristic of conidia of *Exophiala dermatitidis* colony mounted with LPCB stain observed in a 40x magnification.

4.3. Molecular identification

4.3.1: Polymerase Chain Reaction

In this study, we apply automatic method Vitek 2 system for identification of the medically important *Candida* spp. Finally, definite identification of *Candida* spp. was confirmed by Polymerase Chain Reaction. Used universal primers ITS1 and ITS4 successfully to amplify ITS region of *Candida* spp. The expected 375-871 bp amplified ITS DNA product was detected in *Candida* spp. except in negative control, which confirms that all isolates belong to the *Candida* genus; (Figure 4-28) represents the electrophoretic profile of the ITS region of *Candida* spp. isolates. To ensure the *Candida* species identified by morphological characteristics and automatic method Vitek 2 system, the PCR fragments of amplified ITS regions were sequenced, then aligned and registered in NCBI GenBank with the following accession numbers, *C. albicans* (PP033710), *C. parapsilosis* (PP033709), *C. krusei* (PP068836), *C. lusitaniae* (PP068837) and *C. glabrata* (PP068838) as shown in (Table 4-5).

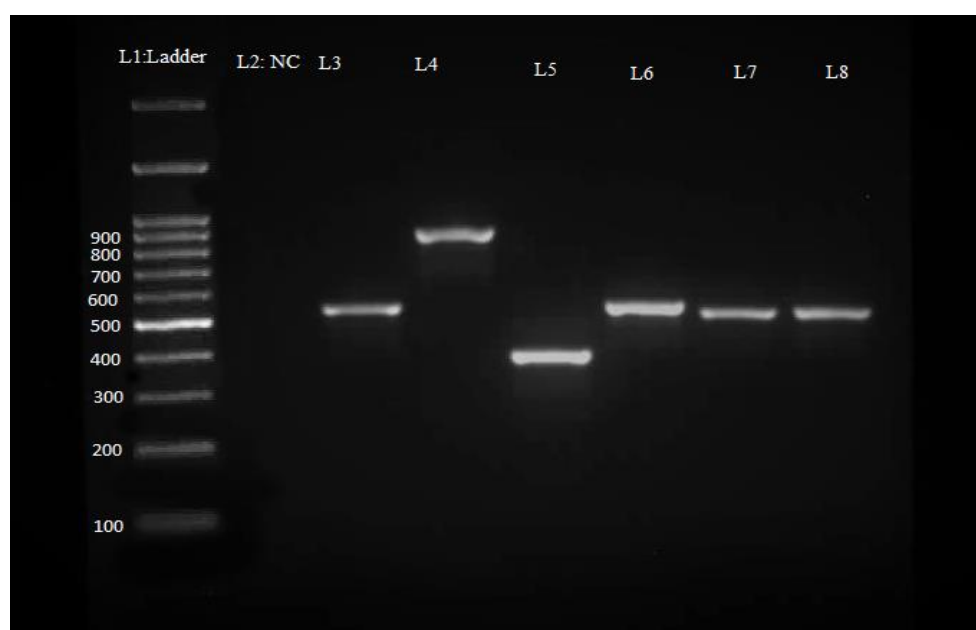


Figure (4-28) The agarose gel electrophoresis technique was used to visualize the ITS-PCR products of *Candida* isolates, which showed distinct bands. Lane 1: Ladder 100 bp (Genedirex), Lane 2: negative control (NC), Lane 3: *C. albicans* (535bp), Lane 4: *C. glabrata* (871bp), Lane 5: *C. lusitaniae*(375bp), Lane 6: *C. albicans* (535bp), Lane 7: *C. krusei* (510bp), Lane 8: *C. parapsilosis* (520bp) respectively by using 1X TBE buffer/ Agarose gel 1.14%.

In the study performed by Nnadi *et al.*, (2020) a molecular technique was used to investigate the occurrence of *Candida* in hospital environments within Nigeria. The present investigation revealed that *Candida parapsilosis* was the highest prevalence 31.25%, then followed by *Candida (Nakaseomyces) glabrata* and *Candida krusei*, both with a prevalence of 28.13%.

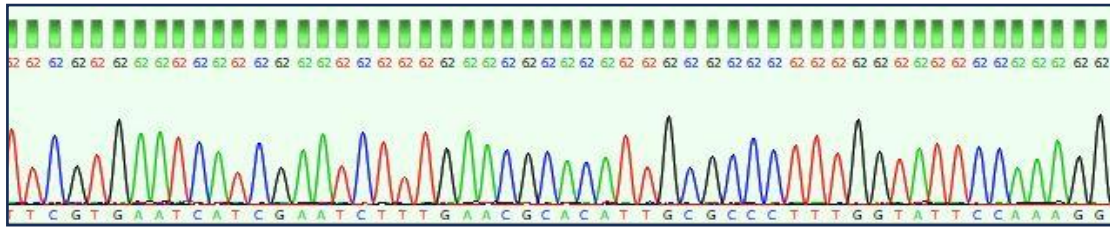
In addition, Nascimento *et al.*, (2023) conducted a study to assess indoor airborne contaminants in hospital environments, with a particular focus on the detection of potentially pathogenic yeasts. Indoor air samples were collected from twelve different healthcare facilities (hospitals and medical clinics). The subsequent identification of the isolates was carried out by the use of polymerase chain reaction. The findings of this study indicate that *C. Parapsilosis* was the highest prevalence among the species examined.

4.3.2: Sequencing Analysis

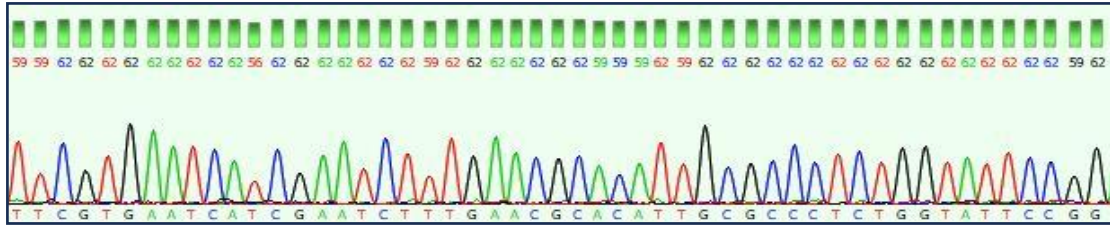
Sequence analysis confirmed the identification of the isolates due to the characteristics of the culture and Vitek identification. For 5 isolates, the chromas software program used DNA sequencing alignment, and then using NCBI BLAST, homology searches were done between the references sequence and our sequenced isolates, NCBI-Genbank accession numbers were obtained for all sequenced isolates placed in a list in (Table 4-5) and (Figure 4-29) examples of the sequenced data for each different *Candida* spp.

Table (4-5) *Candida* spp. isolates obtained from airborne of hospitals in koya city and accession numbers of DNA sequenced of isolates registered in NCBI and Examples of GenBank accession numbers matching to our result.

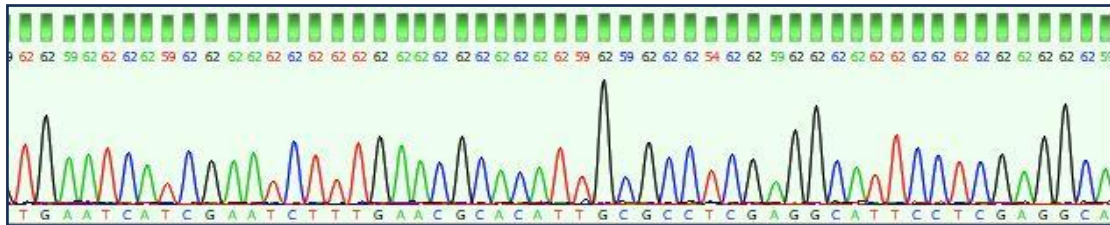
Species name	GenBank sequence accession numbers	Blast accession numbers
<i>C. albicans</i>	PP033710	KP675532.1
<i>C. parapsilosis</i>	PP033709	OP618190.1
<i>C. glabrata</i>	PP068838	LC389225.1
<i>C.lusitaniae (Clavispora lusitaniae)</i>	PP068837	KP764965.1
<i>C. krusei (Pichia kudriavzevii)</i>	PP068836	KP878240.1



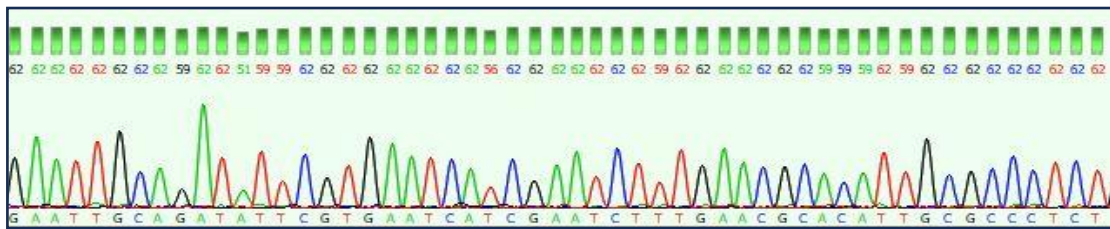
A: *C. albicans*



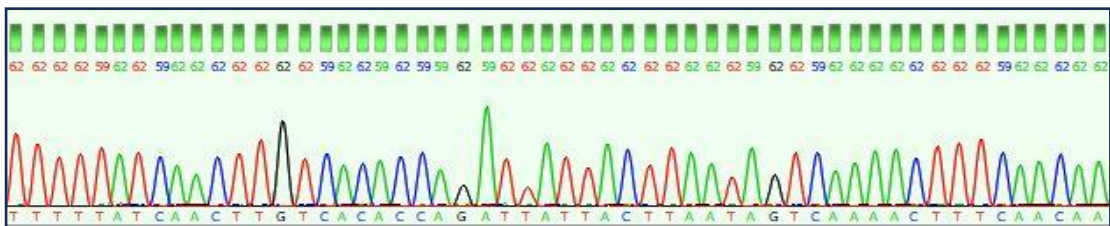
B: *C. parapsilosis*



C: *C. lusitaniae*



D: *C. krusei (Pichia kudriavzevii)*



E: *C. glabrata*

Figure (4-29) Examples of Chromatograms of the Sequenced Data. A) *C. albicans*, B) *C. parapsilosis*, C) *C. lusitaniae*, D) *C. krusei*, E) *C. glabrata*.

4.4: Properties of Nanoparticles

4.4.1: XRD crystallography analysis and thermal stability

X-ray powder crystallography is an essential methodology for identifying the crystalline phase of a substance. The diffraction peaks and their relative planes outlined for zinc oxide nanoparticles at positions $2\theta = 31.7512^\circ$ (010), 34.3769° (002), 36.2408° (011), 47.4743° (012), 56.5420° (110), 62.8302° (013), 66.3786° (020), 67.8857° (112) and 68.9678° (021) (Figure 4-30), provide evidence that iron oxide nanoparticles exist in a crystalline state. The prominent peak at $2\theta = 36.2408^\circ$ (010), which illustrated that significant orientation took place to the assessed facet and demonstrated the high purity of iron oxide nanoparticles after preparation.

However, the diffraction peaks and their relative planes outlined for iron oxide nanoparticles at positions $2\theta = 30.0763^\circ$ (100), 35.4283° (110), 43.2027° (120), 44.5183° (120), 57.1706° (110) and 62.7220° (130) (Figure (4-31), provide evidence that iron oxide nanoparticles exist in a crystalline state. The prominent peak at $2\theta = 35.4283^\circ$ (110), which illustrated that significant orientation took place to the assessed facet and demonstrated the high purity of iron oxide nanoparticles after preparation.

The Debye-Scherrer formula provides a theoretical method for calculating the average crystallite size, which is as follows:

$$D = \frac{K\lambda}{\beta \cos \theta}$$

Since K is the Scherrer constant (0.9), λ is the wavelength of the X-ray, β is the total width at half point of the XRD peak, and θ is the Bragg angle, these four variables are used to determine the XRD peak. Therefore, the measured size of the crystallite particles is approximately 15-20 nm and 18 nm for iron and zinc oxide nanoparticles, respectively (Figure 4-30) and (Figure 4-31).

synthesized nanoparticles possess the same characteristics as the hexagonal phase of zinc oxide. (Figure 4-31) depicted the X-ray diffraction pattern of iron oxide nanoparticles in a similar manner. The diffractogram revealed the presence of peaks at specific angles, namely 18.44°, 19.60°, 23.84°, 33.20°, 35.64°, 40.96°, 49.44°, 54°, and 62.60°(Rajendran & Sengodan, 2017). These peaks suggest that the synthesized iron oxide nanoparticles possess a crystalline phase. Furthermore, the obtained results closely align with the JCPDS card number 19-0629. Previous studies have shown comparable findings in the process of synthesizing magnetite nanoparticles by green methods (Awwad & Salem, 2012). Lail *et al.*, (2023) was applied the X-ray diffraction (XRD) analysis revealed distinct peaks at 2θ values of 31.9°, 35.1°, 36.4°, 47.6°, 56.6°, and 63°, which correspond to the crystallographic planes (100), (002), (101), (102), (110), and (103) respectively. These findings indicate the presence of hexagonal wurtzite crystalline zinc oxide nanoparticles (ZnONPs), as determined by the Joint Committee on Powder Diffraction Standards (JCPDS) database.

The diffraction patterns of the synthesized iron and zinc oxide nanoparticles were measured by Kamal *et al* (2023) within the angular range of 10° to 70°. The synthesized nanoparticle exhibits diffraction peaks that conform to a standard structure, displaying many peaks corresponding to iron at 2θ values of 30.26°, 32.33°, 34.67°, 36.06°, 43.47°, and 46.36°. The observed peaks exhibited a high degree of agreement with the reference to JCPDS card No.76-0958. Measurements were conducted to determine the Full Width at Half Maximum (FWHM) for the planes of reflection (220), (100), (320), (311), (400), and (211). The hexagonal crystalline structure of zinc oxide nanoparticles (NPs) was verified by seeing peaks at 2θ values of 32.9°, 34.99°, 58.65°, and 67.8°, which correspond to the (100), (101), (110), and (200) crystalline planes, respectively. The iron nanoparticles had an average crystalline size of 16.8 nm, whereas the zinc nanoparticles had an average crystalline size of 18.53 nm. These values were derived by analyzing the XRD patterns using Debye-Scherrer's formula (Padmavathy & Vijayaraghavan, 2008)

4.4.2: SEM analysis of nanoparticles

SEM assessment was utilized so that the morphological characteristics of the iron and zinc oxide nanoparticles that were manufactured could be examined. When viewed under varying degrees of magnification, zinc oxide and iron oxide nanoparticles most often take the form of spherical particles (Figure 32 and 4-33, respectively). Iron and zinc oxide nanoparticles were predominantly spherical in shape as depicted by SEM pictures. The SEM picture at two various magnifications reveals that iron and zinc oxide nanoparticles were composed of spherical forms with a restricted size range of 15-20 nm. In addition, the reduction and nucleation development of the reduced atoms agglomerate the grains. More bioavailable metal ions participate in fewer nucleation events, resulting in metal aggregation.

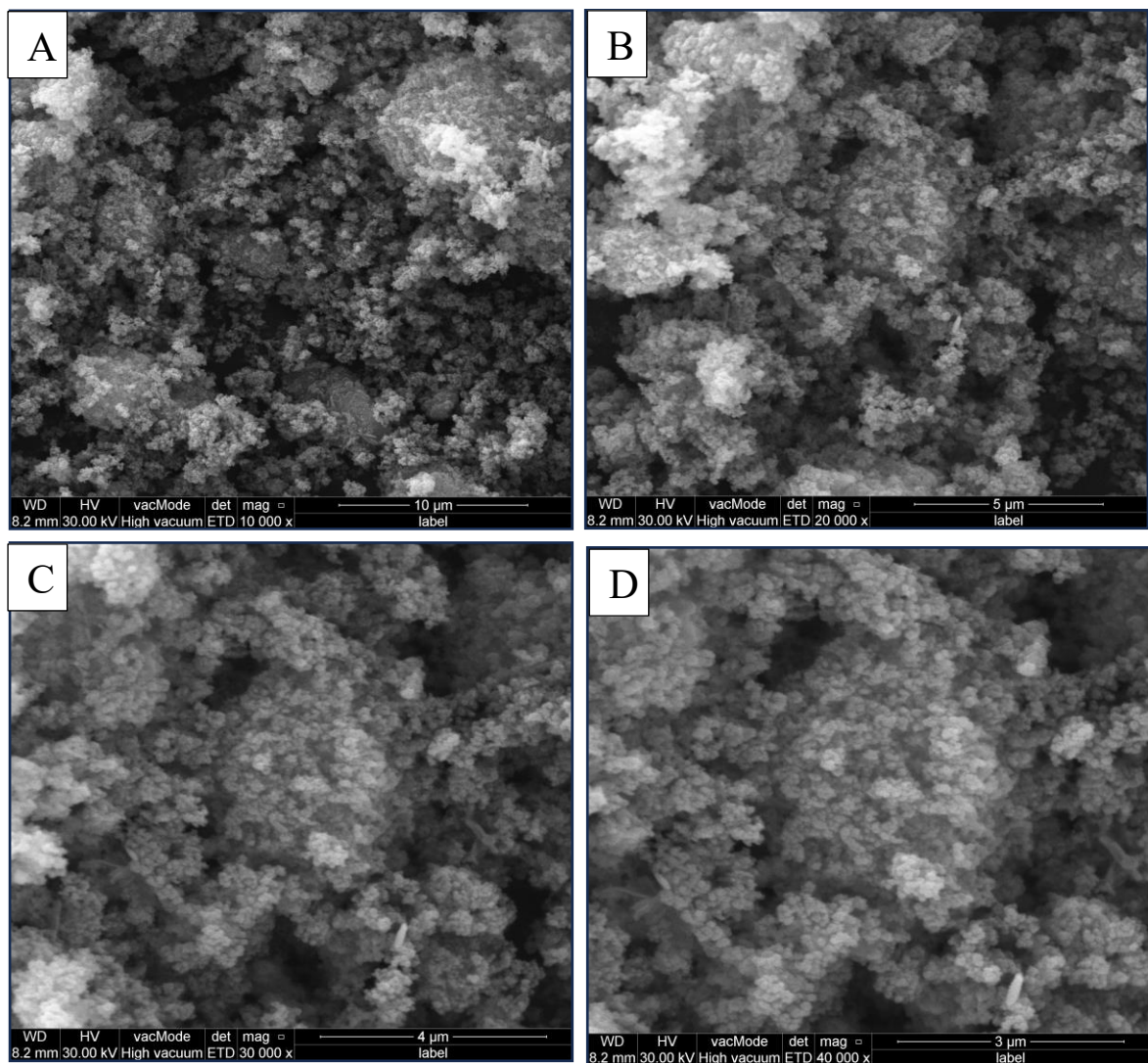
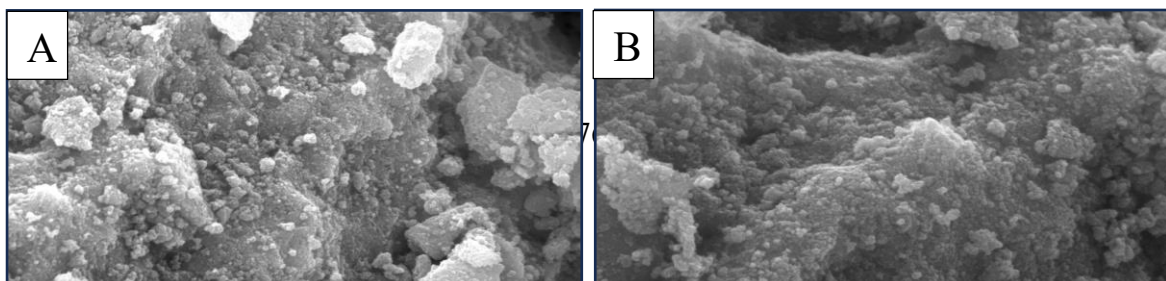


Figure (4-32) SEM photomicrograph of zinc oxide nanoparticles at magnifications of 10 μm (A), 5 μm (B), 4 μm (C), and 3 μm (D).



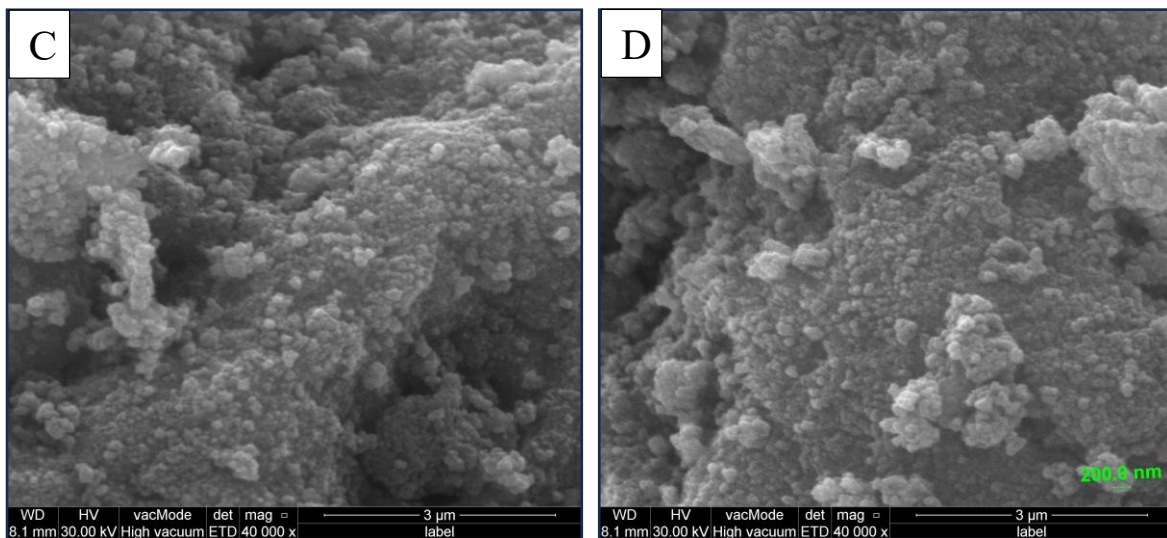


Figure (4-33) SEM photomicrograph of iron oxide nanoparticles at magnifications of 10 μm (A), 5 μm (B), 3 μm (C), and 3 μm (D).

The micrographs presented in figures (4-32 and 4-33) demonstrate the occurrence of network development at the zinc oxide and iron oxide nanoparticles. There was clear indication that the process of agglomeration had occurred. The analysis of the images provided, confirmed that the synthesized zinc oxide and iron oxide nanoparticles exhibited a high degree of agreement with the results obtained from X-ray diffraction (XRD). Furthermore, the zinc oxide nanoparticles that were synthesized had a spherical morphology. In the investigation that performed by Lail *et al.*, (2023) on the characterization of zinc oxide nanoparticles and use the scanning electron microscopy to determine the size of nanoparticles and revealed the presence of nanoparticles with a spherical morphology, exhibiting an average size distribution within the range of 50 to 100 nm.

On the other hand, based on the examination of the scanning electron microscopy (SEM) micrographs, Kamal *et al.*, (2023) was predicted that the iron and zinc nanoparticles synthesized would exhibit irregular shapes. The SEM images reveal that particle agglomeration occurred due to the presence of inter-particle attraction forces. The utilization of scanning electron microscopy (SEM) is crucial in the examination of the dimensions and surface characteristics of the synthesized nanoparticles, since the biological performance of these nanoparticles is heavily influenced by their size and morphology (Sharmila *et al.*, 2017).

4.4.3: MICs Determination of ZnO-NPs, IONPs compared to FLC against different *Candida* species

The susceptibility of different *Candida* species was examined towards ZnONPs and IONPs, and their comparison with Fluconazole. The antifungal activity of ZnO-NPs, IONPs, and FLU were assessed on *Candida* spp. using BMD methods (figures 4-34). The findings of the study indicate that both ZnO-NPs and IONPs exhibit antifungal properties against pathogenic *Candida* spp., effectively inhibiting the growth of all the *Candida* spp. that were examined. The MICs of ZnO-NPs and IONPs against *Candida* species were found to range from 64 to 512 µg/ml and 16-128 µg/ml. Additionally, the MICs for fluconazole (FLU) were observed to be 64-512 µg/ml.

As shown in figure (4-34), the lowest MIC of IONPs in *C. glabrata* and *C. lusitaniae* was 16 µg/ml, *C. albicans* was 32 µg/ml and *C. krusei* was 64 µg/ml. But the highest MIC of IONPs in *C. parapsilosis* was 128 µg/mL. The minimum number of ZnO-NPs required for the growth inhibition of *C. albicans* and *C. lusitaniae* were 64 µg/mL but for *C. glabrata* was 128 µg/ml, for *C. krusei* was 256 µg/ml and for *C. parapsilosis* was 512 µg/ml. The lowest MIC of ZnO-NPs was observed for *C. lusitaniae*, *C. albicans* and *C. glabrata*. The highest MIC values were obtained for *C. parapsilosis* and *C. krusei*.

FLU exhibited the lowest MIC against *C. parapsilosis*, with MIC of 64 µg/ml. *C. glabrata* and *C. lusitaniae* growth was inhibited at MICs of 128 µg/ml. *C. albicans* and *C. krusei* were less sensitive than the other *Candida* spp. examined, with MIC values of the FLU reaching 512 µg/ml and 256 µg/ml, respectively. The FLU susceptibility ordering was *C. parapsilosis* > *C. glabrata* and *C. lusitaniae* > *C. krusei* > *C. albicans*.

The antifungal activity against *Candida parapsilosis* exhibited by (ZnO-NPs) was substantially different when compared to that of fluconazole (FLU). In terms of the antifungal efficacy against *Candida glabrata* and *Candida krusei*, the same MIC were observed between fluconazole (FLC) and zinc oxide nanoparticles (ZnO-NPs). The susceptibility of *C. albicans* and *C. lusitaniae* to ZnO-NPs was shown more sensitive compared to FLU.

There was a significant difference between the MIC of fluconazole compare to IONPs. According to our results the sensitivity of IONPs against candida spp. was higher than FLU. In contrast, the research conducted by Abdulrasool *et al.*, (2022) for the purpose of antifungal effectiveness Fe₃O₄ NPs and FLU against *Candida spp.*, the minimum inhibitory concentration (MIC) values were determined. The MIC of FLU ranged from 15-122 µg/ml, whereas for Fe₃O₄ NPs, it ranged from 59-475 µg/ml. The antifungal activity against *Candida krusei*, *Candida parapsilosis*, *Candida lusitaniae*, and *Candida albicans* species was significantly reduced for Fe₃O₄ nanoparticles in comparison to that of fluconazole (FLU).

These findings are in link with the findings of (Seddighi *et al.*, 2017) which evaluate the antifungal activity of IONPs against different *Candida* spp. in comparison to fluconazole (FLU). The iron oxide nanoparticles (IONPs) exhibited a spherical morphology, with a diameter ranging from 30 to 40 nm. The findings of the study by Seddighi *et al.*, (2017) which are consistent with our findings, indicate that the growth inhibition value for *Candida albicans* and *Candida glabrata* were most susceptible to IONPs. while MIC for *C. lusitaniae* was 250 µg/ml, which is a higher value than what we found.

MICs for ZnO-NPs against *Candida albicans* was 64 $\mu\text{g/ml}$ which is different from the findings of Metwally *et al.*, (2022) that MICs was 250 $\mu\text{g/ml}$. This difference refers to the shape of nanoparticles have rod shape with sizes of 13.58 - 30.70 nm. (Cheon *et al.*, 2019) found that the difference in the antimicrobial activity of NPs was closely linked to the difference in the rate at which NPs ions were released. This was because the surface area of the NPs was different.

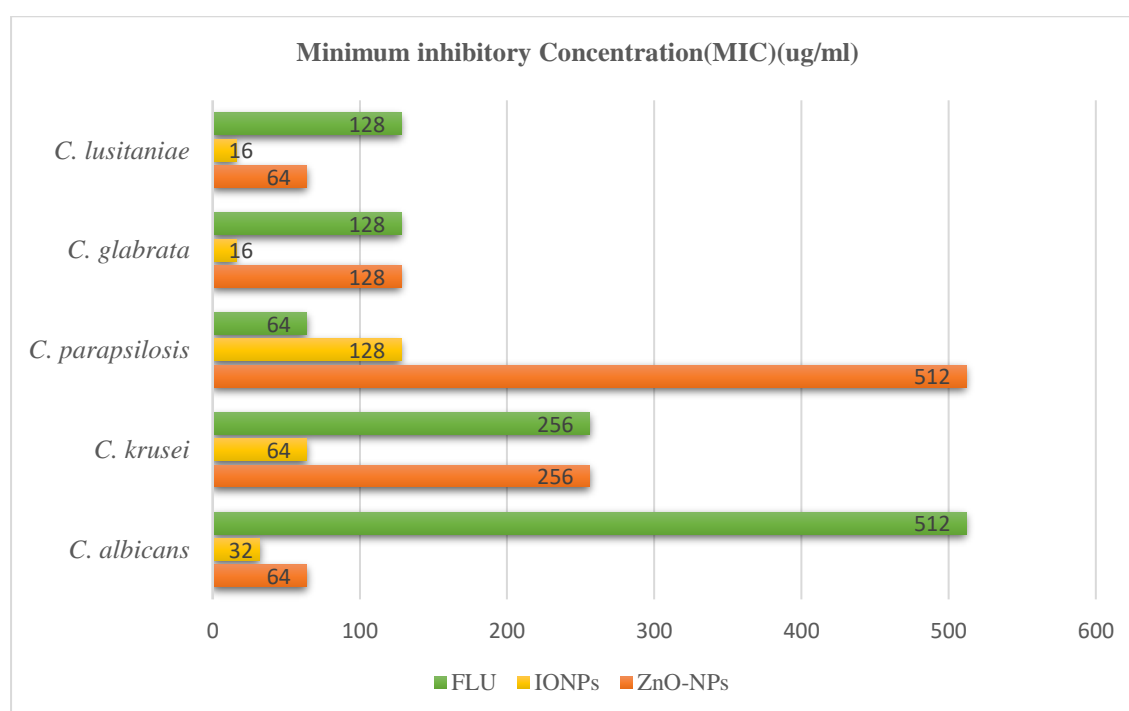


Figure (4-34) Minimum inhibitory concentration (MIC) of ZnO-NPs, IONPs and FLU against different *Candida* species ($\mu\text{g/ml}$)

4.4.4: Inhibitory effect of IONPs against *Candida* species by agar plate well diffusion assay

The present study used the agar well diffusion method to evaluate the efficacy of antimicrobial agents. The current investigation demonstrates a positive relationship between the concentration of iron oxide nanoparticles and the diameter of the growth inhibition zone exhibited by the fungal isolates (Table 4-6). In 1000 μ g/ml concentration of IONPs the high inhibition effect of IONPs which presented in *C. parapsilosis* and *C. glabrata* with inhibition zone of (33.5 mm) and (32 mm) respectively, followed by *C. albicans*, *C. lusitaniae* and *C. krusei* with inhibition zone of (27 mm) (26 mm) and (24 mm). While in 500 μ g/ml concentration the high inhibition effect of IONPs which presented in *C. glabrata* and *C. parapsilosis* followed by *C. albicans* with inhibition zone of (25 mm) (23mm) and (23mm) respectively, while low effect were on *C. krusei* and *C. lusitaniae* with inhibition zone of (19mm) and (17mm). But in 250 μ g/ml the high inhibition effect of IONPs which presented in *C. glabrata* and *C. parapsilosis* and *C. albicans* with inhibition zone of (18 mm) (16mm) and (16mm) respectively. While the low effect in *C. lusitaniae* and *C. krusei* with growth rate (8mm) and (11mm).

In 125 μ g/ml concentration found the high inhibition effect IONPs which presented in *C. albicans* and *C. parapsilosis* with inhibition zone of (10mm), followed by *C. glabrata* with inhibition zone of (9 mm). While not found any effect of IONPs was on *C. Lusitania* and *C. krusei* with inhibition zone of (0 mm) and (6mm). In 62.5 μ g/ml concentration found *Candida spp.* are resistance effect to IONPs.

The findings shown in this study agree with the studies by AL-Husseini & Al-araji, (2021) in which they tested the antifungal properties of Fe₂O₃ nanoparticles on two pathogenic *Candida* species, including (*C. albicans* and *C. glabrata*) using the well diffusion method. The diameter of the growth inhibition zone of the fungal isolates exhibited a positive correlation with the concentration of iron oxide nanoparticles. Specifically, the growth inhibition zone of *C. albicans* displayed measurements of 30.1 mm, 24.2 mm, 20.2 mm, 18 mm, and 14 mm for concentrations of 20 mg/ml, 10 mg/ml, 4 mg/ml, 2 mg/ml, and 1 mg/ml, respectively. In addition, observed that the inhibitory zones of *C. glabrata* exhibited diameters of 37mm, 35.2 mm, 28 mm, 23.7 mm, and 17.9 mm when exposed to Fe₂O₃ NPs.

The study conducted by Sidkey *et al.*, (2020) demonstrated the successful extracellular creation of iron oxide nanoparticles by the utilisation of *Aspergillus flavus*. The antifungal efficacy results of the IONPs demonstrated a maximum inhibition zone of 10 mm against *C. albicans* at a concentration of 10 mg/ml.

The findings of Seddighi *et al.*, (2017) indicated that the diameters of the zones of inhibition of the IONPs were measured to be 51.2 mm and 38 mm against *C. glabrata* and *C. albicans* species, respectively, at a concentration of 1000 µg/ml. In contrast, smaller values of 35 mm, 27.2 mm, and 24.6 mm were observed against *C. krusei*, *C. parapsilosis*, and *C. lusitaniae*, respectively. The observed widths of zones of inhibition against *Candida spp.* in our investigation were found to be lower compared to the findings reported by (Seddighi *et al.*, 2017) .

These findings are partially consistent with the findings reported by Abdulrasool *et al.*, (2022), where the diameters of the zones of inhibition against *C. albicans* and *C. glabrata* species were measured as 36.1 mm and 48.6 mm, respectively, at a concentration of 950 µg/ml for Fe₃O₄ NPs. Comparatively smaller measurements of 23.4, 25.8, and 33.3 mm were acquired in relation to *C. lusitaniae*, *C. parapsilosis*, and *C. krusei*, respectively.

Table (4-6) Zone of inhibition of IONPs at various concentrations against different *Candida* species (mm)

<i>Candida</i> species	Concentration of IONPs (µg/ml)				
	1000	500	250	125	62.5
<i>C. albicans</i>	27	21	16	10	5.2
<i>C. glabrata</i>	32	25	18	9	4
<i>C. parapsilosis</i>	33.5	23	16	10	5
<i>C. krusei</i>	24	17	11	6	3
<i>C. lusitaniae</i>	26	19	8	0	0

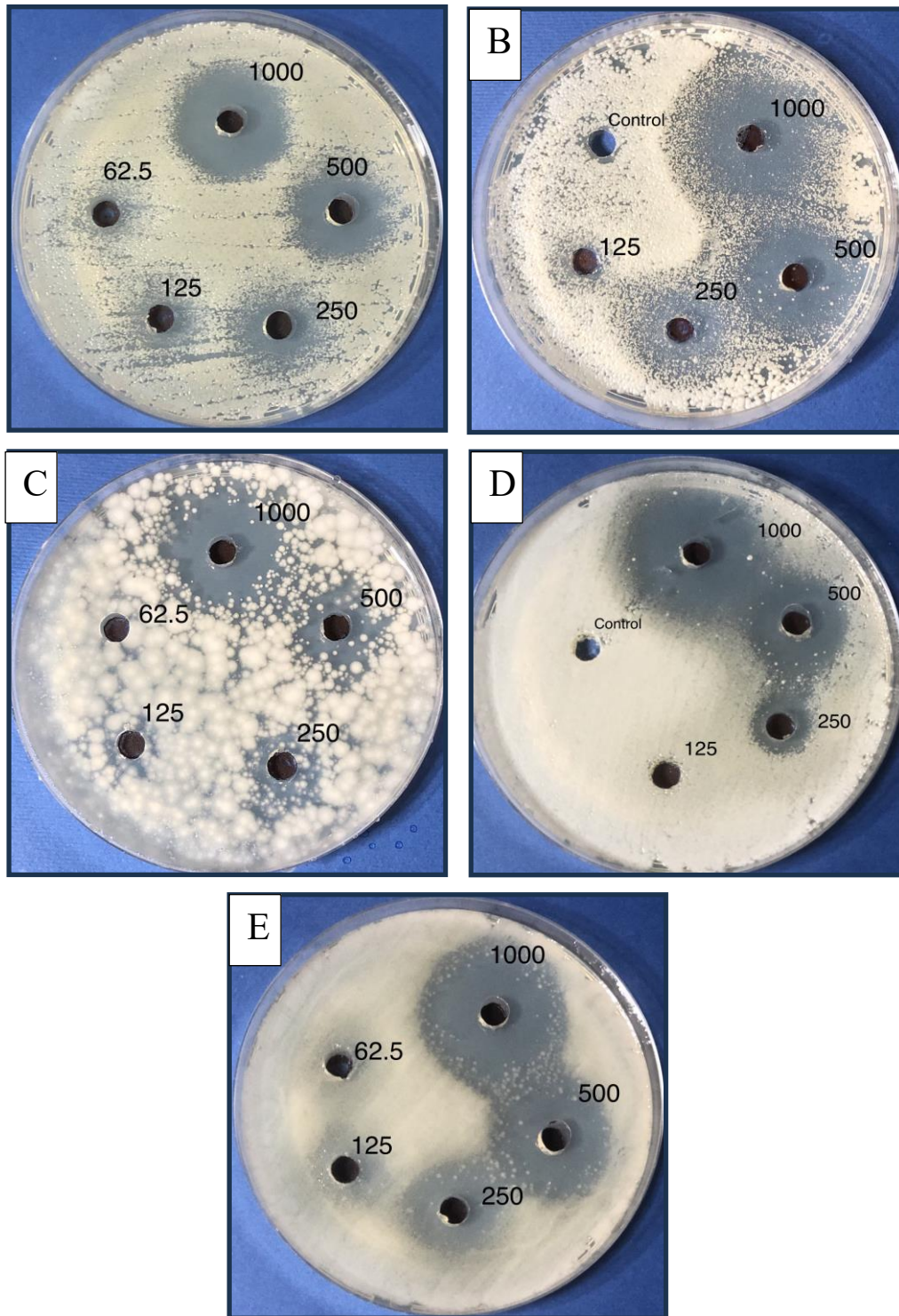


Figure (4-35) Zone of inhibition of IONPs at various concentrations against different *Candida* species. A- *C. albicans*, B- *C. parapsilosis*, C- *C. krusei*, D- *C. lusitaniae*, E- *C. glabrata*.

4.4.5: Inhibitory effect of ZnO-NPs against *Candida* species by agar plate well diffusion assay

Different study using Nano-ZnO as a biological agent and become increasingly common. In Table (4-7) shows the effect of ZnONPs on different species of *Candida*. The results showed that some *Candida* spp. isolate were susceptible to ZnONPs and the inhibition rate increases with the increase of concentration.

ZnONPs at 1000µg/ml showed high inhibition effect presented against *C. lusitaniae* and *C. glabrata* with inhibition zone of (39 mm) and (30 mm) respectively, followed by, *C. krusei*, *C. albicans* and *C. parapsilosis* with inhibition zone of (29 mm) (25 mm) and (21 mm). While in 500µg/ml concentration the high inhibition effect of ZnONPs which presented in *C. lusitaniae* with inhibition zone of (31 mm) *C. glabrata* and *C. krusei* with inhibition zone of (22mm), while low effect was on *C. albicans* and *C. parapsilosis* with inhibition zone of (20mm) and (18mm).

But at 250 µg/ml, the high inhibition effect of ZnONPs which presented in *C. lusitaniae* and *C. glabrata* with inhibition zone of (25 mm) and (20mm) respectively. While the low effect in *C. albicans*, *C. krusei* and *C. parapsilosis* with growth rate (17mm) (15mm) and (14mm).

At 125µg/ml ZnONPs showed high inhibition effect against *C. lusitaniae*, with inhibition zone of (21mm). followed by *C. albicans* and *C. glabrata* with inhibition zone (15 mm). While found low effect of ZnONPs was on *C. parapsilosis* and *C. krusei* with inhibition zone of (11 mm) and (10mm). In 62.5 µg/ml concentration found the high inhibition effect of ZnONPs which presented in *C. lusitaniae*, with inhibition zone of (16mm). *C. parapsilosis* and *C. krusei* are resistance effect to ZnONPs.

The sensitivity of *C.albicans* was sensitive to ZnONPs in our study, which is similar to the results of (Jalal *et al.*, 2018) a maximum zone of inhibition (23 mm) was recorded for *C. albicans* at highest concentration (1000 ug/ml). The findings correlate with the study conducted by Abd & Ali (2015) which demonstrated that *Candida albicans* exhibited sensitivity to various concentrations of zinc oxide nanoparticles. Specifically, *Candida albicans* displayed sensitivity to all concentrations (0.01, 0.05, 0.1, 0.5, 1, 3, and 5.8 mg/ml) of the zinc oxide nanoparticles solution. However, it is important to highlight that at a concentration of 1 mg/ml, the inhibition zones measured 14 mm in their study, whereas our results indicated larger diameters for the inhibition zone at the same concentration.

The study conducted by Yousef & Danial (2013) investigated the antimicrobial efficacy of zinc oxide (ZnO) nanoparticles against *Candida albicans*. The researchers demonstrated that ZnO nanoparticles exhibited an inhibitory zone measuring 18 mm. In the present investigation, the average diameters of the inhibitory zone resulting from the application of zinc nanoparticles were measured to be 25 mm.

Similar anticandidal activity of green synthesized zinc oxide nanoparticles (ZnO NPS) from zinc acetate solution by using lemon peels aqueous extract has also been reported by Metwally *et al.*,(2022) the highest zone of inhibition (24.5 mm) was observed for *C. glabrata*, followed by *C. albicans* (19.5 mm), while the lowest zone of inhibition (16.0 mm) was reported for *C. krusei* at a concentration of 0.5 mg/ml. In a study by Ahmadpour Kermani *et al.*, (2021) disagreed with our findings by reporting no growth inhibition was detected when concentrations of 1024 µg/mL of ZnO-NPs were used for *C. parapsilosis*, *C. lusitaniae*, *C. albicans*, and *C. krusei*.

Table (4-7) Zone of inhibition of ZnO-NPs at various concentrations against different *Candida* species (mm).

<i>Candida</i> species	Concentration of ZnONPs (µg/ml)				
	1000	500	250	125	62.5
<i>C. albicans</i>	25	20	17	15	12
<i>C. glabrata</i>	30	22	20	15	13
<i>C. parapsilosis</i>	21	18	14	11	6
<i>C. krusei</i>	29	22	15	10	5
<i>C. lusitaniae</i>	39	31	25	21	16

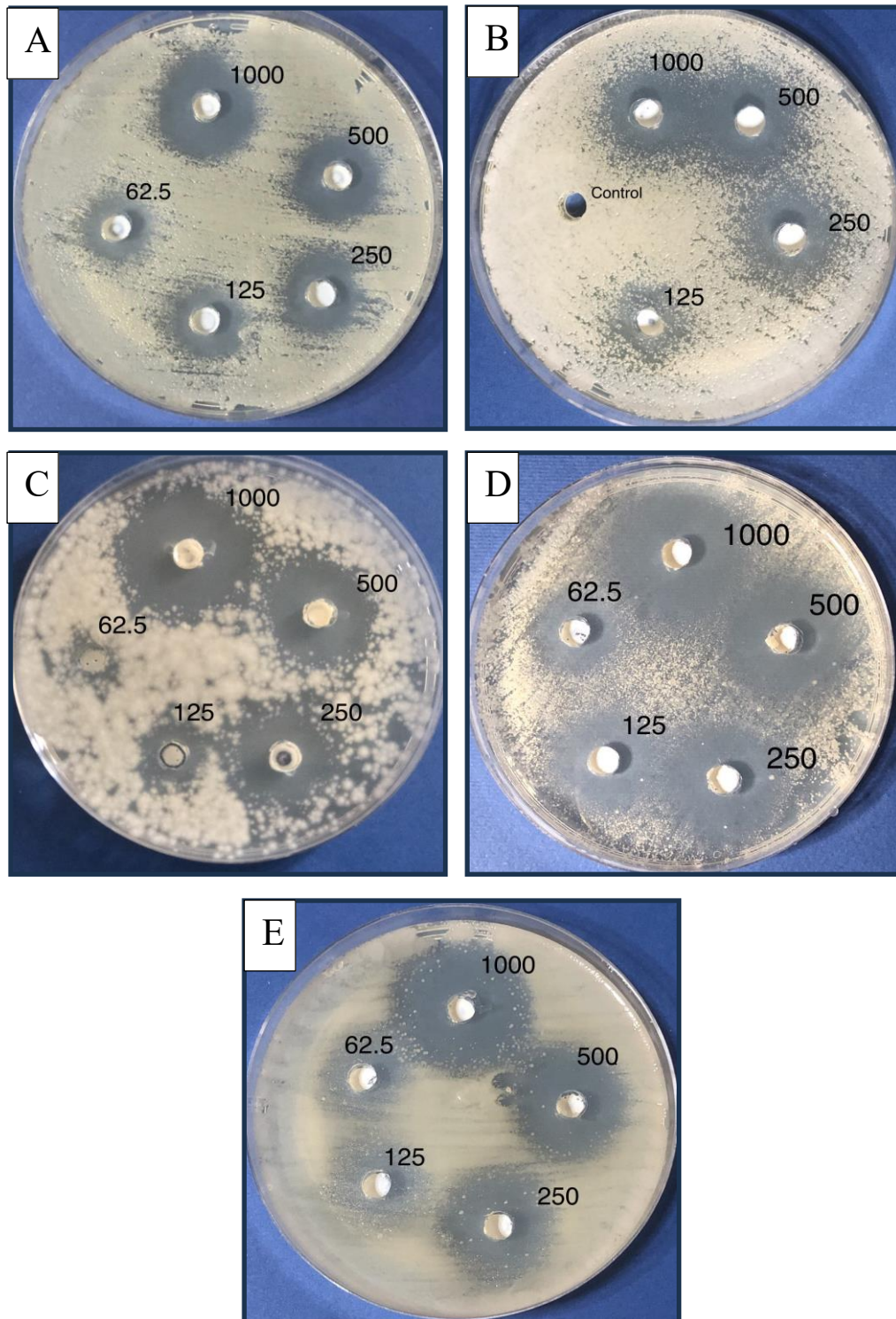


Figure (4-36) Zone of inhibition of ZnO-NPs at various concentrations against different *Candida* species. A- *C. albicans*, B- *C. parapsilosis*, C- *C. krusei*, D- *C. lusitaniae*, E- *C. glabrata*.

4.4.6: Inhibitory effect of FLU against *Candida* species by agar plate well diffusion assay

The susceptibility testing of Fluconazole, in accordance with the Clinical and Laboratory Standards Institute (CLSI) standard, categorises antifungal medications as susceptible (S) if the zone diameter is greater than or equal to 19 mm, intermediate if the zone diameter ranges from 15 to 18 mm, and resistant (R) if the zone diameter is less than or equal to 14 mm. The investigation focused on determining the resistance or sensitivity of the isolated *Candida* spp. to fluconazole. The findings indicated that the previously mentioned strains exhibited resistance to the antifungal compounds, while some strains shown semi-sensitivity and sensitivity. At 1000 µg/ml the highest inhibitory effect of FLU was against *C. parapsilosis*, *C. glabrata*, *C. lusitaniae*, and *C. krusei* respectively, while the *C. albicans* was intermediate sensitive to FLU. FLU compare to ZnONPs and IONPs the diameter of the growth inhibition zone of *C. parapsilosis* higher than nanoparticles. While in 500 µg/ml concentration *C. parapsilosis*, *C. glabrata*, *C. lusitaniae*, and *C. krusei* were sensitive just *C. albicans* was resistant. But in 250 µg/ml concentration *C. parapsilosis* and *C. glabrata* were sensitive. But *C. lusitaniae*, and *C. krusei* were intermediate sensitive to FLU and *C. albicans* was resistant. In 125 µg/ml concentration just *C. parapsilosis* was sensitive, but found the other *Candida* spp. become resistant to FLU. While in 62.5 µg/ml concentration of FLU found the five *Candida* spp. were resistance.

Table (4-8) Zone of inhibition of FLU at various concentrations against different *Candida* species (mm)

<i>Candida</i> species	Concentration of FLU(µg/ml)				
	1000	500	250	125	62.5
<i>C. albicans</i>	15	11	3	0	0
<i>C. glabrata</i>	31	24	19	14	12
<i>C. parapsilosis</i>	40.5	34	29	20	13
<i>C. krusei</i>	23	20.5	16	12	6.5
<i>C. lusitaniae</i>	25	21	17	14	9

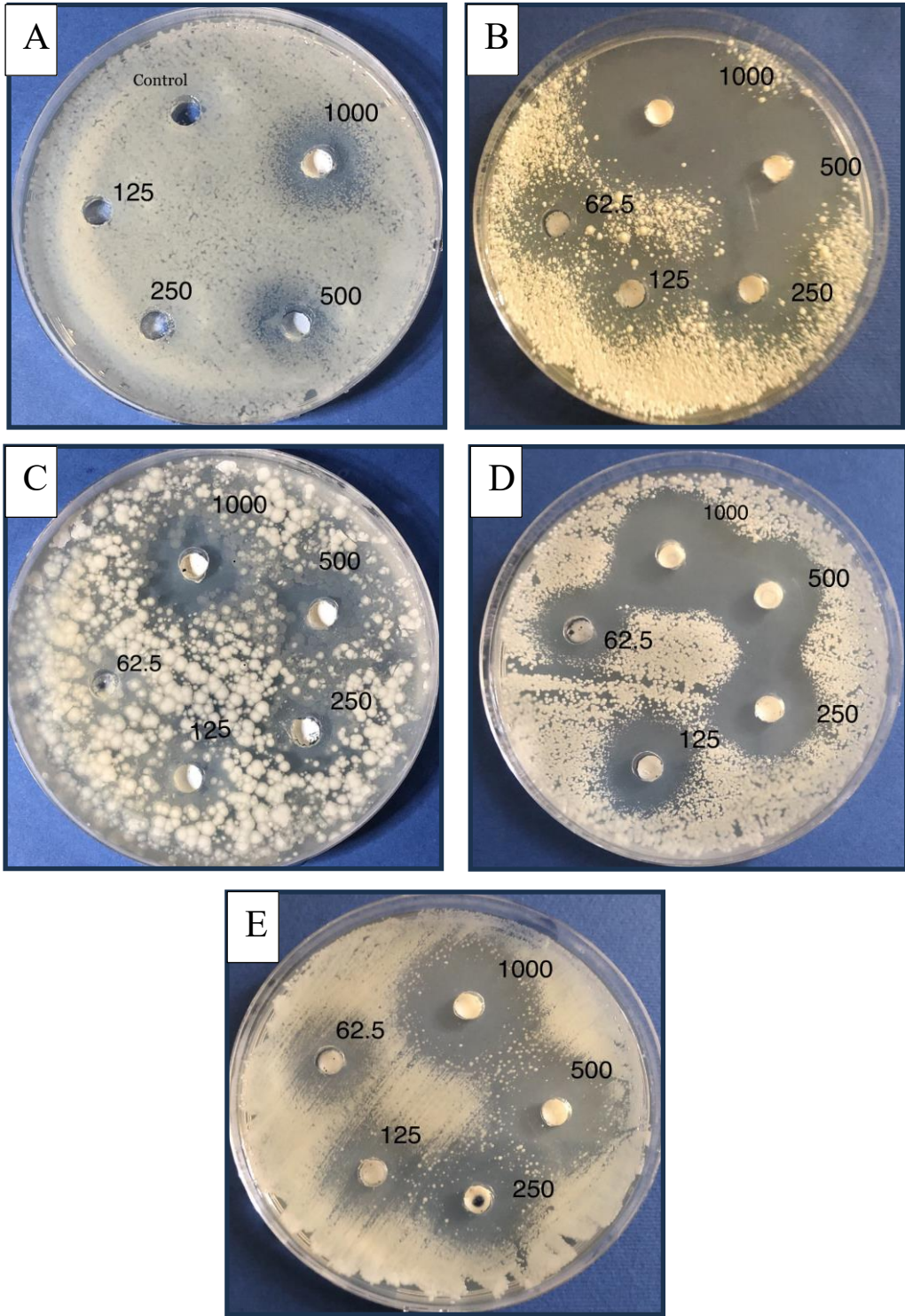


Figure (4-37) Zone of inhibition of FLU at various concentrations against different *Candida* species. A- *C. albicans*, B- *C. parapsilosis*, C- *C. krusei*, D- *C. lusitaniae*, E- *C. glabrata*.

Chapter Five

Conclusions

&

Recommendations

5.1. Conclusions

1- This investigation indicated that the air within the hospital exhibited a general state of contamination.

2-Different types of fungi can cause different pathogenicity, and the body's mechanisms for defence is the key to avoiding fungal infections. Various types of fungi, including filamentous fungi and yeasts were found to contaminate all of the wards. *Candida* is the most common species isolated, followed by *Aspergillus* as the second most common.

3- Sequencing of the internal transcribed spacer (ITS) enables rapid and accurate identification of fungal *Candida* spp. Strains of fungi can be distinguished based on their genetic variation within the ITS region.

4-With the use of XRD pattern for zinc oxide nanoparticles, the prominent peak was 36.24° demonstrated the high purity of zinc oxide nanoparticles. While the XRD pattern for iron oxide nanoparticles the prominent peak was 35.42° demonstrated the high purity of zinc oxide nanoparticles.

5-SEM showed aggregation surface morphology for ZnO-NPs and IONPs which has spherical surface morphology.

6- *Candida* spp. isolates were susceptible to ZnO-NPs and IONPs and the inhibition rate increases with the increase of concentration, while there is resistance of *Candida albicans* to the fluconazole antifungal.

5.2. Recommendations

1-To prevent nosocomial infections, there is a need for more proper hygiene and ongoing nosocomial pathogen monitoring through investing in good ventilation systems, disinfecting the floors regularly, restoration of the buildings, checking the air and ventilation mechanisms regularly, and reduction in visitors.

2- Study of nanoparticles activity against different fungal infection.

3- Study the effects of ZnONPs and IONPs on virulence factor of pathogenic fungi.

4- There is a need for further studies on natural target cells, such as in vivo studies on mouse models to clarify whether nanoparticles could be applicable as an alternative antifungal.

5- Study the ZnONPs and IONPs effected on production of cytokines.

References

References

- Abbasi, F., & Samaei, M. R. (2019). The effect of temperature on airborne filamentous fungi in the indoor and outdoor space of a hospital. *Environmental Science and Pollution Research International*, 26(17), 16868–16876. <https://doi.org/10.1007/s11356-017-0939-5>
- Abd, S. T., & Ali, A. F. (2015). *EFFECT OF ZINC OXIDE NANOPARTICLES ON CANDIDA ALBICANS OF HUMAN SALIVA (IN VITRO STUDY)*.
- Abdeen, S., Isaac, R., Geo, S., S., S., Rose, A., & P.K, P. (2013). Evaluation of Antimicrobial Activity of Biosynthesized Iron and Silver Nanoparticles Using the Fungi Fusarium Oxysporum and Actinomycetes SP. on Human Pathogens. *Nano Biomedicine and Engineering*, 5. <https://doi.org/10.5101/nbe.v5i1.p39-45>
- Ahmadpour Kermani, S., Salari, S., & Ghasemi Nejad Almani, P. (2021). Comparison of antifungal and cytotoxicity activities of titanium dioxide and zinc oxide nanoparticles with amphotericin B against different Candida species: In vitro evaluation. *Journal of Clinical Laboratory Analysis*, 35(1), e23577. <https://doi.org/10.1002/jcla.23577>
- Akeme Yamamoto, A. C., Rodrigues de Paula, C., Basili Dias, L., Tadano, T., Rodrigues Martins, É., Vasconcelos Ribeiro de Souza Amadio, J., & Hahn, R. C. (2012). Epidemiological and clinical characteristics of nosocomial candidiasis in university hospitals in Cuiabá – Mato Grosso, Brazil. *Revista Iberoamericana de Micología*, 29(3), 164–168. <https://doi.org/10.1016/j.riam.2012.01.001>
- Al-Bader, S. M., Ismael, L. Q., & Ahmood, A. A. (2018). Fungal Contamination of Airconditioner Units in Five Hospitals of Erbil Province- Kurdistan Region

- /Iraq. *Science Journal of University of Zakho*, 6(4), Article 4.
<https://doi.org/10.25271/sjuoz.2018.6.4.545>
- AL-Husseini, A. H., & Al-araji, B. T. S. and A. M. (2021). Effect Of Iron Oxide Nanoparticles (Fe₂O₃) On Candida Albicans And Candida Glabrata. *NVEO - NATURAL VOLATILES & ESSENTIAL OILS Journal / NVEO*, 12394–12405.
- Alothman, N. H. A. (2012). *Genotype Comparison of Strains of Candida albicans from Patients with Cutaneous Candidiasis in Nablus Area. M. Sc. Thesis. University of An-Najaf National.*
- Arsène, M. M. J., Viktorovna, P. I., Alla, M., Mariya, M., Nikolaevitch, S. A., Davares, A. K. L., Yurievna, M. E., Rehailia, M., Gabin, A. A., Alekseevna, K. A., Vyacheslavovna, Y. N., Vladimirovna, Z. A., Svetlana, O., & Milana, D. (2023). Antifungal activity of silver nanoparticles prepared using Aloe vera extract against Candida albicans. *Veterinary World*, 16(1), 18–26.
<https://doi.org/10.14202/vetworld.2023.18-26>
- Aslam, S., Tahir, A., Aslam, M. F., Alam, M. W., Shedayi, A. A., & Sadia, S. (2017). Recent advances in molecular techniques for the identification of phytopathogenic fungi – a mini review. *Journal of Plant Interactions*, 12(1), 493–504. <https://doi.org/10.1080/17429145.2017.1397205>
- Awwad, A. M., & Salem, N. M. (2012). A Green and Facile Approach for Synthesis of Magnetite Nanoparticles. *Nanoscience and Nanotechnology*, 2(6), 208–213.
- Babič, M. N., Zupančič, J., Gunde-Cimerman, N., de Hoog, S., & Zalar, P. (2018). Ecology of the Human Opportunistic Black Yeast *Exophiala dermatitidis* Indicates Preference for Human-Made Habitats. *Mycopathologia*, 183(1), 201–212. <https://doi.org/10.1007/s11046-017-0134-8>

- Balajee, S. A. (2009). *Aspergillus terreus* complex. *Medical Mycology*, *47 Suppl 1*, S42-46. <https://doi.org/10.1080/13693780802562092>
- Baldin, C., & Ibrahim, A. S. (2017). Molecular mechanisms of mucormycosis—The bitter and the sweet. *PLOS Pathogens*, *13*(8), e1006408. <https://doi.org/10.1371/journal.ppat.1006408>
- Bamrungsap, S., Zhao, Z., Chen, T., Wang, L., Li, C., Fu, T., & Tan, W. (2012). Nanotechnology in therapeutics: A focus on nanoparticles as a drug delivery system. *Nanomedicine (London, England)*, *7*(8), 1253–1271. <https://doi.org/10.2217/nnm.12.87>
- Barac, A., Ong, D. S. Y., Jovancevic, L., Peric, A., Surda, P., Tomic Spiric, V., & Rubino, S. (2018). Fungi-Induced Upper and Lower Respiratory Tract Allergic Diseases: One Entity. *Frontiers in Microbiology*, *9*, 583. <https://doi.org/10.3389/fmicb.2018.00583>
- Barbedo, L. S., Figueiredo-Carvalho, M. H. G., Muniz, M. de M., & Zancopé-Oliveira, R. M. (2016). The identification and differentiation of the *Candida parapsilosis* complex species by polymerase chain reaction-restriction fragment length polymorphism of the internal transcribed spacer region of the rDNA. *Memórias Do Instituto Oswaldo Cruz*, *111*(4), 267–270. <https://doi.org/10.1590/0074-02760150466>
- Barker, K. S., & Rogers, P. D. (2006). Recent insights into the mechanisms of antifungal resistance. *Current Infectious Disease Reports*, *8*(6), 449–456. <https://doi.org/10.1007/s11908-006-0019-3>
- Bastos, R. W., Valero, C., Silva, L. P., Schoen, T., Drott, M., Brauer, V., Silva-Rocha, R., Lind, A., Steenwyk, J. L., Rokas, A., Rodrigues, F., Resendiz-Sharpe, A., Lagrou, K., Marcet-Houben, M., Gabaldón, T., McDonnell, E., Reid, I., Tsang,

- A., Oakley, B. R., ... Goldman, G. H. (2020). Functional Characterization of Clinical Isolates of the Opportunistic Fungal Pathogen *Aspergillus nidulans*. *MSphere*, 5(2), 10.1128/msphere.00153-20. <https://doi.org/10.1128/msphere.00153-20>
- Branchini, M. L., Pfaller, M. A., Rhine-Chalberg, J., Frempong, T., & Isenberg, H. D. (1994). Genotypic variation and slime production among blood and catheter isolates of *Candida parapsilosis*. *Journal of Clinical Microbiology*, 32(2), 452–456. <https://doi.org/10.1128/jcm.32.2.452-456.1994>
- Brandelli, A. (2012). Nanostructures as promising tools for delivery of antimicrobial peptides. *Mini Reviews in Medicinal Chemistry*, 12(8), 731–741. <https://doi.org/10.2174/138955712801264774>
- Brion, L. P., Uko, S. E., & Goldman, D. L. (2007). Risk of resistance associated with fluconazole prophylaxis: Systematic review. *The Journal of Infection*, 54(6), 521–529. <https://doi.org/10.1016/j.jinf.2006.11.017>
- Burnik, C., Altintas, N. D., Ozkaya, G., Serter, T., Selçuk, Z. T., Firat, P., Arıkan, S., Cuenca-Estrella, M., & Topeli, A. (2007). Acute respiratory distress syndrome due to *Cryptococcus albidus* pneumonia: Case report and review of the literature. *Medical Mycology*, 45(5), 469–473. <https://doi.org/10.1080/13693780701386015>
- Byadarahally Raju, S., & Rajappa, S. (2011). Isolation and Identification of *Candida* from the Oral Cavity. *ISRN Dentistry*, 2011, 487921. <https://doi.org/10.5402/2011/487921>
- Caggiano, G., Lovero, G., De Giglio, O., Barbuti, G., Montagna, O., Laforgia, N., & Montagna, M. T. (2017). Candidemia in the Neonatal Intensive Care Unit: A

- Retrospective, Observational Survey and Analysis of Literature Data. *BioMed Research International*, 2017, 7901763. <https://doi.org/10.1155/2017/7901763>
- Caggiano, G., Napoli, C., Coretti, C., Lovero, G., Scarafilo, G., De Giglio, O., & Montagna, M. T. (2014). Mold contamination in a controlled hospital environment: A 3-year surveillance in southern Italy. *BMC Infectious Diseases*, 14, 595. <https://doi.org/10.1186/s12879-014-0595-z>
- Calumby, R. J. N., Silva, J. A., Silva, D. P. da, Moreira, R. T. de F., Araujo, M. A. dos S., Almeida, L. M. de, Grillo, L. A. M., & Alvino, V. (2019). Isolamento e identificação da microbiota fúngica anemófila em Unidade de Terapia Intensiva/ Isolation and identification of anemophilic fungal microbiota in an Intensive Care Unit. *Brazilian Journal of Development*, 5(10), Article 10. <https://doi.org/10.34117/bjdv5n10-186>
- Cannon, R. D., Lamping, E., Holmes, A. R., Niimi, K., Baret, P. V., Keniya, M. V., Tanabe, K., Niimi, M., Goffeau, A., & Monk, B. C. (2009). Efflux-mediated antifungal drug resistance. *Clinical Microbiology Reviews*, 22(2), 291–321, Table of Contents. <https://doi.org/10.1128/CMR.00051-08>
- Carmen V., S. (2017, April). *Atlas of Clinically Important Fungi* | Wiley. Wiley.Com. <https://www.wiley.com/en-us/Atlas+of+Clinically+Important+Fungi-p-9781119069669>
- Charles, M. P., Noyal, M. J., Easow, J. M., & M, R. (2011). Invasive pulmonary aspergillosis caused by *Aspergillus versicolor* in a patient on mechanical ventilation. *The Australasian Medical Journal*, 4(11), 632–634. <https://doi.org/10.4066/AMJ.2011.905>

- Cheon, J. Y., Kim, S. J., Rhee, Y. H., Kwon, O. H., & Park, W. H. (2019). Shape-dependent antimicrobial activities of silver nanoparticles. *International Journal of Nanomedicine*, *14*, 2773–2780. <https://doi.org/10.2147/IJN.S196472>
- Choi, S., Son, H.-J., Jung, J., Jae Kim, M., Pil Chong, Y., Lee, S.-O., Choi, S.-H., Hee Woo, J., Soo Kim, Y., & Kim, S.-H. (2019). 1703. Bacterial or Fungal Co-Infection in Patients with Mucormycosis. *Open Forum Infectious Diseases*, *6*(Supplement_2), S623–S624. <https://doi.org/10.1093/ofid/ofz360.1567>
- Chopra, S., Mahajan, G., & Singh, Y. (2020a). *Monitoring of Airborne Fungi in a Hospital Unit*. *31*(1).
- Chopra, S., Mahajan, G., & Singh, Y. (2020b). *Monitoring of Airborne Fungi in a Hospital Unit*. *31*(1).
- Cordeiro, R. A., Brilhante, R. S. N., Pantoja, L. D. M., Moreira Filho, R. E., Vieira, P. R. N., Rocha, M. F. G., Monteiro, A. J., & Sidrim, J. J. C. (2010). Isolation of pathogenic yeasts in the air from hospital environments in the city of Fortaleza, northeast Brazil. *The Brazilian Journal of Infectious Diseases: An Official Publication of the Brazilian Society of Infectious Diseases*, *14*(1), 30–34. <https://doi.org/10.1590/s1413-86702010000100007>
- Costa, C., Ribeiro, J., Miranda, I. M., Silva-Dias, A., Cavalheiro, M., Costa-de-Oliveira, S., Rodrigues, A. G., & Teixeira, M. C. (2016). Clotrimazole Drug Resistance in *Candida glabrata* Clinical Isolates Correlates with Increased Expression of the Drug:H⁺ Antiporters CgAqr1, CgTpo1_1, CgTpo3, and CgQdr2. *Frontiers in Microbiology*, *7*, 526. <https://doi.org/10.3389/fmicb.2016.00526>
- Deak, E., Wilson, S. D., White, E., Carr, J. H., & Balajee, S. A. (2009). *Aspergillus terreus* Accessory Conidia Are Unique in Surface Architecture, Cell Wall

- Composition and Germination Kinetics. *PLOS ONE*, 4(10), e7673.
<https://doi.org/10.1371/journal.pone.0007673>
- Delavy, M., Dos Santos, A. R., Heiman, C. M., & Coste, A. T. (2019). Investigating Antifungal Susceptibility in *Candida* Species With MALDI-TOF MS-Based Assays. *Frontiers in Cellular and Infection Microbiology*, 9, 19.
<https://doi.org/10.3389/fcimb.2019.00019>
- Demirel, R., Sen, B., Kadaifciler, D., Yoltas, A., Okten, S., Ozkale, E., Berikten, D., Samson, R. A., Haliki Uztan, A., Yilmaz, N., Abaci Gunyar, O., Aydogdu, H., Asan, A., Kivanc, M., Ozdil, S., & Sakartepe, E. (2017). Indoor airborne fungal pollution in newborn units in Turkey. *Environmental Monitoring and Assessment*, 189(7), 362. <https://doi.org/10.1007/s10661-017-6051-y>
- Deorukhkar, S. C., & Saini, S. (2015). Virulence factors attributed to pathogenicity of non albicans *Candida* species isolated from Human Immunodeficiency virus infected patients with oropharyngeal candidiasis. *Annals of Pathology and Laboratory Medicine*, 2(2), Article 2.
- Deorukhkar, S. C., & Saini, S. (2016). Why *Candida* Species have Emerged as Important Nosocomial Pathogens? *International Journal of Current Microbiology and Applied Sciences*, 5(1), 533–545.
<https://doi.org/10.20546/ijcmas.2016.501.054>
- Deorukhkar, S., & Saini, S. (2013). Evaluation of Phospholipase Activity in Biofilm Forming *Candida* Species Isolated from Intensive Care Unit Patients. *Microbiology Research Journal International*, 440–447.
<https://doi.org/10.9734/BMRJ/2013/4359>
- Devi, R. S., & Gayathri, R. (2014). Green Synthesis of Zinc Oxide Nanoparticles by using *Hibiscus rosa-sinensis*. 4, 2444–2446.

- Di Filippo, P., Pomata, D., Riccardi, C., Buiarelli, F., & Perrino, C. (2013). Fungal contribution to size-segregated aerosol measured through biomarkers. *Atmospheric Environment*, *64*, 132–140. <https://doi.org/10.1016/j.atmosenv.2012.10.010>
- Diba, K., P, K., SH, M., Rezaie, S., & Mahmoudi, M. (2007, December). *Identification of aspergillus species using morphological characteristics*. <https://www.pjms.com.pk/issues/octdec207/article/article9.html>
- Diekema, D., Arbefeville, S., Boyken, L., Kroeger, J., & Pfaller, M. (2012). The changing epidemiology of healthcare-associated candidemia over three decades. *Diagnostic Microbiology and Infectious Disease*, *73*(1), 45–48. <https://doi.org/10.1016/j.diagmicrobio.2012.02.001>
- Dissanayake, N. M., Current, K. M., & Obare, S. O. (2015). Mutagenic Effects of Iron Oxide Nanoparticles on Biological Cells. *International Journal of Molecular Sciences*, *16*(10), 23482–23516. <https://doi.org/10.3390/ijms161023482>
- Dizaj, S. M., Vazifehasl, Zh., Salatin, S., Adibkia, Kh., & Javadzadeh, Y. (2015). Nanosizing of drugs: Effect on dissolution rate. *Research in Pharmaceutical Sciences*, *10*(2), 95–108.
- Djearamane, S., Ling Shing, W., Yang Mooi, L., & Lee, P. F. (2020). Oxidative stress effects of zinc oxide nanoparticles on fresh water microalga *Haematococcus pluvialis*. *Ecology, Environment and Conservation*, *26*, 2020–2663.
- Eghtedar Nejad, E., Ghasemi Nejad Almani, P., Mohammadi, M. A., & Salari, S. (2020). Molecular identification of *Candida* isolates by Real-time PCR-high-resolution melting analysis and investigation of the genetic diversity of *Candida* species. *Journal of Clinical Laboratory Analysis*, *34*(10), e23444. <https://doi.org/10.1002/jcla.23444>

Ellis, D., Davis, S., Alexiou, H., Handke, R., & Bartley, R. (2007). *DESCRIPTIONS OF MEDICAL FUNGI*.

Eskandari, M., Ahmadi, V., & Ahmadi, SH. (2009). Low temperature synthesis of ZnO nanorods by using PVP and their characterization. *Physica B: Condensed Matter*, 404(14), 1924–1928. <https://doi.org/10.1016/j.physb.2009.03.024>

Ezealigo, U. S., Ezealigo, B. N., Aisida, S. O., & Ezema, F. I. (2021). Iron oxide nanoparticles in biological systems: Antibacterial and toxicology perspective. *JCIS Open*, 4, 100027. <https://doi.org/10.1016/j.jciso.2021.100027>

Ezenwa, B. N., Oladele, R. O., Akintan, P. E., Fajolu, I. B., Oshun, P. O., Oduyebo, O. O., & Ezeaka, V. C. (2017). Invasive candidiasis in a neonatal intensive care unit in Lagos, Nigeria. *The Nigerian Postgraduate Medical Journal*, 24(3), 150–154. https://doi.org/10.4103/npmj.npmj_104_17

Fernstrom, A., & Goldblatt, M. (2013). Aerobiology and Its Role in the Transmission of Infectious Diseases. *Journal of Pathogens*, 2013, e493960. <https://doi.org/10.1155/2013/493960>

Gangneux, J.-P., Bougnoux, M.-E., Hennequin, C., Godet, C., Chandenier, J., Denning, D. W., Dupont, B., & LIFE program, the Société française de mycologie médicale SFMM-study group. (2016). An estimation of burden of serious fungal infections in France. *Journal De Mycologie Medicale*, 26(4), 385–390. <https://doi.org/10.1016/j.mycmed.2016.11.001>

García-Carnero, L. C., & Mora-Montes, H. M. (2022). Mucormycosis and COVID-19-Associated Mucormycosis: Insights of a Deadly but Neglected Mycosis. *Journal of Fungi*, 8(5), Article 5. <https://doi.org/10.3390/jof8050445>

García-Suárez, J., Gómez-Herruz, P., Cuadros, J. A., & Burgaleta, C. (2011). Epidemiology and outcome of *Rhodotorula* infection in haematological

- patients. *Mycoses*, 54(4), 318–324. <https://doi.org/10.1111/j.1439-0507.2010.01868.x>
- Gibbons, J. G., & Rokas, A. (2013). The function and evolution of the *Aspergillus* genome. *Trends in Microbiology*, 21(1), 14–22. <https://doi.org/10.1016/j.tim.2012.09.005>
- Golah, H. A., Al-Garadi, M. A., Salah, M., Baghza, N., Al-Mahdi, H., Al-Dhorani, M., & Al-Sharma, A. (2017). Isolation and Identification of Airborne Pathogenic Fungi from the Hospitals at Dhamar Governorate, Yemen. *International Journal of Microbiology and Biotechnology*, 2(4), Article 4. <https://doi.org/10.11648/j.ijmb.20170204.13>
- Gonçalves, C. L., Fv, M., Gf, F., Jf, M., Ec, P., Ch, F., Jn, V., Jp, V., & Ps, N. (2018). Airborne fungi in an intensive care unit. *Brazilian Journal of Biology = Revista Brasileira de Biologia*, 78(2). <https://doi.org/10.1590/1519-6984.06016>
- Gong, J., Xiao, M., Wang, H., Kudinha, T., Wang, Y., Zhao, F., Wu, W., He, L., Xu, Y.-C., & Zhang, J. (2018). Genetic Differentiation, Diversity, and Drug Susceptibility of *Candida krusei*. *Frontiers in Microbiology*, 9. <https://www.frontiersin.org/articles/10.3389/fmicb.2018.02717>
- Gontero, D., Lessard-Viger, M., Brouard, D., Bracamonte, A., Boudreau, D., & Veglia, A. (2017). Smart multifunctional nanoparticles design as sensors and drug delivery systems based on supramolecular chemistry. *Microchemical Journal*, 130, 316–328. <https://doi.org/10.1016/j.microc.2016.10.007>
- Gopal, K. A., Kalaivani, V., & Anandan, H. (2020). Pulmonary Infection by *Chrysosporium* Species in a Preexisting Tuberculous Cavity. *International Journal of Applied and Basic Medical Research*, 10(1), 62–64. https://doi.org/10.4103/ijabmr.IJABMR_382_18

- Gudkov, S. V., Burmistrov, D. E., Serov, D. A., Rebezov, M. B., Semenova, A. A., & Lisitsyn, A. B. (2021). Do Iron Oxide Nanoparticles Have Significant Antibacterial Properties? *Antibiotics*, *10*(7), Article 7. <https://doi.org/10.3390/antibiotics10070884>
- Gudlaugsson, O., Gillespie, S., Lee, K., Vande Berg, J., Hu, J., Messer, S., Herwaldt, L., Pfaller, M., & Diekema, D. (2003). Attributable mortality of nosocomial candidemia, revisited. *Clinical Infectious Diseases: An Official Publication of the Infectious Diseases Society of America*, *37*(9), 1172–1177. <https://doi.org/10.1086/378745>
- Guo, Y., Ge, S., Luo, H., Rehman, A., Li, Y., & He, S. (2020). Occurrence of *Trichophyton verrucosum* in cattle in the Ningxia Hui autonomous region, China. *BMC Veterinary Research*, *16*(1), 187. <https://doi.org/10.1186/s12917-020-02403-6>
- Ha, J. F., Italiano, C. M., Heath, C. H., Shih, S., Rea, S., & Wood, F. M. (2011). Candidemia and invasive candidiasis: A review of the literature for the burns surgeon. *Burns*, *37*(2), 181–195. <https://doi.org/10.1016/j.burns.2010.01.005>
- Hadi, H., & Jassim Alsultany, S. (2020). *Isolation and identification Candida species among renal failure Iraqi patients.*
- Hagen, F., Lumbsch, H. T., Arsic Arsenijevic, V., Badali, H., Bertout, S., Billmyre, R. B., Bragulat, M. R., Cabañes, F. J., Carbia, M., Chakrabarti, A., Chaturvedi, S., Chaturvedi, V., Chen, M., Chowdhary, A., Colom, M.-F., Cornely, O. A., Crous, P. W., Cuétara, M. S., Diaz, M. R., ... Boekhout, T. (2017). Importance of Resolving Fungal Nomenclature: The Case of Multiple Pathogenic Species in the *Cryptococcus* Genus. *MSphere*, *2*(4), e00238-17. <https://doi.org/10.1128/mSphere.00238-17>

- Henriet, S. S. V., Verweij, P. E., & Warris, A. (2012). *Aspergillus nidulans* and chronic granulomatous disease: A unique host-pathogen interaction. *The Journal of Infectious Diseases*, *206*(7), 1128–1137. <https://doi.org/10.1093/infdis/jis473>
- Hosseini SS, Mohammadi Sh, Joshaghani HR, & Eskandari M. (2011). Antifungal effect of Sodium Dodecil Sulfate and Nano particle ZnO on growth inhibition of standard strain of *Candida albicans*. *Journal of Gorgan University of Medical Sciences*, *12*(4), 64–69.
- Howell, A., Isaacs, D., Halliday, R., & Australasian Study Group For Neonatal Infections. (2009). Oral nystatin prophylaxis and neonatal fungal infections. *Archives of Disease in Childhood. Fetal and Neonatal Edition*, *94*(6), F429-433. <https://doi.org/10.1136/adc.2008.157123>
- Huang, Y.-H., Lin, I.-H., Chang, T.-C., & Tseng, S.-H. (2015). Early Diagnosis and Successful Treatment of *Cryptococcus albicus* Keratitis. *Medicine*, *94*(19), e885. <https://doi.org/10.1097/MD.0000000000000885>
- Humphrey, J. M., Walsh, T. J., & Gulick, R. M. (2016). Invasive *Aspergillus* Sinusitis in Human Immunodeficiency Virus Infection: Case Report and Review of the Literature. *Open Forum Infectious Diseases*, *3*(3), ofw135. <https://doi.org/10.1093/ofid/ofw135>
- Jacob, J. H., Irshaid, F. I., & Alhalib, M. A. (2016). Estimation and Identification of Airborne Bacteria and Fungi in the Outdoor Atmosphere of Al-Mafraq Area—Jordan. *Jordan Journal of Biological Sciences*, *9*(1), 3–10. <https://doi.org/10.12816/0027002>
- Jacob Kizhakedathil, M. P., Koppula, A. R., & C., S. D. (2017). A Brief Review on Invasive Aspergillosis and the Host Immune Response and the Target Drugs. *Immunology, Endocrine & Metabolic Agents - Medicinal ChemistryCurrent*

- Medicinal Chemistry - Immunology, Endocrine & Metabolic Agents*), 17(1), 4–14. <https://doi.org/10.2174/1871522217666170706151211>
- Jalal, M., Ansari, M. A., Ali, S. G., Khan, H. M., & Rehman, S. (2018). Anticandidal activity of bioinspired ZnO NPs: Effect on growth, cell morphology and key virulence attributes of *Candida* species. *Artificial Cells, Nanomedicine, and Biotechnology*, 46(sup1), 912–925. <https://doi.org/10.1080/21691401.2018.1439837>
- Kamal, A., Saba, M., Kamal, A., Batool, M., Asif, M., Al-Mohaimed, A. M., Al Farraj, D. A., Habib, D., & Ahmad, S. (2023). Bioinspired Green Synthesis of Bimetallic Iron and Zinc Oxide Nanoparticles Using Mushroom Extract and Use against *Aspergillus niger*; The Most Devastating Fungi of the Green World. *Catalysts*, 13(2), Article 2. <https://doi.org/10.3390/catal13020400>
- Kano, R., Kitagawat, M., Oota, S., Oosumi, T., Murakami, Y., Tokuriki, M., & Hasegawa, A. (2008). First case of feline systemic *Cryptococcus albidus* infection. *Medical Mycology*, 46(1), 75–77. <https://doi.org/10.1080/13693780701541106>
- Karimiyan, A., Najafzadeh, H., Ghorbanpour, M., & Hekmati-Moghaddam, S. H. (2015). Antifungal Effect of Magnesium Oxide, Zinc Oxide, Silicon Oxide and Copper Oxide Nanoparticles Against *Candida albicans*. *Zahedan Journal of Research in Medical Sciences*, 17(10), Article 10. <https://doi.org/10.17795/zjrms-2179>
- Kaur, R., Mehra, B., Dhakad, M. S., Goyal, R., & Dewan, R. (2017). Pulmonary aspergillosis as opportunistic mycoses in a cohort of human immunodeficiency virus-infected patients: Report from a tertiary care hospital in North India. *International Journal of Health Sciences*, 11(2), 45–50.

- Kemoui, E. K. (2012). *ISOLATION AND CHARACTERIZATION OF YEAST FROM Gallus gallus*.
- Khan, I., Saeed, K., & Khan, I. (2019). Nanoparticles: Properties, applications and toxicities. *Arabian Journal of Chemistry*, 12(7), 908–931. <https://doi.org/10.1016/j.arabjc.2017.05.011>
- Khattab, A., & Levetin, E. (2008). Effect of sampling height on the concentration of airborne fungal spores. *Annals of Allergy, Asthma & Immunology: Official Publication of the American College of Allergy, Asthma, & Immunology*, 101(5), 529–534. [https://doi.org/10.1016/S1081-1206\(10\)60293-1](https://doi.org/10.1016/S1081-1206(10)60293-1)
- Khawcharoenporn, T., Apisarnthanarak, A., & Mundy, L. M. (2007). Non-neoformans Cryptococcal Infections: A Systematic Review. *Infection*, 35(2), 51. <https://doi.org/10.1007/s15010-007-6142-8>
- Kiasat, N., Fatahinia, M., Mahmoudabadi, A. Z., & Shokri, H. (2017). Qualitative and Quantitative Assessment of Airborne Fungal Spores in the Hospitals Environment of Ahvaz City (2016). *Jundishapur Journal of Microbiology*, 10(10), Article 10. <https://doi.org/10.5812/jjm.14143>
- Kidd, S., Halliday, C., & Ellis, D. (2022). *Descriptions of Medical Fungi* (4th ed.). CABI. <https://doi.org/10.1079/9781800622340.0000>
- Kim, K. Y., Kim, Y. S., & Kim, D. (2010). Distribution characteristics of airborne bacteria and fungi in the general hospitals of Korea. *Industrial Health*, 48(2), 236–243. <https://doi.org/10.2486/indhealth.48.236>
- Kojic, E. M., & Darouiche, R. O. (2004, April 1). *Candida Infections of Medical Devices / Clinical Microbiology Reviews*. <https://journals.asm.org/doi/10.1128/CMR.17.2.255-267.2004>

- Kołodziejczak-Radzimska, A., & Jesionowski, T. (2014). Zinc Oxide—From Synthesis to Application: A Review. *Materials*, 7(4), Article 4. <https://doi.org/10.3390/ma7042833>
- Kullberg, B. J., & Arendrup, M. C. (2015). Invasive Candidiasis. *The New England Journal of Medicine*, 373(15), 1445–1456. <https://doi.org/10.1056/NEJMra1315399>
- Kumar, D., Resident, S., Singhd, S., Sengupta, A., Sarfraz, A., & Bhattacharyya, S. (2020). ISOLATION OF FUNGUS FROM HOSPITAL ENVIRONMENT AND EQUIPMENTS IN A TERTIARY CARE HOSPITAL IN EASTERN INDIA Nahid Anjum* Senior Resident, Department of Microbiology, AIIMS Patna *Corresponding Author Sayan Bhattacharyya. *International Journal of Scientific Research*, 8.
- Kumar, H., & Rani, R. (2013). Structural and Optical Characterization of ZnO Nanoparticles Synthesized by Microemulsion Route. *International Letters of Chemistry, Physics and Astronomy*, Vol. 14, 26–36.
- Kumar, R., Nayak, M., Sahoo, G. C., Pandey, K., Sarkar, M. C., Ansari, Y., Das, V. N. R., Topno, R. K., Bhawna, null, Madhukar, M., & Das, P. (2019). Iron oxide nanoparticles based antiviral activity of H1N1 influenza A virus. *Journal of Infection and Chemotherapy: Official Journal of the Japan Society of Chemotherapy*, 25(5), 325–329. <https://doi.org/10.1016/j.jiac.2018.12.006>
- Lacerda, J. F., & Oliveira, C. M. (2013). Diagnosis and treatment of invasive fungal infections focus on liposomal amphotericin B. *Clinical Drug Investigation*, 33 Suppl 1, S5-14. <https://doi.org/10.1007/s40261-012-0023-3>
- Lail, N., Sattar, A., Omer, M. O., Hafeez, M. A., Khalid, A. R., Mahmood, S., Shabbir, M. A., Ahmed, W., Aleem, M. T., Alouffi, A., & Almutairi, M. M. (2023).

- Biosynthesis and characterization of zinc oxide nanoparticles using *Nigella sativa* against coccidiosis in commercial poultry. *Scientific Reports*, 13(1), Article 1. <https://doi.org/10.1038/s41598-023-33416-4>
- Lalueza, A., López-Medrano, F., del Palacio, A., Alhambra, A., Alvarez, E., Ramos, A., Pérez, A., Lizasoain, M., Meije, Y., García-Reyne, A., & Aguado, J. M. (2011). *Cladosporium macrocarpum* brain abscess after endoscopic ultrasound-guided celiac plexus block. *Endoscopy*, 43 Suppl 2 UCTN, E9-10. <https://doi.org/10.1055/s-0030-1255804>
- Latgé, J.-P., & Chamilos, G. (2019). *Aspergillus fumigatus* and Aspergillosis in 2019. *Clinical Microbiology Reviews*, 33(1), e00140-18. <https://doi.org/10.1128/CMR.00140-18>
- Le, T., Huu Chi, N., Kim Cuc, N. T., Sieu, T. P. M., Shikuma, C. M., Farrar, J., & Day, J. N. (2010). AIDS-Associated *Penicillium marneffeii* Infection of the Central Nervous System. *Clinical Infectious Diseases*, 51(12), 1458–1462. <https://doi.org/10.1086/657400>
- Li, X., Zhang, T., & Wang, S. (2019). Aerosolization of *Aspergillus niger* spores from colonies on different positions of a circular tube. *E3S Web of Conferences*, 111, 02030. <https://doi.org/10.1051/e3sconf/201911102030>
- Lobato, R., Vargas, V., & Silveira, É. (2009). Sazonalidade e prevalência de fungos anemófilos em ambiente hospitalar no Sul do Rio Grande do Sul, Brasil. *Revista Da Faculdade de Ciências Médicas de Sorocaba*, 11.
- Lockhart, S. R., Etienne, K. A., Vallabhaneni, S., Farooqi, J., Chowdhary, A., Govender, N. P., Colombo, A. L., Calvo, B., Cuomo, C. A., Desjardins, C. A., Berkow, E. L., Castanheira, M., Magobo, R. E., Jabeen, K., Asghar, R. J., Meis, J. F., Jackson, B., Chiller, T., & Litvintseva, A. P. (2017). Simultaneous

- Emergence of Multidrug-Resistant *Candida auris* on 3 Continents Confirmed by Whole-Genome Sequencing and Epidemiological Analyses. *Clinical Infectious Diseases: An Official Publication of the Infectious Diseases Society of America*, 64(2), 134–140. <https://doi.org/10.1093/cid/ciw691>
- Lockhart, S. R., Messer, S. A., Pfaller, M. A., & Diekema, D. J. (2008). Geographic distribution and antifungal susceptibility of the newly described species *Candida orthopsilosis* and *Candida metapsilosis* in comparison to the closely related species *Candida parapsilosis*. *Journal of Clinical Microbiology*, 46(8), 2659–2664. <https://doi.org/10.1128/JCM.00803-08>
- Lohrenz, S., Minion, J., Pandey, M., & Karunakaran, K. (2018). Blastomycosis in Southern Saskatchewan 2000-2015: Unique presentations and disease characteristics. *Medical Mycology*, 56(7), 787–795. <https://doi.org/10.1093/mmy/myx131>
- Lunardi, L. W., Aquino, V. R., Zimmerman, R. A., & Goldani, L. Z. (2006). Epidemiology and outcome of *Rhodotorula fungemia* in a tertiary care hospital. *Clinical Infectious Diseases: An Official Publication of the Infectious Diseases Society of America*, 43(6), e60-63. <https://doi.org/10.1086/507036>
- Lutzoni, F., Kauff, F., Cox, C. J., McLaughlin, D., Celio, G., Dentinger, B., Padamsee, M., Hibbett, D., James, T. Y., Baloch, E., Grube, M., Reeb, V., Hofstetter, V., Schoch, C., Arnold, A. E., Miadlikowska, J., Spatafora, J., Johnson, D., Hambleton, S., ... Vilgalys, R. (2004). Assembling the fungal tree of life: Progress, classification, and evolution of subcellular traits. *American Journal of Botany*, 91(10), 1446–1480. <https://doi.org/10.3732/ajb.91.10.1446>
- M. Abdulrasool, M., Nabeel Mustafa, A., Ahmed, M., W. Alwash, S., Taha Ibrahim, I., Jihad Hammady, F., & S. Abed, A. (2022). The Effectiveness of Chitosan-

- Coated Iron Oxide Nanoparticles as Antifungals against Various Candida Species. *Journal of Nanostructures*, 12(3), 718–725.
<https://doi.org/10.22052/JNS.2022.03.024>
- M. Bassam Aboul-Nasr, Abdel-Naser A. Zohri, & Enas Mahmoud Amer. (2014). Indoor Surveillance of Airborne Fungi Contaminating Intensive Care Units and Operation Rooms in Assiut University Hospitals, Egypt. *J. of Health Science*, 2(1). <https://doi.org/10.17265/2328-7136/2014.01.003>
- Maldonado-Vega, M., Peña-Cabriales, J. J., Castellanos-Arévalo, A. P., Camarena-Pozos, D., Arévalo-Rivas, B., & Valdés-Santiago, L. (2014). *BIOAEROSOLES Y EVALUACIÓN DE LA CALIDAD DEL AIRE EN DOS CENTROS HOSPITALARIOS UBICADOS EN LEÓN, GUANAJUATO, MÉXICO*. 30(4), 351–363.
- Marimuthu, S., Antonisamy, A. J., Malayandi, S., Rajendran, K., Tsai, P.-C., Pugazhendhi, A., & Ponnusamy, V. K. (2020). Silver nanoparticles in dye effluent treatment: A review on synthesis, treatment methods, mechanisms, photocatalytic degradation, toxic effects and mitigation of toxicity. *Journal of Photochemistry and Photobiology B: Biology*, 205, 111823.
<https://doi.org/10.1016/j.jphotobiol.2020.111823>
- Martin, K. J., & Rygiewicz, P. T. (2005). Fungal-specific PCR primers developed for analysis of the ITS region of environmental DNA extracts. *BMC Microbiology*, 5, 28. <https://doi.org/10.1186/1471-2180-5-28>
- Martínez-Herrera, E. O., Frías De-León, M. G., Duarte-Escalante, E., Calderón-Ezquerro, M. D. C., Jiménez-Martínez, M. D. C., Acosta-Altamirano, G., Rivera-Becerril, F., Toriello, C., & Reyes-Montes, M. D. R. (2016). Fungal diversity and *Aspergillus* in hospital environments. *Annals of Agricultural and*

- Environmental Medicine*, 23(2), 264–269.
<https://doi.org/10.5604/12321966.1203888>
- Matare, T., Nziramasanga, P., Gwanzura, L., & Robertson, V. (2017). Experimental Germ Tube Induction in *Candida albicans*: An Evaluation of the Effect of Sodium Bicarbonate on Morphogenesis and Comparison with Pooled Human Serum. *BioMed Research International*, 2017, 1976273.
<https://doi.org/10.1155/2017/1976273>
- McCarty, T. P., & Pappas, P. G. (2016). Invasive Candidiasis. *Infectious Disease Clinics of North America*, 30(1), 103–124.
<https://doi.org/10.1016/j.idc.2015.10.013>
- McGinnis, M. R., & Tying, S. K. (1996). Introduction to Mycology. In S. Baron (Ed.), *Medical Microbiology* (4th ed.). University of Texas Medical Branch at Galveston. <http://www.ncbi.nlm.nih.gov/books/NBK8125/>
- Metwally, R. S., M. H. Kheiralla, Z., M. Ashour, S., & S. Zaki, S. (2022). Anticandidal Activity of Green Synthesized Zinc Oxide Nanoparticles Using Lemon Peel Extract. *Journal of Scientific Research in Science*, 39(2), 62–81.
<https://doi.org/10.21608/jsrs.2022.275788>
- Miceli, A., & Krishnamurthy, K. (2023). Blastomycosis. In *StatPearls*. StatPearls Publishing. <http://www.ncbi.nlm.nih.gov/books/NBK441987/>
- Minnebruggen, G. V., Francois, I. E. J. A., Cammue, B. P. A., Thevissen, K., Vroome, V., Borgers, M., & Shroot, B. (2010). A General Overview on Past, Present and Future Antimycotics. *The Open Mycology Journal*, 4(1).
<https://benthamopen.com/ABSTRACT/TOMYCJ-4-22>
- Mitchell, M. J., Billingsley, M. M., Haley, R. M., Wechsler, M. E., Peppas, N. A., & Langer, R. (2021). Engineering precision nanoparticles for drug delivery.

Nature Reviews Drug Discovery, 20(2), Article 2.

<https://doi.org/10.1038/s41573-020-0090-8>

Moazeni, M., Asgari, S., & Nabili, M. (2018). *Nosocomial Fungal Infections: Epidemiology, Diagnosis, Treatment and Prevention*.

Montone, K. T. (2016). Pathology of Fungal Rhinosinusitis: A Review. *Head and Neck Pathology*, 10(1), 40–46. <https://doi.org/10.1007/s12105-016-0690-0>

Nakasone, K. K., Peterson, S. W., & Jong, S.-C. (2004). Preservation and distribution of fungal cultures. *Biodiversity of Fungi : Inventory and Monitoring Methods. Amsterdam : Elsevier Academic Press, 2004: Pages 37-47., 3.*
<https://www.fs.usda.gov/research/treesearch/7115>

NaPier, E., & Redd, T. (2022). Alternaria fungus growing on top of cyanoacrylate glue in a patient with perforated corneal ulcer. *American Journal of Ophthalmology Case Reports*, 28, 101717. <https://doi.org/10.1016/j.ajoc.2022.101717>

Napoli, C., Marcotrigiano, V., & Montagna, M. T. (2012). Air sampling procedures to evaluate microbial contamination: A comparison between active and passive methods in operating theatres. *BMC Public Health*, 12(1), 594. <https://doi.org/10.1186/1471-2458-12-594>

Narayanasamy, S., Dat, V. Q., Thanh, N. T., Ly, V. T., Chan, J. F.-W., Yuen, K.-Y., Ning, C., Liang, H., Li, L., Chowdhary, A., Youngchim, S., Supparatpinyo, K., Aung, N. M., Hanson, J., Andrianopoulos, A., Dougherty, J., Govender, N. P., Denning, D. W., Chiller, T., ... Le, T. (2021). A global call for talaromycosis to be recognised as a neglected tropical disease. *The Lancet Global Health*, 9(11), e1618–e1622. [https://doi.org/10.1016/S2214-109X\(21\)00350-8](https://doi.org/10.1016/S2214-109X(21)00350-8)

Nascimento, J. P. M. do, Santos, R. dos, Silva, M. S. dos S., Araújo, M. A. de, Anhezini, L., Santos, D. É. dos, & Silva-Filho, E. A. da. (2023). *Indoor Air Contamination*

by Yeasts in Healthcare Facilities: Risks of Invasive Fungal Infectio.

<https://doi.org/10.20944/preprints202307.1717.v1>

Nnadi, E., Nanpyal, M., Kaduna, N., Jonathan, B., & Karalti, I. (2020a). Species Diversity of *Candida* from Hospital Environment in Plateau State, Nigeria. *American Journal of Biomedical and Life Sciences*, 8, 15–19. <https://doi.org/10.11648/j.ajbls.20200801.14>

Nnadi, E., Nanpyal, M., Kaduna, N., Jonathan, B., & Karalti, I. (2020b). Species Diversity of *Candida* from Hospital Environment in Plateau State, Nigeria. *American Journal of Biomedical and Life Sciences*, 8, 15–19. <https://doi.org/10.11648/j.ajbls.20200801.14>

Okten, S., & Asan, A. (2012). Airborne fungi and bacteria in indoor and outdoor environment of the Pediatric Unit of Edirne Government Hospital. *Environmental Monitoring and Assessment*, 184(3), 1739–1751. <https://doi.org/10.1007/s10661-011-2075-x>

Padmavathy, N., & Vijayaraghavan, R. (2008). Enhanced bioactivity of ZnO nanoparticles-an antimicrobial study. *Science and Technology of Advanced Materials*, 9(3), 035004. <https://doi.org/10.1088/1468-6996/9/3/035004>

Pappas, P. G., Kauffman, C. A., Andes, D. R., Clancy, C. J., Marr, K. A., Ostrosky-Zeichner, L., Reboli, A. C., Schuster, M. G., Vazquez, J. A., Walsh, T. J., Zaoutis, T. E., & Sobel, J. D. (2016). Clinical Practice Guideline for the Management of Candidiasis: 2016 Update by the Infectious Diseases Society of America. *Clinical Infectious Diseases: An Official Publication of the Infectious Diseases Society of America*, 62(4), e1-50. <https://doi.org/10.1093/cid/civ933>

- Pappas, P. G., Lionakis, M. S., Arendrup, M. C., Ostrosky-Zeichner, L., & Kullberg, B. J. (2018). Invasive candidiasis. *Nature Reviews Disease Primers*, 4(1), Article 1. <https://doi.org/10.1038/nrdp.2018.26>
- Park, B.-G., & Lee, M.-K. (2008). Appropriate Condition of Germ Tube Formation as Presumptive Identification Test for *Candida albicans*. *Korean Journal of Medical Mycology*, 20–25.
- Park, D.-U., Yeom, J.-K., Lee, W. J., & Lee, K.-M. (2013). Assessment of the Levels of Airborne Bacteria, Gram-Negative Bacteria, and Fungi in Hospital Lobbies. *International Journal of Environmental Research and Public Health*, 10(2), 541–555. <https://doi.org/10.3390/ijerph10020541>
- Paul, N. C., Deng, J. X., Lee, H. B., & Yu, S.-H. (2015). Characterization and Pathogenicity of *Alternaria burnsii* from Seeds of *Cucurbita maxima* (Cucurbitaceae) in Bangladesh. *Mycobiology*, 43(4), 384–391. <https://doi.org/10.5941/MYCO.2015.43.4.384>
- Peay, K. G., Kennedy, P. G., & Bruns, T. D. (2008). Fungal Community Ecology: A Hybrid Beast with a Molecular Master. *BioScience*, 58(9), 799–810. <https://doi.org/10.1641/B580907>
- Pemán, J., Cantón, E., & Espinel-Ingroff, A. (2009). Antifungal drug resistance mechanisms. *Expert Review of Anti-Infective Therapy*, 7(4), 453–460. <https://doi.org/10.1586/eri.09.18>
- Ponce-Caballero, C., Gamboa-Marrufo, M., López-Pacheco, M., Cerón-Palma, I., Quintal-Franco, C., Giacomán-Vallejos, G., & Loría-Arcila, J. H. (2013). Seasonal variation of airborne fungal propagules indoor and outdoor of domestic environments in Mérida, Mexico. *Atmósfera*, 26(3), 369–377. [https://doi.org/10.1016/S0187-6236\(13\)71083-X](https://doi.org/10.1016/S0187-6236(13)71083-X)

- Presente, S., Bonnal, C., Normand, A.-C., Gaudonnet, Y., Fekkar, A., Timsit, J.-F., & Kernéis, S. (2023). Hospital Clonal Outbreak of Fluconazole-Resistant *Candida parapsilosis* Harboring the Y132F ERG11p Substitution in a French Intensive Care Unit. *Antimicrobial Agents and Chemotherapy*, 67(3), e0113022. <https://doi.org/10.1128/aac.01130-22>
- Prodan, A. M., Iconaru, S. L., Ciobanu, C. S., Chifiriuc, M. C., Stoicea, M., & Predoi, D. (2013). Iron Oxide Magnetic Nanoparticles: Characterization and Toxicity Evaluation by *In Vitro* and *In Vivo* Assays. *Journal of Nanomaterials*, 2013, e587021. <https://doi.org/10.1155/2013/587021>
- Prucek, R., Tuček, J., Kilianová, M., Panáček, A., Kvítek, L., Filip, J., Kolář, M., Tománková, K., & Zbořil, R. (2011). The targeted antibacterial and antifungal properties of magnetic nanocomposite of iron oxide and silver nanoparticles. *Biomaterials*, 32(21), 4704–4713. <https://doi.org/10.1016/j.biomaterials.2011.03.039>
- Qiu, Y., Zhang, J.-Q., Pan, M.-L., Zeng, W., Tang, S.-D., & Tan, C.-M. (2019). Determinants of prognosis in *Talaromyces marneffei* infections with respiratory system lesions. *Chinese Medical Journal*, 132(16), 1909. <https://doi.org/10.1097/CM9.0000000000000345>
- Qudiesat, K., Abu-Elteen, K., Elkarmi, A., Hamad, M., & Abussaud, M. (2009). *Assessment of airborne pathogens in healthcare settings*.
- Rajendran, S. P., & Sengodan, K. (2017). Synthesis and Characterization of Zinc Oxide and Iron Oxide Nanoparticles Using *Sesbania grandiflora* Leaf Extract as Reducing Agent. *Journal of Nanoscience*, 2017, e8348507. <https://doi.org/10.1155/2017/8348507>

- Rajniak, P., Tsinontides, S. C., Pham, D., Hunke, W. A., Reynolds, S. D., & Chern, R. T. (2008). Sterilizing filtration—Principles and practice for successful scale-up to manufacturing. *Journal of Membrane Science*, 325(1), 223–237. <https://doi.org/10.1016/j.memsci.2008.07.049>
- Rashed, A., El-Katatny, M., Hetta, A., & Hashem, Z. (2020). Validation of moist and dry heat processes used for sterilization and depyrogenation during ampoules manufacturing. *Journal of Advanced Biomedical and Pharmaceutical Sciences*, 0(0), 0–0. <https://doi.org/10.21608/jabps.2020.27282.1083>
- Rasmussen, J. W., Martinez, E., Louka, P., & Wingett, D. G. (2010). Zinc oxide nanoparticles for selective destruction of tumor cells and potential for drug delivery applications. *Expert Opinion on Drug Delivery*, 7(9), 1063–1077. <https://doi.org/10.1517/17425247.2010.502560>
- Reddy, K. M., Feris, K., Bell, J., Wingett, D. G., Hanley, C., & Punnoose, A. (2007). Selective toxicity of zinc oxide nanoparticles to prokaryotic and eukaryotic systems. *Applied Physics Letters*, 90(213902), 213902-1-213902–213903. <https://doi.org/10.1063/1.2742324>
- Ripeau, J.-S., Aumont, F., Belhumeur, P., Ostrosky-Zeichner, L., Rex, J. H., & de Repentigny, L. (2002). Effect of the echinocandin caspofungin on expression of *Candida albicans* secretory aspartyl proteinases and phospholipase in vitro. *Antimicrobial Agents and Chemotherapy*, 46(9), 3096–3100. <https://doi.org/10.1128/AAC.46.9.3096-3100.2002>
- Robbins, N., Uppuluri, P., Nett, J., Rajendran, R., Ramage, G., Lopez-Ribot, J. L., Andes, D., & Cowen, L. E. (2011). Hsp90 governs dispersion and drug resistance of fungal biofilms. *PLoS Pathogens*, 7(9), e1002257. <https://doi.org/10.1371/journal.ppat.1002257>

- Roemer, T., & Krysan, D. J. (2014). Antifungal drug development: Challenges, unmet clinical needs, and new approaches. *Cold Spring Harbor Perspectives in Medicine*, 4(5), a019703. <https://doi.org/10.1101/cshperspect.a019703>
- Rogers, W. J. (2012). 2—Steam and dry heat sterilization of biomaterials and medical devices. In S. Lerouge & A. Simmons (Eds.), *Sterilisation of Biomaterials and Medical Devices* (pp. 20–55). Woodhead Publishing. <https://doi.org/10.1533/9780857096265.20>
- Rudramurthy, G. R., Swamy, M. K., Sinniah, U. R., & Ghasemzadeh, A. (2016). Nanoparticles: Alternatives Against Drug-Resistant Pathogenic Microbes. *Molecules*, 21(7), Article 7. <https://doi.org/10.3390/molecules21070836>
- Rudramurthy, S. M., Paul, R. A., Chakrabarti, A., Mouton, J. W., & Meis, J. F. (2019). Invasive Aspergillosis by *Aspergillus flavus*: Epidemiology, Diagnosis, Antifungal Resistance, and Management. *Journal of Fungi*, 5(3), 55. <https://doi.org/10.3390/jof5030055>
- Saleem, S. S., Alnakshabandie, W. M., & Saadullah, A. A. M. (2017). Fungal contamination of Azadi Teaching Hospital and Hevi Paediatric Hospital Environments, Duhok, Iraq. *Tikrit Journal of Pure Science*, 22(6), Article 6. <https://doi.org/10.25130/tjps.v22i6.788>
- Sang, H., Zheng, X. E., Zhou, W. Q., He, W., Lv, G. X., Shen, Y. N., Kong, Q. T., & Liu, W. D. (2012). A case of subcutaneous phaeohyphomycosis caused by *Cladosporium cladosporioides* and its treatment. *Mycoses*, 55(2), 195–197. <https://doi.org/10.1111/j.1439-0507.2011.02057.x>
- Sardi, J. C. O., Scorzoni, L., Bernardi, T., Fusco-Almeida, A. M., & Mendes Giannini, M. J. S. (2013). *Candida* species: Current epidemiology, pathogenicity, biofilm

- formation, natural antifungal products and new therapeutic options. *Journal of Medical Microbiology*, 62(1), 10–24. <https://doi.org/10.1099/jmm.0.045054-0>
- Sardi, J., Pitangui, N., & Giannini, F. (2013). A Mini Review of Candida Species in Hospital Infection: Epidemiology, Virulence Factor and Drugs Resistance and Prophylaxis. *Tropical Medicine & Surgery*, 01(05). <https://doi.org/10.4172/2329-9088.1000141>
- Savastano, C., de Oliveira Silva, E., Gonçalves, L. L., Nery, J. M., Silva, N. C., & Dias, A. L. T. (2016). Candida glabrata among Candida spp. From environmental health practitioners of a Brazilian Hospital. *Brazilian Journal of Microbiology: [Publication of the Brazilian Society for Microbiology]*, 47(2), 367–372. <https://doi.org/10.1016/j.bjm.2015.05.001>
- Saxena, P., & Mani, R. K. (2014). Preventing hospital acquired infections: A challenge we must accept. *Indian Journal of Critical Care Medicine: Peer-Reviewed, Official Publication of Indian Society of Critical Care Medicine*, 18(3), 125–126. <https://doi.org/10.4103/0972-5229.128699>
- Schoch, C. L., Seifert, K. A., Huhndorf, S., Robert, V., Spouge, J. L., Levesque, C. A., & Chen, W. (2012, February 24). Nuclear ribosomal internal transcribed spacer (ITS) region as a universal DNA barcode marker for Fungi. <https://doi.org/10.1073/pnas.1117018109>
- Seddighi, N. S., Salari, S., & Izadi, A. R. (2017). Evaluation of antifungal effect of iron-oxide nanoparticles against different Candida species. *IET Nanobiotechnology*, 11(7), 883–888. <https://doi.org/10.1049/iet-nbt.2017.0025>
- Sellart-Altisent, M., Torres-Rodríguez, J. M., Gómez de Ana, S., & Alvarado-Ramírez, E. (2007). [Nasal fungal microbiota in allergic and healthy subjects]. *Revista*

- Iberoamericana De Micologia*, 24(2), 125–130. [https://doi.org/10.1016/s1130-1406\(07\)70027-x](https://doi.org/10.1016/s1130-1406(07)70027-x)
- Seneviratne, C., Jin, L., & Samaranyake, L. (2008). Biofilm lifestyle of *Candida*: A mini review. *Oral Diseases*, 14(7), 582–590. <https://doi.org/10.1111/j.1601-0825.2007.01424.x>
- Setlhare, G., Malebo, N., Shale, K., & Lues, R. (2014). Identification of airborne microbiota in selected areas in a health-care setting in South Africa. *BMC Microbiology*, 14(1), 100. <https://doi.org/10.1186/1471-2180-14-100>
- Sharmila, G., Farzana Fathima, M., Haries, S., Geetha, S., Manoj Kumar, N., & Muthukumar, C. (2017). Green synthesis, characterization and antibacterial efficacy of palladium nanoparticles synthesized using *Filicium decipiens* leaf extract. *Journal of Molecular Structure*, 1138, 35–40. <https://doi.org/10.1016/j.molstruc.2017.02.097>
- Sharpe, R. A., Bearman, N., Thornton, C. R., Husk, K., & Osborne, N. J. (2015). Indoor fungal diversity and asthma: A meta-analysis and systematic review of risk factors. *The Journal of Allergy and Clinical Immunology*, 135(1), 110–122. <https://doi.org/10.1016/j.jaci.2014.07.002>
- Shekhany, K. A. M. (2021). Isolation and genotyping of *Candida albicans* involved in vaginal candidiasis among pregnant women in Sulaymaniyah and Erbil cities. *Zanco Journal of Medical Sciences (Zanco J Med Sci)*, 25(1), 493–502. <https://doi.org/10.15218/zjms.2021.012>
- Shelton, B. G., Kirkland, K. H., Flanders, W. D., & Morris, G. K. (2002). Profiles of airborne fungi in buildings and outdoor environments in the United States. *Applied and Environmental Microbiology*, 68(4), 1743–1753. <https://doi.org/10.1128/AEM.68.4.1743-1753.2002>

- Shoham, S., & Marr, K. A. (2012). Invasive fungal infections in solid organ transplant recipients. *Future Microbiology*, 7(5), 639–655. <https://doi.org/10.2217/fmb.12.28>
- Shukla, S., Arora, V., Jadaun, A., Kumar, J., Singh, N., & Jain, V. K. (2015). Magnetic removal of Entamoeba cysts from water using chitosan oligosaccharide-coated iron oxide nanoparticles. *International Journal of Nanomedicine*, 10, 4901–4917. <https://doi.org/10.2147/IJN.S77675>
- Sidkey, N., Goudal, A., Shawky, H., & Abdel-hady, Y. (2020). BIOSYNTHESIS, CHARACTERIZATION AND ANTIMICROBIAL ACTIVITY OF IRON OXIDE NANOPARTICLES SYNTHESIZED BY FUNGI. *Al-Azhar Journal of Pharmaceutical Sciences*, 62(2), 164–179. <https://doi.org/10.21608/ajps.2020.118382>
- Silva, S., Negri, M., Henriques, M., Oliveira, R., Williams, D. W., & Azeredo, J. (2012). Candida glabrata, Candida parapsilosis and Candida tropicalis: Biology, epidemiology, pathogenicity and antifungal resistance. *FEMS Microbiology Reviews*, 36(2), 288–305. <https://doi.org/10.1111/j.1574-6976.2011.00278.x>
- Singh, S., Kanaujia, R., Rudramurthy, S. M., Singh, S., Kanaujia, R., & Rudramurthy, S. M. (2021). Immunopathogenesis of Aspergillosis. In *The Genus Aspergillus—Pathogenicity, Mycotoxin Production and Industrial Applications*. IntechOpen. <https://doi.org/10.5772/intechopen.98782>
- Sivagnanasundaram, P., Amarasekara, R. W. K., Madegedara, R. M. D., Ekanayake, A., & Magana-Arachchi, D. N. (2019). Assessment of Airborne Bacterial and Fungal Communities in Selected Areas of Teaching Hospital, Kandy, Sri Lanka. *BioMed Research International*, 2019, 7393926. <https://doi.org/10.1155/2019/7393926>

- Souza, A. K. P., Nascimento, J. P. M. do, Araújo, M. A. dos S., Pedrosa, K. P. da S., Tenorio, B. M., Pires, L. L. S., Lima, G. B. C. de, Barboza, R. I. dos S., & Filho, E. A. da S. (2019). Airborne Fungi in Neonatal Intensive Care Unit of a Public Hospital in Brazil. *International Journal of Current Microbiology and Applied Sciences*, 8(12), 1210–1219. <https://doi.org/10.20546/ijcmas.2019.812.149>
- Steinbach, W. J., Benjamin, D. K., Kontoyiannis, D. P., Perfect, J. R., Lutsar, I., Marr, K. A., Lionakis, M. S., Torres, H. A., Jafri, H., & Walsh, T. J. (2004). Infections due to *Aspergillus terreus*: A multicenter retrospective analysis of 83 cases. *Clinical Infectious Diseases: An Official Publication of the Infectious Diseases Society of America*, 39(2), 192–198. <https://doi.org/10.1086/421950>
- Storti, L. R., Pasquale, G., Scomparim, R., Galastri, A. L., Alterthum, F., Gambale, W., & Rodrigues Paula, C. (2012). *Candida* spp. Isolated from inpatients, the environment, and health practitioners in the Pediatric Unit at the University Hospital of the Jundiaí Medical College, State of São Paulo, Brazil. *Revista Da Sociedade Brasileira De Medicina Tropical*, 45(2), 225–231. <https://doi.org/10.1590/s0037-86822012000200017>
- Sudharsanam, S., Swaminathan, S., Ramalingam, A., Thangavel, G., Annamalai, R., Steinberg, R., Balakrishnan, K., & Srikanth, P. (2012). Characterization of indoor bioaerosols from a hospital ward in a tropical setting. *African Health Sciences*, 12(2), 217–225. <https://doi.org/10.4314/ahs.v12i2.22>
- Thomaz, D. Y., de Almeida, J. N., Sejas, O. N. E., Del Negro, G. M. B., Carvalho, G. O. M. H., Gimenes, V. M. F., de Souza, M. E. B., Arastehfar, A., Camargo, C. H., Motta, A. L., Rossi, F., Perlin, D. S., Freire, M. P., Abdala, E., & Benard, G. (2021). Environmental Clonal Spread of Azole-Resistant *Candida parapsilosis* with Erg11-Y132F Mutation Causing a Large Candidemia

- Outbreak in a Brazilian Cancer Referral Center. *Journal of Fungi (Basel, Switzerland)*, 7(4), 259. <https://doi.org/10.3390/jof7040259>
- Tocco, I., Zavan, B., Bassetto, F., & Vindigni, V. (2012). Nanotechnology-Based Therapies for Skin Wound Regeneration. *Journal of Nanomaterials*, 2012, e714134. <https://doi.org/10.1155/2012/714134>
- Tong, X., Xu, H., Zou, L., Cai, M., Xu, X., Zhao, Z., Xiao, F., & Li, Y. (2017). High diversity of airborne fungi in the hospital environment as revealed by meta-sequencing-based microbiome analysis. *Scientific Reports*, 7, 39606. <https://doi.org/10.1038/srep39606>
- Torabi, L. R., & Doudi, M. (2016). The Effect of Gold Nano Particles Compared to Dioxide Titanium Nano Particles on Vital Factors of Isolated *Candida albicans* in Patients with Oral Candidiasis in Vitro. *Zahedan Journal of Research in Medical Sciences*, 18(12), Article 12. <https://doi.org/10.17795/zjrms-5666>
- Tormo-Molina, R., Gonzalo-Garijo, M. A., Fernández-Rodríguez, S., & Silva-Palacios, I. (2012). Monitoring the occurrence of indoor fungi in a hospital. *Revista Iberoamericana de Micología*, 29(4), 227–234. <https://doi.org/10.1016/j.riam.2012.04.002>
- Tortora, G. J., Funke, B. R., & Case, C. L. (2010). *Microbiology: An introduction* (10th ed). Pearson Benjamin Cummings. <http://books.google.com/books?id=wUkqAQAAMAAJ>
- Tran, N., Mir, A., Mallik, D., Sinha, A., Nayar, S., & Webster, T. J. (2010). Bactericidal effect of iron oxide nanoparticles on *Staphylococcus aureus*. *International Journal of Nanomedicine*, 5, 277–283. <https://doi.org/10.2147/ijn.s9220>
- Usuda, D., Higashikawa, T., Hotchi, Y., Usami, K., Shimosawa, S., Tokunaga, S., Osugi, I., Katou, R., Ito, S., Yoshizawa, T., Asako, S., Mishima, K., Kondo, A.,

- Mizuno, K., Takami, H., Komatsu, T., Oba, J., Nomura, T., & Sugita, M. (2021). *Exophiala dermatitidis*. *World Journal of Clinical Cases*, *9*(27), 7963–7972. <https://doi.org/10.12998/wjcc.v9.i27.7963>
- Venceslau, E., Oliveira, I., & Martins, R. (2012). Frequência de fungos anemófilos em áreas críticas de unidade hospitalar de Aracaju, Sergipe, Brasil Frequency of airborne fungus in critical areas at hospital unit of Aracaju, Sergipe, Brazil. *RBAC*, *44*, 26–30.
- Verma, A., Wüthrich, M., Deepe, G., & Klein, B. (2015). Adaptive Immunity to Fungi. *Cold Spring Harbor Perspectives in Medicine*, *5*(3), a019612. <https://doi.org/10.1101/cshperspect.a019612>
- Viegas, C., Sabino, R., Veríssimo, C., & Rosado, L. (2011). *Assessment of fungal contamination in a Portuguese maternity unit*. 127–133. <https://doi.org/10.2495/EHR110121>
- Wasly, H. (2018). X-RAY ANALYSIS FOR DETERMINATION THE CRYSTALLITE SIZE AND LATTICE STRAIN IN ZnO NANOPARTICLES. *Journal of Al-Azhar University Engineering Sector*, *13*(49), 1312–1320. <https://doi.org/10.21608/aej.2018.18943>
- White, Bruns, T., Lee, S., & Taylor, J. (1990). *White, T. J., T. D. Bruns, S. B. Lee, and J. W. Taylor. Amplification and direct sequencing of fungal ribosomal RNA Genes for phylogenetics* (pp. 315–322).
- White, J. K., Nielsen, J. L., & Madsen, A. M. (2020). Potential Respiratory Deposition and Species Composition of Airborne Culturable, Viable, and Non-Viable Fungi during Occupancy in a Pig Farm. *Atmosphere*, *11*(6), Article 6. <https://doi.org/10.3390/atmos11060639>

- Wirth, F., & Goldani, L. Z. (2012). Epidemiology of Rhodotorula: An Emerging Pathogen. *Interdisciplinary Perspectives on Infectious Diseases*, 2012, 465717. <https://doi.org/10.1155/2012/465717>
- Wu, W., Wu, Z., Yu, T., Jiang, C., & Kim, W.-S. (2015). Recent progress on magnetic iron oxide nanoparticles: Synthesis, surface functional strategies and biomedical applications. *Science and Technology of Advanced Materials*, 16(2), 023501. <https://doi.org/10.1088/1468-6996/16/2/023501>
- Xiao, L., Madison, V., Chau, A. S., Loebenberg, D., Palermo, R. E., & McNicholas, P. M. (2004). Three-dimensional models of wild-type and mutated forms of cytochrome P450 14alpha-sterol demethylases from *Aspergillus fumigatus* and *Candida albicans* provide insights into posaconazole binding. *Antimicrobial Agents and Chemotherapy*, 48(2), 568–574. <https://doi.org/10.1128/AAC.48.2.568-574.2004>
- Yousef, J., & Danial, E. (2013). In Vitro Antibacterial Activity and Minimum Inhibitory Concentration of Zinc Oxide and Nano-particle Zinc oxide Against Pathogenic Strains [dataset]. In *International JOURNAL OF HEALTH SCIENCE* (Vol. 2). <https://doi.org/10.5923/j.health.20120204.04>
- Zhang, Z.-Y., & Xiong, H.-M. (2015). Photoluminescent ZnO Nanoparticles and Their Biological Applications. *Materials*, 8(6), Article 6. <https://doi.org/10.3390/ma8063101>

دراسة تأثير ZnONPs و IONPs بالتراكيز (١٠٠٠، ٥٠٠، ٢٥٠، ١٢٥ و ٦٢,٥) ميكروغرام/مل ضد (٥) عزلات من فطر *Candida* بواسطة مقياس الانتشار الجيد لطبق الأجار. لقد لفتنا الانتباه إلى العمل الممتاز لـ NPs، وأظهرت النتائج أن التأثير التثبيطي العالي لـ ZnONPs والذي ظهر في *C. lusitaniae* و *C. glabrata* متبوعاً بـ *C. krusei*. في حين أن التأثير التثبيطي العالي لـ IONPs ظهر في *C. parapsilosis* و *C. glabrata*. أظهرت النتائج أن *Candida spp*. كانوا عرضة لـ NPs ويزداد معدل التثبيط مع زيادة التركيز.

للحصول على الحد الأدنى من التركيز المثبط بواسطة طرق التخفيف الدقيق ، وجدنا أن MIC من ZnO-NPs و IONPs ضد *Candida spp*. تم الإبلاغ عن أنها ٦٤-٥١٢ ميكروجرام/مل، ١٦-١٢٨ و ٦٤-٥١٢ ميكروجرام/مل بالنسبة لـ FLC. تكشف نتائجنا أن MICs لمضادات الفطريات ضد *Candida spp*. كان نشاطاً جيداً جداً في المختبر، وكان أقل MIC لـ IONPs في *C. glabrata* و *C. lusitaniae* هو ١٦ ميكروغرام/مل. في حين لوحظ أن أدنى تركيز MIC لـ ZnO-NPs في *C. lusitaniae* و *C. albicans* كان ٦٤ ميكروغرام/مل.

الخلاصة

على الرغم من وجود الجراثيم في بيئات مختلفة ، إلا أن محيط المستشفى الداخلي قد يتسبب في انتشار الفطريات المسببة للأمراض بين المرضى في المستشفيات. كان الهدف من هذه الدراسة هو عزل وتعريف الفطريات المحمولة جواً الموجودة في بيئة المستشفيات في مدينة كوية التعرف الجزيئي للفطريات المعزولة من أنواع المبيضات *Candida*. تم أجريت الدراسة في خمسة مستشفيات ومنشآت رعاية صحية حكومية ، والتي تم تضمينها ؛ مستشفى الشهيد دكتور خالد ، مركز الصحي شهيد دكتور هندرين ، مركز الصحي الحاجي قادر ، مركز الصحي باواجي ومركز الصحي الشهيد دكتور كاوه والأسنان. تمت زراعة ٢٢٥ عينة هواء من أماكن مختلفة في كل من هذه المستشفيات. باستخدام أطباق بتري معقمة مليئة بأجار Sabouraud dextrose agar (SDA) والكلورامفينيكول ، يتم تحديد كل عينة بشكل صحيح ثم يتم أخذها إلى المختبر للمعالجة والتحليل الميكروبيولوجي. تم رصد ١٦ نوع من الفطريات المسببة للأمراض في جميع مستشفيات مدينة كويه ، وفقاً للنتائج. وزعت هذه العزلات في مستشفى شهيد دكتور خالد (٣٢٪) ، مركز الصحي شهيد دكتور هندرين (١٧٪) ، مركز الصحي الحاجي قادر (١٥٪) ، مركز الصحي البواجي (١٢٪) ، ومركز الصحي الشهيد دكتور كاوه والأسنان (٢٣٪).

وأظهرت نتائج التحليل المختبري أنه من ١٩٨ عينة إيجابية تم تحليلها، تم تحديد ٦٠,٥% منها على أنها فطريات mould، بينما تم تحديد ٣٩,٥% المتبقية على أنها عزلات خميرة. ومن أكثر الفطريات المحمولة جواً شيوعاً ما يلي: توزع الفطر mould بنسبة (٢٥,٢٦%) *Aspergillus spp.*، *Penicillium Sp.* (8.25%)، و *Curvularia sp* (٦,١٩%) حيث توزعت عزلات الخميرة بنسبة (٢٨,٣٥%) *Candida Spp.*، و *Cryptococcus sp* (6.87%)، و *Rhodotorula spp* (٣,٦١%).

لتحديد الأنواع عزلة من المبيضات، كان التشخيص الجزيئي ضرورياً. كشفت نتائج تفاعل البلمرة المتسلسل أن البادئات العامة لقليل النوكليوتيد ITS1 (18S) و ITS4 (28S) تعمل على تضخيم جينات (rRNA) وجين S٥,٨ للفطر. لقد حددنا بدقة مستويات الأنواع لـ *C. albicans* و *C. glabrata* و *C. parapsilosis* و *C. lusitaniae* باستخدام هذه البادئات، التي تم تسجيلها في قاعدة بيانات المركز الوطني لمعلومات التكنولوجيا الحيوية.

يهدف جزء إضافي من هذه الدراسة إلى تقييم النشاط المضاد للفطريات لجزيئات أكسيد المعادن النانوية، وخاصة أكسيد الزنك وأكسيد الحديد ضد أنواع مختلفة من المبيضات، مقارنة بالفلوكونازول (FLC). تم تشخيص جزيئات أكسيد الزنك وأكسيد الحديد النانوية بواسطة تحليل حيود الأشعة السينية (XRD) والمجهر الإلكتروني الماسح (SEM).

جمهورية العراق الفيدرالي
حوكمة إقليم كردستان
وزارة التعليم العالي والبحث العلمي
جامعة كويه



**النشاط المضاد للفطريات لجسيمات أكسيد الحديد وأكسيد الزنك النانوية ضد
الفطريات المحمولة جوا المعزولة من بيئة المستشفيات في مدينة كويه**

رسالة مقدمة الى فاكولتي العلوم والصحة في جامعة كويه وهي جزء من متطلبات
نيل شهادة الماجستير في علم الأحياء المجهرية الطبية

من قبل

ايمان محمد ميرزا

حاصلة شهادة بكالوريوس في قسم علم الأحياء المجهرية الطبية كلية العلوم الصحية
جامعة هولير الطبية سنة ٢٠١٦

بإشراف

أ.م.د. طه جلال عمر

١٤٤٥هـ

کاربرگهري ZnONPs و IONPs لئیکۆلئینهوه له چریه جیاوازهکان (۱۰۰۰-۵۰۰-۲۵۰-۱۲۵-
۶۲,۵) $\mu\text{g/ml}$ بهرامبهر (۵) جیاکردنهوهی candida په رینگهی agar plate well diffusion . نئیمه
سهرنجمان راکئیشا بۆ کردهوه نایابهکهی تهنۆلکهی نانۆیی ، ئهنجامهکان ئهو کاربهرییه رینگریه بهرزهی
ZnONPs نیشانی دا لههژی *C. lusitaniae* و *C. glabrata* ، بههوایدا *C. Krusei* له کاتیکدا
کاربهری بهربهستی بهرزهی IONPs لههژی *C. parapsilosis* و *C. glabrata* پئشککش کرا.
ئهنجامهکان ئهوهیان دهرخست که کاندیدا ههستیازه بۆ NPs. و ریزههی رینگریکردن لهگهل زیادبوونی چری
نانۆیهکه زیاد دهکات.

کهترین چری رینگری لهلایهن میتودهکانی broth microdilution ، نئیمه ئهوهمان بۆ دهركهوت
که MIC له ZnO-NPs و IONPs بهرامبهر به *Candida spp*. راپۆرت کراوه که ۶۴-۵۱۲ و ۱۶-۱۲۸
 $\mu\text{g/ml}$ و ۶۴-۵۱۲ $\mu\text{g/ml}$ بۆ FLC. ئهنجامهکانمان ئهوه ئاشکرا دهکهن که MIC بۆ هژی *Candida*
spp. چالاکییهکی زۆر باش بوون، کهترین MIC ی ئوکسیدی ناسن پۆ *C. glabrata* و *C.*
lusitaniae ۱۶ $\mu\text{g/ml}$ بوون. له کاتیکدا که مترین MIC بۆ ئوکسیدی زینک *C* و *C lusitaniae*
albicans ۶۴ $\mu\text{g/ml}$ بوو.

پوخته

سهره‌رای نمره راستیهی که سپوره‌کان له ژینگه‌ی جوراوجوردا بوونیان هه‌یه، به‌لام هه‌وای ناو نه‌خوشخانه له‌وانه‌یه بیهته هوی بلاو بوونه‌وی نه‌خوشی که‌رووی له‌نیو نه‌خوشه‌کان له نه‌خوشخانه‌کاندا. نامانجی نهم لیکولینه‌ویه جیاکر دنه‌وه و ناسینه‌وهی نهم که‌رووانه بوو که له ژینگه‌ی نه‌خوشخانه‌کانی شاری کویه بوونیان هه‌یه، ناسینه‌وهی که‌رووی گهردیله‌یی بو جوره‌کانی (*Candida*). به قه‌باره‌ی باند (۳۷۵-۸۷۱ bp). لیکولینه‌ومه‌که له پینج نه‌خوشخانه و دامه‌زراوه‌ی چاودیری تهن‌روستی حکومهت نه‌جامدراوه، که بریتین له؛ نه‌خوشخانه‌ی شه‌هید دکتور خالید، مه‌ل‌بندی تهن‌روستی شه‌هید دکتور ههن‌دین، مه‌ل‌بندی تهن‌روستی حاجی قادر، مه‌ل‌بندی تهن‌روستی باواجی، مه‌ل‌بندی تهن‌روستی دکتور کاوه و سه‌نته‌ری ددان. له ههر په‌کیک له نه‌خوشخانه‌کاندا ۲۲۵ نمونه‌ی هه‌وا له به‌شه جیاوازمه‌کانی نه‌خوشخانه‌که‌دا هه‌بوون. ههر نمونه‌یه‌که به شیوه‌یه‌کی گونجاو وهرگیراوه، پاشان ده‌بریت بو تاقیگه بو پرۆسه‌کردن و شیکردنه‌وه‌ی مایکروبیالۆجی. به‌گیروه‌ی نه‌جامه‌کان، له هه‌موو نه‌خوشخانه‌کانی شاری کویه ۱۶ که‌رووی جیاواز له نه‌خوشخانه‌کانی شاری کویه بینه‌راوه. نهم ریژه‌یه له نه‌خوشخانه‌ی شه‌هید دکتور خالید (۳۲٪) و مه‌ل‌بندی تهن‌روستی شه‌هید دکتور ههن‌دین (۱۷٪) و مه‌ل‌بندی تهن‌روستی حاجی قادر (۱۵٪) و مه‌ل‌بندی تهن‌روستی باواجی (۱۲٪) و مه‌ل‌بندی تهن‌روستی دکتور کاوه و سه‌نته‌ری ددان (۲۳٪) دابه‌ش بوون.

نه‌جامه‌کانی شیکردنه‌وه‌ی تاقیگه‌که نه‌مه‌یان ناشکرا کرد که له کوی ۱۹۸ نمونه‌ی پۆزه‌تیف شیکردنه‌وه‌یان بو کراوه، کوی گشتی ۶۰،۵٪ و مک که‌رووی *Mold* ناسینه‌اون، له کاتیگدا ۳۹،۵٪ ی ماوه‌که به جیاکراوه‌ی *yeast* ناسینه‌اون. باوترین که‌روومه‌کانی هه‌وا بریتین له: که‌رووه *Mold* کان دابه‌شکراوه: *Aspergillus spp.* (۲۵،۲۶٪)، *Penicillium* (۸،۲۵٪)، *Curvularia sp.* (۶،۱۹٪) و *yeast* جیاکراوه‌کان دابه‌ش بوون و مک (*Candida Spp.*) (۲۸،۳۵٪)، *Cryptococcus sp.* (۶،۸۷٪)، *Candida Spp.* (۳،۶۱٪) و *Rhodotorula spp.*

بو دۆزینه‌وه‌ی وردی جیاکراوه‌ترین جوره‌کانی *candida*، ده‌ست‌نیشان‌کردنی گهردی پۆیه‌سته. نه‌جامه‌کانی کارلیکی زنجیره‌یی پۆلیمه‌یز نه‌مه‌یان ناشکرا کرد که ITS1 (18S) و ITS4 (28S) ئولیگونوکلیوتایدی جیهانی جینی rRNA و جینی ۵،۸S که‌روومه‌کیان گهره‌تر کردوه. نهمه به وردی جوره‌کانمان دیاریکرد بو *C. albicans*، *C. glabrata*، *C. parapsilosis*، *C. krusei* و *C. lusitaniae* به به‌کار هینانی نهم سه‌ره‌تایینه، که له سه‌نته‌ری نیشتمانی بو بنکه‌دراره‌ی زانیاری بایۆتکنۆلۆجی تومارکران.

به‌شیکی دیکه‌ی نهم لیکولینه‌ویه نامانجی هه‌لسه‌نگاندنی چالاک‌ی دژه که‌روو نانوته‌نۆکانی ئوکسیدی کانزایه، به‌تایه‌تی ئوکسیدی زینک و ئوکسیدی ناسن به‌رامبه‌ر به‌جوره جیاوازمه‌کانی *candida*، به به‌راورد له‌گه‌ل (FLC) *fluconazole* تاییه‌تمه‌ندیه‌کانی ئوکسیدی زینک و ته‌نۆته‌نۆکانی ئوکسیدی ناسن به شیکردنه‌وه‌ی جیاوازی تیشکی ئیکس (XRD). و مایکروسکۆپی ئه‌لیکترۆن (SEM) دیاریکران.

کۆماری فیدرالی عێراق
حوکمهتی ههریمی کوردستان
وهزارهتی خویندنی بالآ و
تویژینهوهی زانستی زانکۆی کۆیه



چالاکي دژه کهروویي تهنۆلکهی ئۆکسیدی ناسن و ئۆکسیدی زینک دژي
ئهوکهر ووانهی له ههوا جیاکراونهتهوه له ژینگهی نهخۆشخانهکانی شاری کۆیه

ماستر نامهبهکه پيشکeshی

فاکهلتی ئهنجومهنی زانست و تهندروستی کراوه له زانکۆی کۆیه وهک بهشیک له
پیداویستی به دهست هێانی بروانامهی ماستر له زانستی میدیکهل مایکروبايولوجی

له لایهن

ایمان محمد میرزا

بهکالتوریۆس له میدیکهل مایکروبايولوجی

کۆلیژی زانسته تهندروستیهکان/ زانکۆی ههولیری پزیشکی/ سالی ۲۰۱۶

سهرپهرشتیار

پ.ی.د. طه جلال عمر

2023ز